RITA Intelligent Transportation Systems
Joint Program Office

Microscopic Analysis of Traffic Flow in Inclement Weather

Part 2

www.its.dot.gov/index.htm
Final Report — December 01, 2010
FHWA- JPO-11-020

U.S. Department of Transportation
Federal Highway Administration
Research and Innovative Technology Administration

Produced by
ITS Joint Program Office
Research and Innovative Technology Administration
U.S. Department of Transportation

Notice

Report Documentation Page

Form Approved
OMB No. 0704-0188

1. REPORT DATE (DD MM YYYY)	2. REPORT TYPE	3. DATES COVERED
01 12 2010	Research	July 2009 to December 2010

4. TITLE AND SUBTITLE
Microscopic Analysis of Traffic Flow in Inclement Weather -Part 2

5a. CONTRACT NUMBER
DTFH61-06-D-00004

5b. GRANT NUMBER

5c. PROGRAM ELEMENT NUMBER

5d. PROJECT NUMBER

5e. TASK NUMBER

5f. WORK UNIT NUMBER

6. AUTHOR(S)
Hesham Rakha, Ismail Zohdy, Sangjun Park, Daniel Krechmer

7. PERFORMING ORGANIZATION NAME(S) AND ADDRESS(ES)
Cambridge Systematics, Inc.
4800 Hampden Lane, Suite 800
Bethesda, MD 20814

Virginia Tech Transportation Institute
3500 Transportation Research Plaza (0536)
Blacksburg, VA 24061

8. PERFORMING ORGANIZATION REPORT NUMBER
FHWA-JPO-11-020

9. SPONSORING/MONITORING AGENCY NAME(S) AND ADDRESS(ES)
Research and Innovative Technology Administration
U.S. Department of Transportation
1200 New Jersey Avenue, NE
Washington, DC 20590

10. SPONSORING/MONITOR'S ACRONYM(S)

11. SPONSORING/MONITOR'S REPORT NUMBER(S)

12a. DISTRIBUTION/AVAILABILITY STATEMENT
No restrictions. This document is available to the public through the National Technical Information Service, Springfield, VA 22161.

12b. DISTRIBUTION CODE

13. SUPPLEMENTARY NOTES
COTM's for FHWA are Roemer Alfelor and C. Y. David Yang.

14. ABSTRACT (Maximum 200 words)
This report documents the second part of the FHWA research study involving analysis of the microscopic impacts of adverse weather on traffic flow, but is a third phase of the research effort on the impacts of weather on traffic flow. The first phase of FHWA research involved macroscopic analysis, which focused on the impacts of adverse weather on aggregate traffic flow. The second phase of research analyzed the impacts of adverse weather on microscopic traffic behavior. This report documents the results of three research efforts (1) The impacts of icy roadway conditions on driver behavior at a microscopic level, using field-measured car-following data,; (2) An investigation of the influence of weather precipitation and roadway surface condition on left-turn gap-acceptance behavior using traffic and weather data collected during the winter of 2009-2010 at a signalized intersection in Blacksburg, Virginia; and (3)The development and demonstration of methodologies for the use of weather-related adjustment factors in microsimulation models, including general approaches to construct simulation models accounting for the impact of precipitation. For the third effort, the general approach was applied to the calibration of the VISSIM and INTEGRATION simulation software.

15. SUBJECT TERMS
Weather-responsive traffic management, WRTM, weather and traffic flow analysis, microscopic traffic models, gap acceptance and weather, car following weather, lane changing.

16. SECURITY CLASSIFICATION OF:			17. LIMITATION OF ABSTRACT	18. NUMBER OF PAGES	19a. NAME OF RESPONSIBLE PERSON
Unclassified				93	Roemer Alfelor
a. REPORT	b. ABSTRACT	c. THIS PAGE			19b. TELEPHONE NUMBER
					(202) 366-9242

Preface/Acknowledgments

Acknowledgments
We would like to thank Roemer Alfelor and C. Y. David Yang, the FHWA Contracting Officer's Task Managers, for their continued support and technical guidance during this project. This report is based upon work supported by the Federal Highway Administration under contract number DTFH61-01-C00181. Any opinions, findings, and conclusions or recommendations expressed in this publication are those of the authors and do not necessarily reflect the views of the Federal Highway.

Administration
The authors would also like to thank Dr. Takashi Nakatsuji of the Hokkaido University for providing the experiment data used in this study and Mr. Mitsuru Tanaka of McCormick Taylor, Inc. for organizing the data and translating the data description document for the study documented in Chapter 2.

Quality Assurance Statement

The Federal Highway Administration (FHWA) provides high-quality information to serve Government, industry, and the public in a manner that promotes public understanding. Standards and policies are used to ensure and maximize the quality, objectivity, utility, and integrity of its information. FHWA periodically reviews quality issues and adjusts its programs and processes to ensure continuous quality improvement.

Table of Contents

List of Tables

List of Figures

List of Attributes

1.0 Introduction

Weather causes a variety of impacts on the transportation system. While severe winter storms, hurricanes, or flooding can result in major stoppages or evacuations of transportation systems and cost millions of dollars, the day-to-day weather events such as rain, fog, snow, and freezing rain can have a serious impact on the mobility and safety of the transportation system users. The application of IntelliDriveTM technologies, Road Weather Information Systems (RWIS), and weather/traffic data collection and forecasting technologies, presents new opportunities to improve the safety and mobility of the traveling public during adverse weather conditions. Key to these opportunities are: 1) improved knowledge and understanding of how individual drivers behave during adverse weather; and 2) how their decisions collectively impact traffic flow. This, in turn, will support weather-responsive traffic management strategies such as real-time modification of traffic signal and ramp meter timings, automated deicing systems, and variable speed limits. Despite the documented impacts of adverse weather on transportation, understanding of the linkages between inclement weather conditions and traffic flow remain tenuous. This report documents the second part of the FHWA research study involving analysis of the microscopic impacts of adverse weather on traffic flow, but is a third phase of the research effort into the impacts of weather on traffic flow.

The first phase of FHWA research involved macroscopic analysis, which focused on the impact of adverse weather on aggregate traffic flow. This research was conducted using data from Traffic Management Centers in Baltimore, Seattle, and the Twin Cities of Minneapolis-St. Paul, and the National Weather Service stations at airports in those cities. The research found that both rain and snow did impact free-flow speed, speed-at-capacity, and capacity. Impacts varied with precipitation intensity. The complete report is available from the FHWA web site http://ops.fhwa.dot.gov/publications/weatherempirical/index.htm.

The second phase of research analyzed the impacts of adverse weather on microscopic traffic behavior. Microscopic analysis describes individual driver responses to weather conditions, such as changing lanes, merging on to a freeway, making left turns across traffic at an intersection, or adjusting the distance behind a lead vehicle. Studies that videotape individual vehicle movements at intersections or freeway merge locations are providing a rich source of data for microscopic analysis. For this phase of the study, video recorded data was utilized to accomplish two primary goals:

1. Better understand how drivers respond to adverse weather, focusing on three types of driving behavior: car following, gap acceptance, and lane changing.
2. Incorporate microscopic models in existing microsimulation tools, so they can be used to model and evaluate weather-responsive traffic management strategies.

The microsimulation packages evaluated include CORSIM, VISSIM, AIMSUM2, Paramics, and INTEGRATION.

This phase was most successful in modeling gap acceptance behavior. Research used video collected at three intersections in Blacksburg, VA, to determine whether drivers alter their gap acceptance behavior during rainy weather. Findings indicate a more cautious approach to left turn gap acceptance during

rainy weather, a factor that would influence the effectiveness of signal timing plans. This report can be found at http://ntl.bts.gov/lib/32000/32500/32539/tfiw_final.pdf.

This report documents the continuation of research on the impacts of adverse weather on traffic flow at the microscopic level. The results are documented in subsequent sections as follows:

- Section 2.0 documents research findings on the impacts of icy roadway conditions on driver behavior at a microscopic level, using field-measured car-following data, in addition to the study of the typical variability in driver behavior. Specifically, the study uses two car-following experiment datasets, one gathered under dry roadway conditions and another gathered under icy roadway conditions, in order to calibrate the Van Aerde car-following model and build a database of two sets of driver-specific parameters. The two sets of parameters are statistically compared to quantify changes in driver behavior as a result of icy roadway conditions. Specifically, this study quantifies the impact of icy roadway conditions on five driver-specific parameters namely: free-flow speed, headway-at-capacity (reciprocal of capacity), the speed-at-capacity, spacing at jam density (reciprocal of jam density), and driver perception-reaction time. The research also considers the vehicle acceleration and deceleration constraints considering the roadway surface conditions. The dataset utilized was obtained from the University of Hokkaido in Japan.
- Section 3.0 includes the results of an investigation of the influence of weather precipitation (rain or snow) and roadway surface condition (icy, snowy, or wet) on left-turn gap-acceptance behavior. The weather condition in the study is divided into six categories for the different combinations of weather precipitation and roadway surface condition. Logit models are fit to the data to model driver gap acceptance behavior and compute driver-specific critical gap sizes. The data were collected for six months, including the winter of 2009-2010, at a signalized intersection in Blacksburg, Virginia, which was outfitted with CCTV and an Environmental Sensor Station used to measure temperature and precipitation. Analysis of over 11,000 observations revealed that drivers are more conservative during snow precipitation compared to rain precipitation. In the case of the roadway surface condition, drivers require larger gaps for wet surface conditions compared to snowy and icy surface conditions, and, as would be expected, require smallest gaps for dry roadway conditions. In addition, the models show that the drivers require larger gaps as the distance required to clear the conflict point increases. The study also illustrates how inclement weather and number of opposing lanes affect permissive left-turn saturation flow rates.
- Section 4.0 documents the final portion of this project, which involved development and demonstration of methodologies for the use of weather-related adjustment factors in microsimulation models. The specific objective was to identify the methodologies for modeling traffic stream behavior under inclement weather conditions using state-of-the-art microscopic simulation software. Specifically, this study investigates general approaches to construct simulation models accounting for the impact of rain and snow precipitation by means of calibrating car-following, lane-changing, and gap-acceptance models. Thereafter, the general approach is applied to the calibration of the VISSIM and INTEGRATION software. The original project plan called for use of the CORSIM model rather than INTEGRATION. However, an evaluation of both models showed that the CORSIM model has a limited ability to incorporate weather-related adjustment factors. INTEGRATION on the other hand offers much greater capability to incorporate

weather-related factors. The results of the test showed that while rain and snow conditions significantly affected the traffic flow conditions in the case of the INTEGRATION simulation runs, the weather impacts were not significant for the VISSIM results. Further research is needed with validation through field data.

- Section 5.0 summarizes the conclusions and recommendations from all three studies.

2.0 Impacts of Icy Roadway Conditions on Driver Car-Following Behavior

The objective of this study is to quantify the impacts of icy roadway conditions on driver behavior at a microscopic level, using field-measured car-following data, in addition to the study of the typical variability in driver behavior. Specifically, the study uses two car-following experiment datasets, one gathered under dry roadway conditions and another gathered under icy roadway conditions, in order to calibrate the Van Aerde car-following model and build a database of two sets of driver-specific parameters. The two sets of parameters are statistically compared to quantify changes in driver behavior as a result of icy roadway conditions.

The research presented in this section differs from earlier research, which quantified the weather impacts on macroscopic traffic stream behavior, by analyzing individual driver behavior. Specifically, this study quantifies the impact of icy roadway conditions on five driver-specific parameters namely: free-flow speed, the headway-at-capacity (reciprocal of capacity), the speed-at-capacity, the spacing at jam density (reciprocal of jam density), and the driver perception-reaction time. The research also considers the vehicle acceleration and deceleration constraints considering the roadway surface conditions.

2.1 Data Collection Procedures

Car-following experiments conducted under clean and dry conditions were performed at a test track in Hokkaido, Japan, from October 16, 2000, through October 18, 2000. The track has two straight 1.2-kilometer (km) sections and two 50-meter radius half-circular sections. A total of 10 passenger cars were driven multiple times along the track while the lead vehicle was directed to follow one of the nine different predefined speed patterns: half-, one-, two-, or three-wave; random; or four constant speed patterns. Vehicle position and speed were recorded every deci-second using real-time kinematic (RTK) GPS receivers that were attached to the vehicles. All the drivers were male, and their ages and driving experiences are summarized in Table 2.1.

Table 2.1 Road Surface and Driver Characteristics

Road Surface Condition	Driver ID	Position ID			Age	Driving Experience
		Scenario A	Scenario B	Scenario C		
Dry and Clean	D1	G1 or G10	G1 or G10	–	30	10
	D2	G2	G8	–	21	3
	D3	G3	G7	–	25	3
	D4	G4	G6	–	24	5
	D5	G5	G5	–	25	7
	D6	G6	G4	–	23	3
	D7	G7	G3	–	22	2
	D8	G8	G2	–	24	3
	D9	G9	G9	–	30	10
	D10	G10 or G1	G10 or G1	–	60	40
Icy and Slippery	D1	G1	G1	G1	60	40
	D2	G2	G3	G4	21	2
	D3	G4	G2	G2	21	2
	D4	G3	G4	G3	30	11

For icy and slippery roadway experiments, four passenger cars equipped with GPS receivers were tested at the same facility between December 18 and December 19, 2001. The same speed patterns with a set of lower minimum and maximum speeds (relative to the dry roadway testing experiments) were tested.

Based on the car-following datasets, this study only utilizes the two-, three-wave, and random speed pattern datasets because the calibration of Perception/Reaction Time (PRT) using the one-, half-, or constant- speed pattern datasets sometimes yields unreasonable results, including extremely short or long PRTs. PRT is defined as the total time required for a driver to perceive a need for action and to carry out that action.

2.2 Model Calibration Procedures

The Van Aerde car-following model was calibrated to the Hokkaido data because it provides the highest level of flexibility in matching field data in comparison to other models. Relative reductions in four macroscopic traffic parameters have been calculated in other studies as a function of the rain and snow intensity. These parameters include the traffic stream free-flow speed (u_f), speed-at-capacity (u_c), capacity (q_c), and jam density (k_j). Specifically, the speed-at-capacity can be less than the free-flow speed. Alternatively, the GM-1 model (The GM-1 model is the first car-following model developed by General Motors assumes that the speed-at-capacity equals the free-flow speed. Additionally, vehicle dynamics and collision avoidance models were utilized to ensure more realistic car-following behavior. In other words, the objective function used in the optimization incorporates these three models to estimate an array of realistic vehicle speed and headway estimates of a following vehicle and compares them to the car-following measurements to compute an error measure. Given the objective function, a heuristic

algorithm developed for this study was utilized to search for the optimum set of parameters by minimizing the total sum of squared error between the observed and estimated speed and position trajectories. The detailed calibration procedure is presented in the next section.

Optimization of Car-Following Parameters

A custom-built bi-level optimization algorithm was developed and used to calibrate the model parameters. The first level involved the calibration of the driver perception-reaction times. Given the driver and speed pattern-specific PRTs, the second optimization level involved the calibration of the remaining car-following parameters. Specifically, the distance headway of the following vehicle was offset by the driver PRT because the vehicle speed at instance *t* depends on the distance headway *T* seconds earlier (the PRT).

Driver's perception-reaction time often changes during a trip depending on the driving and the surrounding environment. However, it is reasonable to assume that the PRT remains constant if the trip is relatively short. Consequently, the optimum lag time was computed for each trip by minimizing the difference in speed between the lead and the following vehicle profiles, as illustrated in Figure 2.1. Figure 2.1(a) illustrates the speeds of the lead and following vehicles over time when the lead vehicle was directed to follow the three-wave speed pattern. The figure demonstrates that the speed of the following vehicle is offset by a temporal duration. The circle highlights the area which is shown in more detail in Figures 2.1(b) and 2.1(c). As can be seen in Figures 2.1(b) and2.1(c), the speed of the following vehicle fits well with that of the lead vehicle when it is offset by 1.7 seconds.

Figure 2.1 Illustration of PRT Calibration

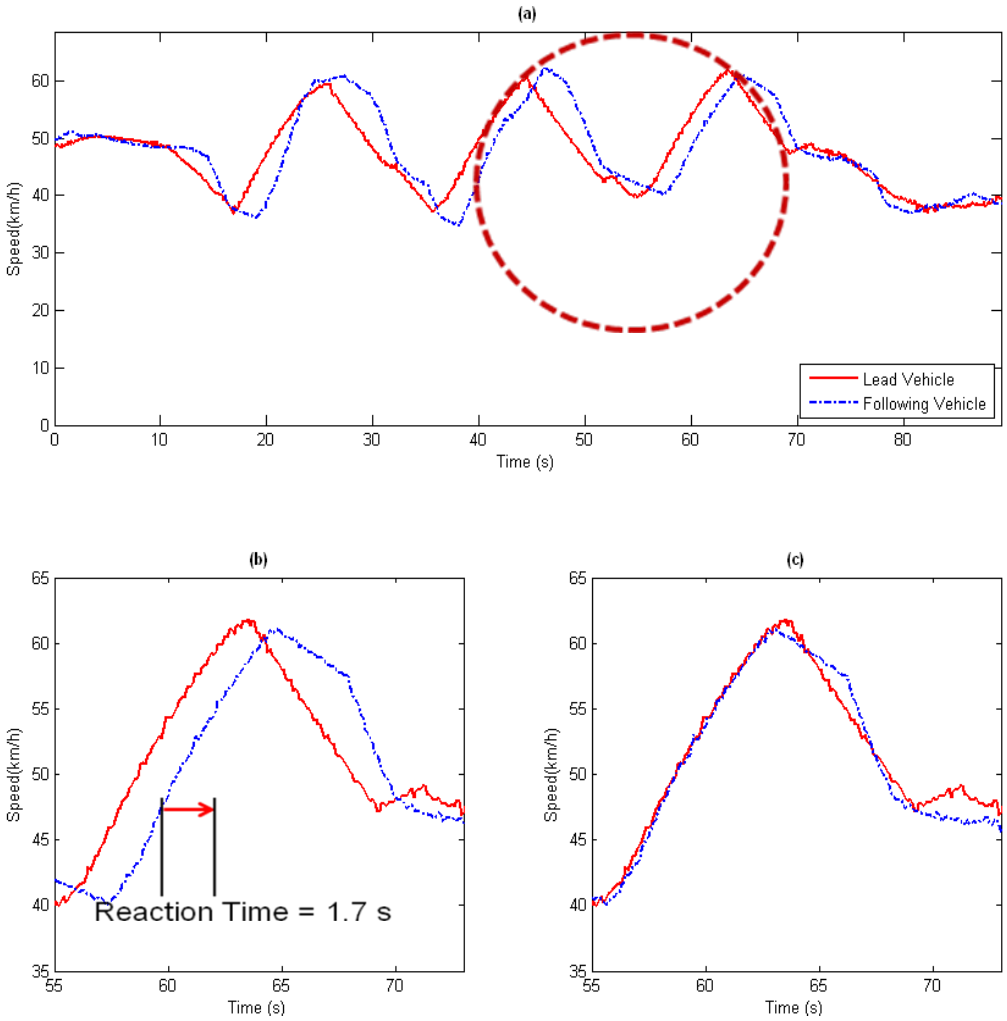

As previously mentioned, the second level offsets the distance headway by the driver PRT and then calibrates the four car-following parameters.

For the optimization, a simple and efficient algorithm was developed and used. The algorithm started by generating a set of car-following parameters and evaluating these parameters. The optimization algorithm consists of multiple iterations. In each iteration, the algorithm generates a set of car-following parameters ranging from a lower bound to an upper bound at predefined step sizes. Specifically, a relatively wider search range is defined for each of the parameters. The parameters are then varied using a large step size in the first iteration. Once the optimal parameters have been found in the first iteration, new lower and upper boundaries for the second iteration are generated centered on the optimal parameter set. These boundaries are reduced in size. Subsequently, new parameter sets are generated by varying the parameter values within the new range using a smaller step size. These procedures are repeated until the predefined number of iterations is reached or the change of the objective function is within a user-defined range. In summary, the four car-following parameter ranges and the step sizes are reduced as the iteration number increases as illustrated in Figure 2.2.

Figure 2.2 Example Illustration of Bi-Level Heuristic Algorithm

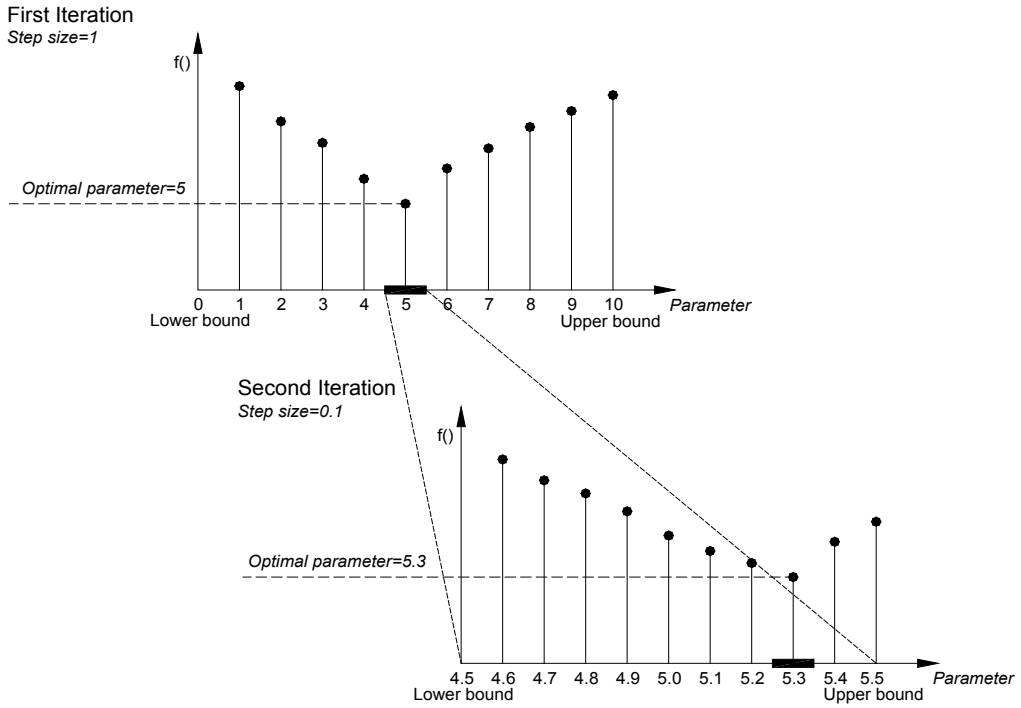

For the enhancement of optimization speed, two sets of boundary conditions were prepared as shown in Table 2.2. Specifically, a smaller size of parameters was initially optimized to derive reasonable boundary conditions. However, the boundary condition of k_j was calculated from the average test vehicle length and vehicle spacing when completely stopped. Given the boundary conditions, the car-following parameters were optimized; sample optimization results are illustrated in Figure 2.3. In this scenario, the observed and estimated distance headways and speeds of the second vehicle in the platoon are plotted over a three-wave car-following test under dry roadway conditions.

Table 2.2 Boundary Conditions

Classification	Dry		Icy	
	Lower Bound	Upper Bound	Lower Bound	Upper Bound
q_c	1,700	2,700	800	2,000
k_j	180	195	180	195
u_c	30	60	15	50
u_f	60	120	30	100

Figure 2.3 Sample Optimized Speed and Headway Profile

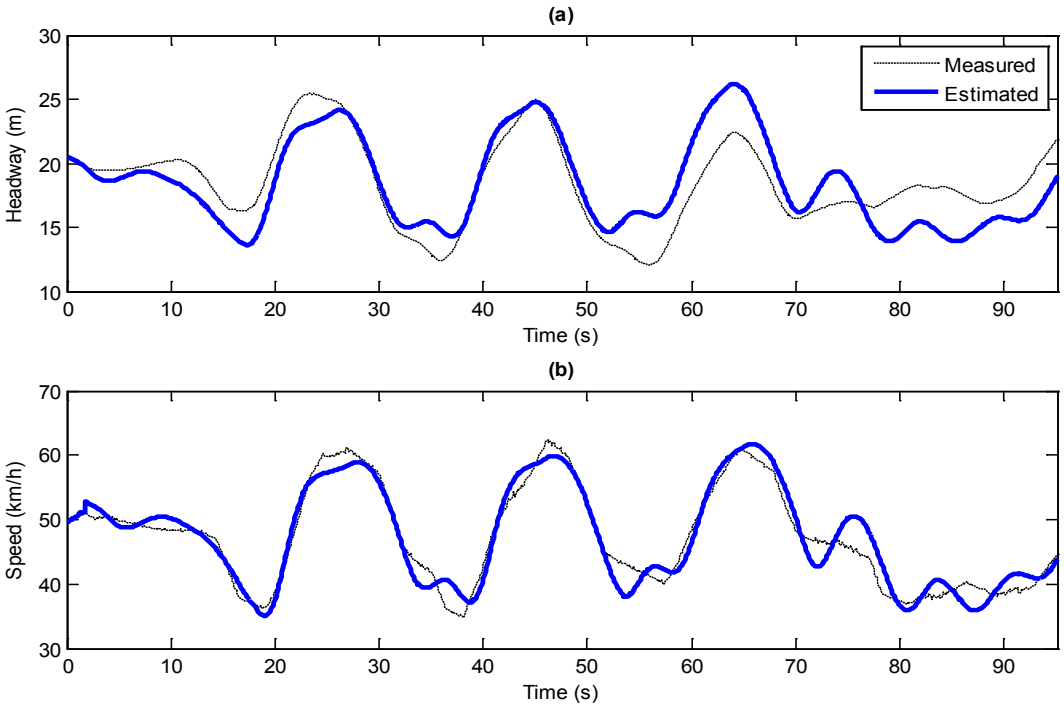

2.3 Calibration Results

Once the model was calibrated, differences between dry and icy roadway car-following parameters were quantified. Effectively, statistical tests were conducted to identify any significant differences. One-way ANOVA and Kruskal-Wallis tests were utilized to assess any significant impacts of roadway surface conditions or driver behavior. The Kruskal-Wallis test was implemented because the distribution for some calibrated parameters violated the normality assumption that is required to conduct ANOVA tests.

Behavior on Dry Roadway Conditions

This section analyzes how driver car-following behavior on a dry roadway surface is affected by factors other than the roadway conditions. In fact, differences across drivers and the impact of driving experience were studied using one-way ANOVA and Kruskal-Wallis tests. Driver age and gender were not studied because all the drivers were male, and most of them were in their early 20s. The differences in all parameters across the various drivers or driving experiences were statistically significant at the 5 percent significance level. However, the p-values of the tests on the capacity q_c and PRT parameters are noticeably smaller than those of other parameters. Consequently, realistic modeling of car-following behavior would require that one accounts for differences in driver behavior. In other words, individual driver differences in car-following parameters should be taken into account in the modeling of car-following behavior because these differences were found to be significant.

Behavior on Icy Roadway Conditions

The effects of driver and the platoon position under icy roadway conditions were also tested using one-way ANOVA and Kruskal-Wallis tests. While more insight into the effects could be provided if a two-way ANOVA test was used to analyze the interaction between the two variables, the structure of the experiments did not allow this type of test because each driver was tested in only two of three positions in the platoon. The effects of the driver are only significant on the capacity q_c, the free-flow speed u_f, and PRT parameters based on the Kruskal-Wallis tests. Such result may be attributed to the fact that the effects of icy roadway conditions are more significant than those of other factors when compared to the results of dry roadway conditions. The effects of position are only significant on the jam density k_j and PRT parameters based on the Kruskal-Wallis tests.

Effect of Roadway Conditions: Dry versus Icy

The effects of roadway conditions on the car-following behavior are significant as illustrated in Figure 2.4. Icy roadway conditions negatively affect q_c, u_c, and u_f. However, it is not clear from the histograms whether k_j and PRT were affected by the icy conditions. In order to study the effects in a quantitative manner, one-way ANOVA tests were conducted to ascertain if the means of the two groups of calibrated parameters were the same. Since one of the assumptions of ANOVA is that data are normally distributed, the normality of each of the parameter sets was tested using normal Quantile-Quantile (Q-Q) plots. As can be seen in Figure 2.5, the normality of the data was not completely satisfied. Consequently, the analysis was also conducted using the Kruskal-Wallis test – which is a nonparametric statistical method that tests equality of the medians of different groups – in order to provide more confidence in the study findings.

As expected from the parameter distributions, the results of the one-way ANOVA tests demonstrate that all of the mean parameters for dry roadway experiments are not equal to those for icy roadway experiments, excluding the kj parameters at the 5 percent significance level. Furthermore, the Kruskal-Wallis tests show similar results, although the p-values are different when compared to the one-way ANOVA test results. Since kj does not significantly depend on the roadway surface condition but rather on the length of vehicles with some variations in vehicle spacing when completely stopped, the fact that there are no differences in the kj parameters is reasonable. The descriptive statistics of the calibrated results, including minimum, maximum, quantiles, median, and mean measures are provided in Table 2.3. When comparing the mean values of the parameters, the mean, uf, uc, and qc parameters for the icy roadway experiments are 28 percent, 13 percent, and 46 percent less than those for the dry roadway experiments, respectively. However, the mean PRT for the icy roadway experiments is 13 percent greater than that for the dry experiments.

Figure 2.4 Histograms of the Calibrated Parameters and PRT

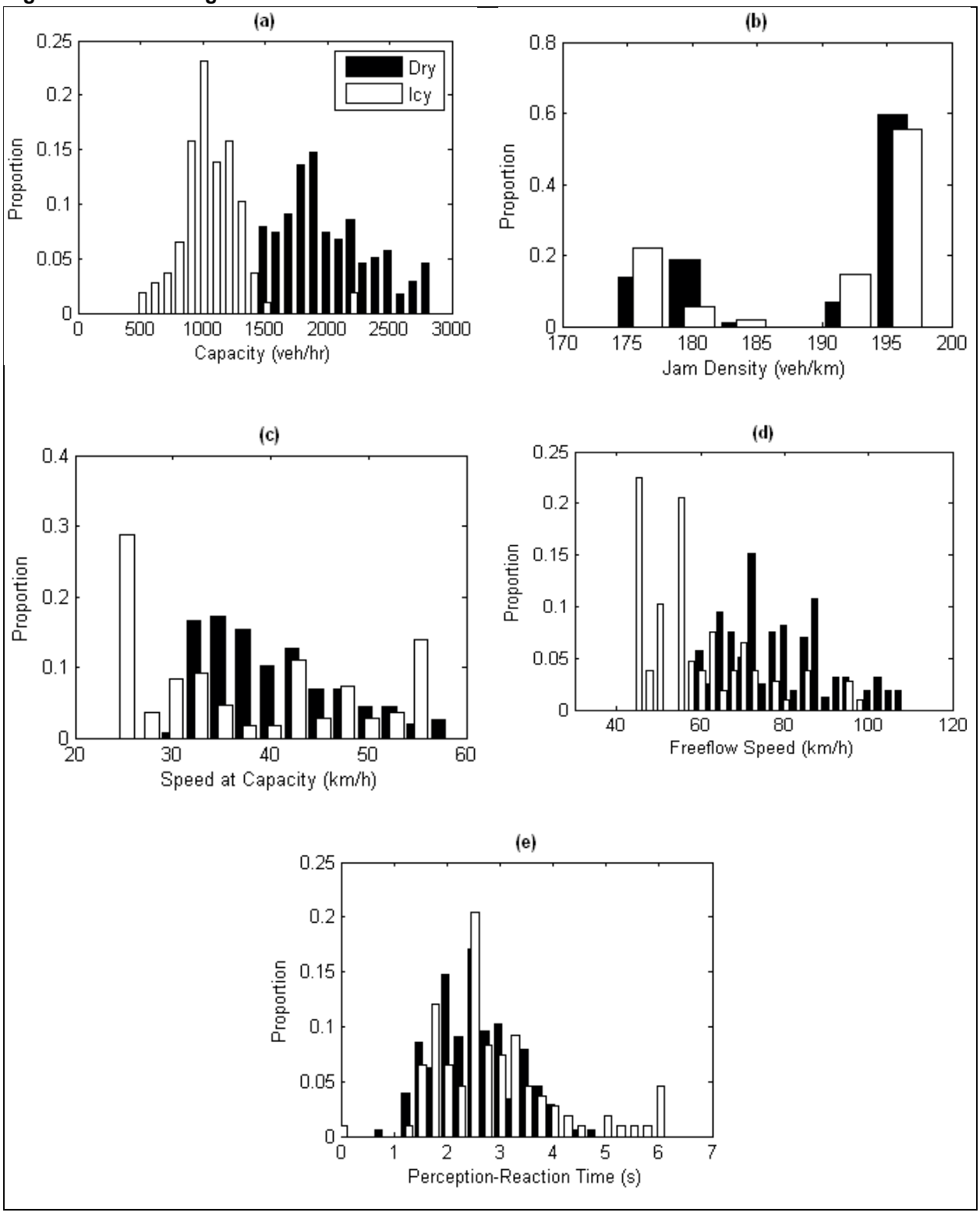

Figure 2.5 Normal Q-Q Plots

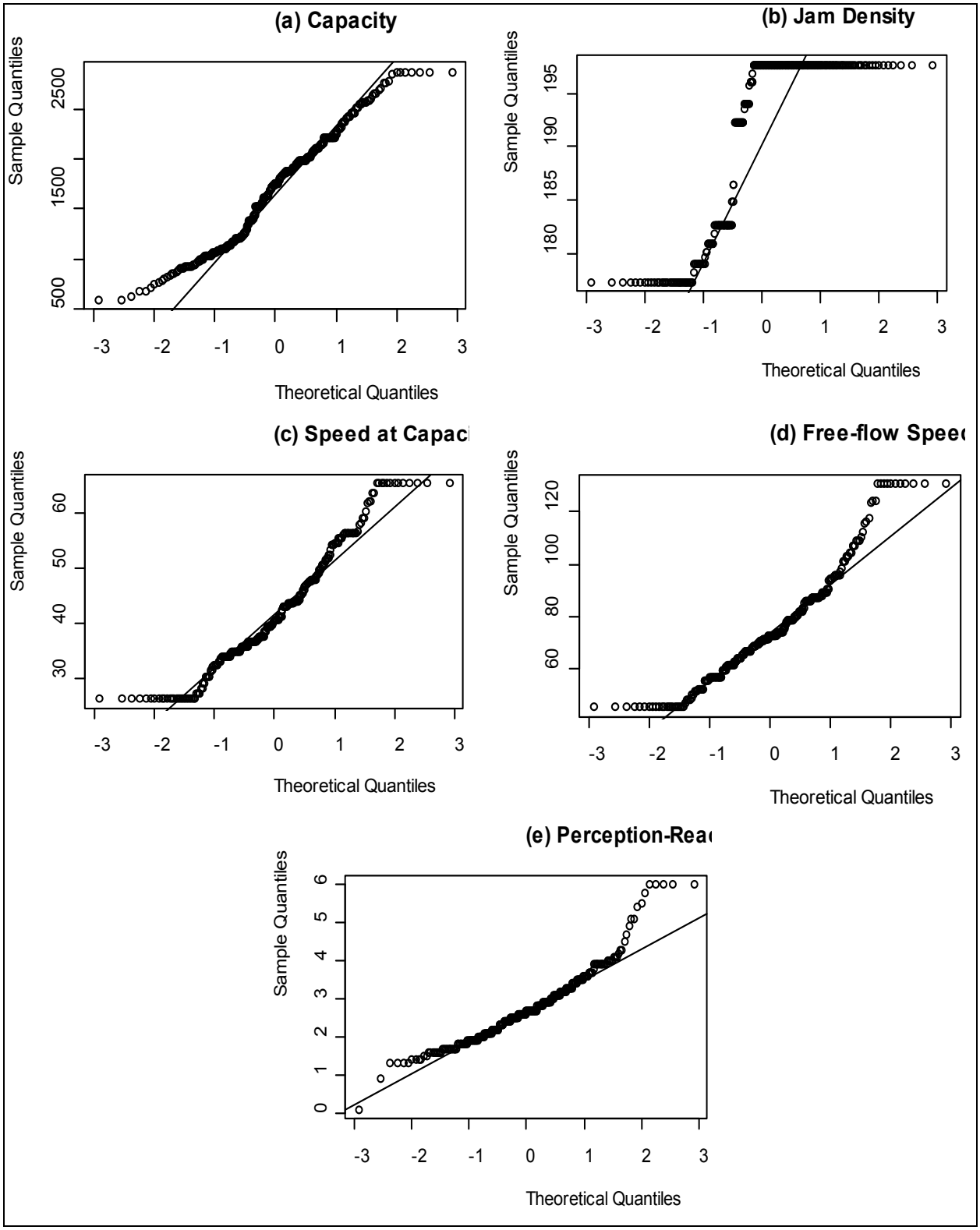

Table 2.3 Descriptive Statistics of the Calibration Results

Classification		u_f (km/h)	u_c (km/h)	q_c (veh/h)	k_j (veh/km)	PRT (s)
Dry Surface	Min	61	32	1,519	177	0.9
	1st Quantile	71	37	1,803	183	2.1
	Median	80	41	1,992	198	2.6
	Mean	84	44	2,064	192	2.6
	3rd Quantile	90	49	2,257	198	3.1
	Max	131	65	2,881	198	4.9
Icy Surface	Min	45	26	583.3	177	0.1
	1st Quantile	49	27	953.7	183	2.2
	Median	57	35	1,090.7	198	2.7
	Mean	60	38	1,106.3	191	3.0
	3rd Quantile	69	48	1,224.1	198	3.4
	Max	113	56	2,216.7	198	6.0

Impacts of Roadway Surface Conditions on the Speed-Flow-Density Relationship

This section analyzes the impacts of icy roadway conditions on the steady-state speed-flow-density relationship, while the earlier section presented the relative differences in the mean parameters. To generate the speed-flow-density diagrams, the median parameters were used. Specifically, the u_f, u_c, q_c, and k_j of 80 km/h, 41 km/h, 1,992 veh/h, and 198 veh/km were used to create the diagrams for dry roadway conditions. The u_f, u_c, q_c, and k_j of 57 km/h, 35 km/h, 1,091 veh/h, and 198 veh/km were used to create those for icy roadway conditions. The effects of icy roadway conditions on the speed-flow-density relationship are fairly significant, as illustrated in Figure 2.6. The thick and thin lines represent the dry and icy roadway cases, and the dots on the lines in subplots (b) through (d) represent the four parameters. The significant differences between the dry and icy roadway cases are clearly shown in each of the three planes. Subplots (e) and (f) show the differences in flow rates and speeds between the dry and icy roadway cases as a function of density. Thus the two plots show the differences at the same density levels. The maximum flow difference is 994 veh/h/lane, which happens at a density of 58 veh/km/lane, as can be seen in subplot (e). The maximum speed difference is 23 km/h, which happens at the density of 33 veh/km/lane, as seen in subplot (f). The valley observed at low densities in subplot (f) is due to icy and dry speed-density curves not being parallel to each other as can be seen in subplot (d). Specifically, the icy speed-density line decreases at a higher rate as a function of speed when compared to the dry speed-density line in the density range of approximately 25 to 50 veh/km.

Figure 2.6 Speed-Flow-Density Diagrams and Differences in Flow and Speed

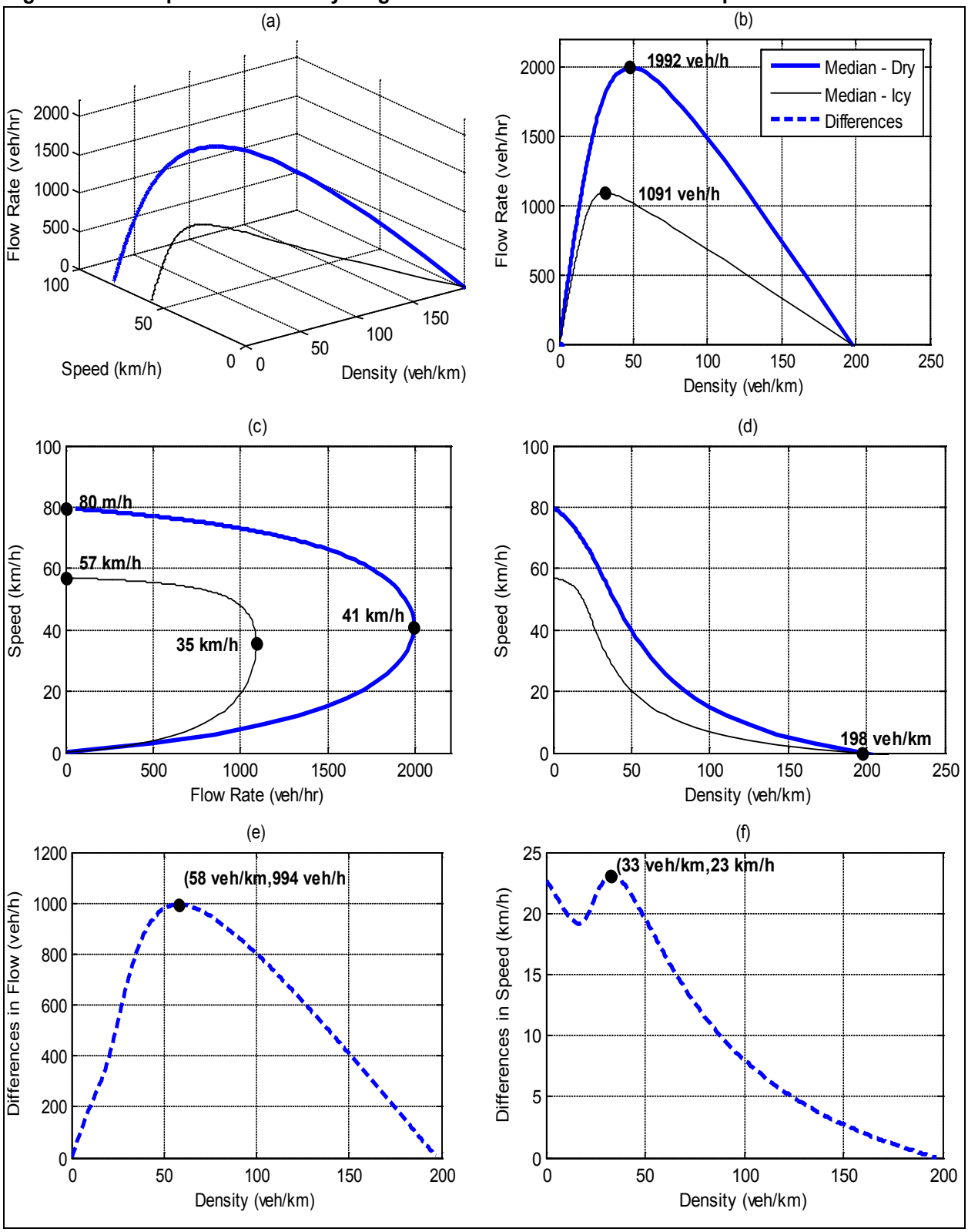

Driver Parameter Distributions

The two sets of parameters were fitted to parametric distributions to determine a suitable distribution for modeling the impacts of icy roadway conditions. Therefore, the beta, gamma, lognormal, and GEV (Generalized Extreme Value) distributions were considered since these distributions provide a high level of flexibility in capturing different shapes than other frequently used distributions such as the normal and exponential distributions. In order to calibrate the parameters of the beta distribution, the data were normalized to range between 0.0 and 1.0 since the beta distribution is defined on that interval. Figures 2.7 and 2.8 show the empirical probability density functions of the five parameters for dry and icy roadway conditions in addition to the fitted distributions. From the visual inspection of the plots, the GEV distribution is likely to be most suitable for modeling differences in driver behavior. Additionally, the goodness-of-fit for each model was computed using the Kolmogorov-Smirnov test, as shown in Table 2.4. The bold figures represent the most suitable distributions (minimum values), while the figures in parentheses represent the rank. Based on the test results, the GEV, beta, and lognormal distributions are suitable for modeling specific parameters since they had the minimum values. However, the GEV distribution presents relatively good test statistics when compared to other distributions. The fitted GEV parameters are shown in Table 2.5.

Figure 2.7 Distribution Fitting for Dry Roadway Conditions

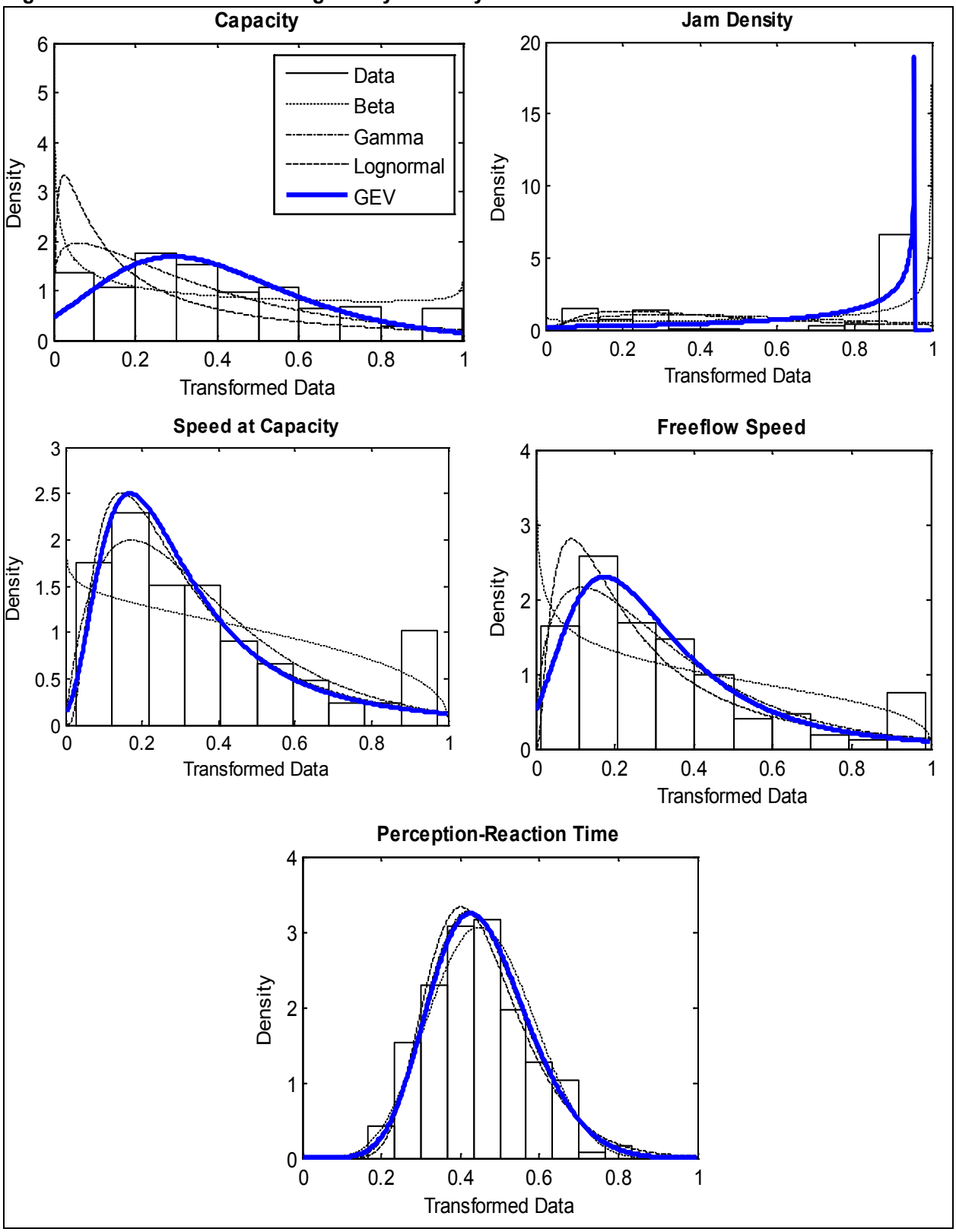

Figure 2.8 Distribution Fitting for Icy Roadway Conditions

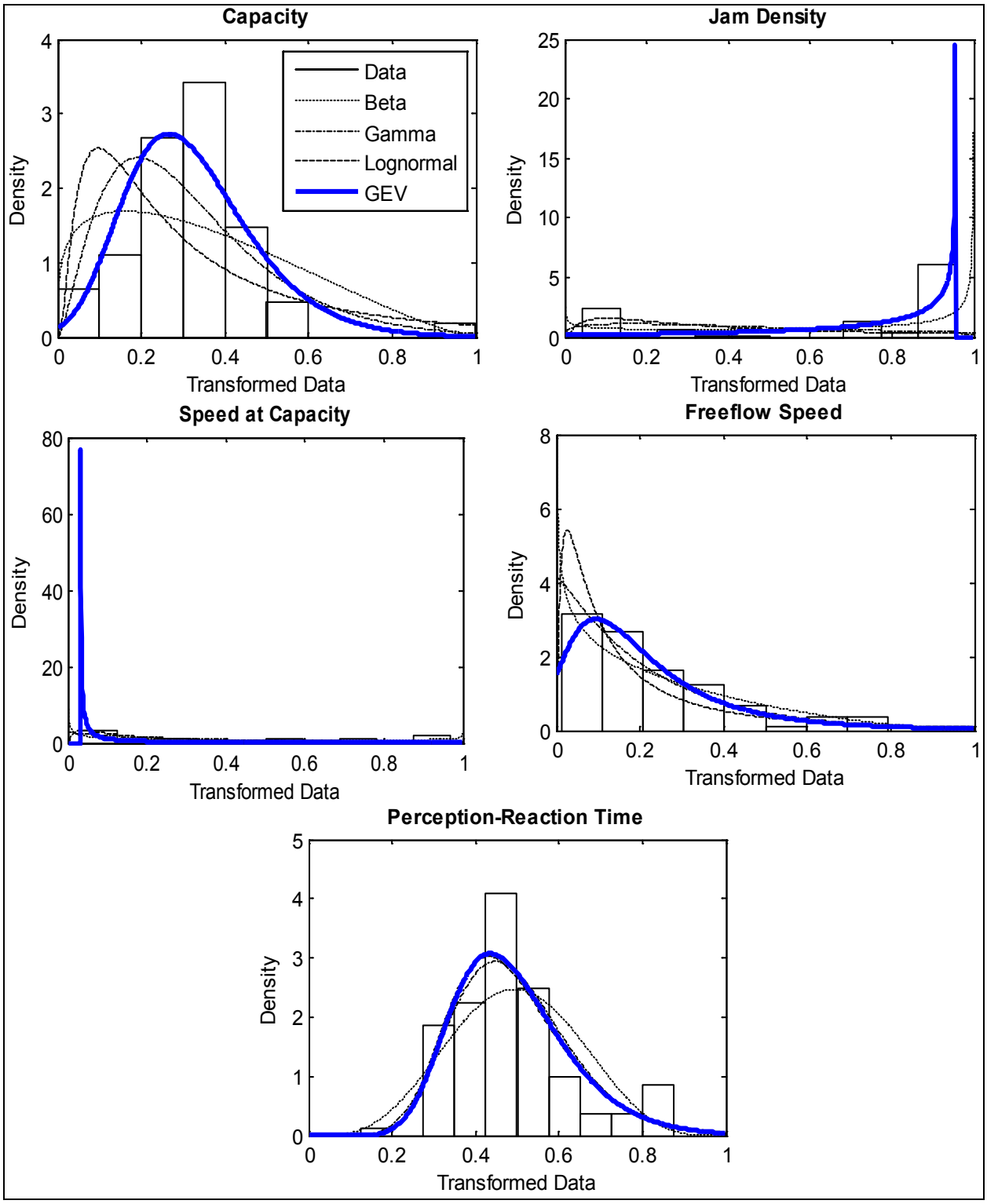

Table 2.4 Kolmogorov-Smirnov Test Results

Classification		GEV	Gamma	Beta	Lognormal
Dry	q_c	0.0447 (1)	0.1489 (3)	0.1309 (2)	0.2183 (4)
	k_j	0.5739 (4)	0.3380 (2)	0.3583 (3)	0.3190 (1)
	u_c	0.0702 (2)	0.0879 (3)	0.1515 (4)	0.0630 (1)
	u_f	0.0583 (2)	0.0557 (1)	0.1720 (4)	0.1058 (3)
	PRT	0.0435 (1)	0.0514 (2)	0.0622 (3)	0.0676 (4)
Icy	q_c	0.0866 (1)	0.1637 (2)	0.1971 (3)	0.2435 (4)
	k_j	0.5278 (4)	0.3454 (2)	0.3183 (1)	0.3605 (3)
	u_c	0.3156 (4)	0.1664 (2)	0.1375 (1)	0.1803 (3)
	u_f	0.1329 (2)	0.1449 (3)	0.1250 (1)	0.2038 (4)
	PRT	0.0774 (2)	0.0886 (3)	0.1486 (4)	0.0769 (1)

Table 2.5 Fitted GEV Parameters

	Dry Roadway Condition			Icy Roadway Condition		
Classification	**K**	**Sigma**	**Mu**	**K**	**Sigma**	**Mu**
q_c	-0.0494	0.2187	0.2823	-0.0785	0.1351	0.2556
k_j	-1.4969	0.5082	0.6159	-1.5967	0.5075	0.6375
u_c	0.3550	0.1557	0.2142	4.3269	0.0581	0.0446
u_f	0.2035	0.1632	0.2042	0.2464	0.1257	0.1233
PRT	-0.1714	0.1152	0.4047	-0.0674	0.1200	0.4288

Modeling Differences in Driver Behavior

Since there might be correlations between the calibrated parameters, it is reasonable to identify relationships between the parameters and develop regression models that capture these interactions. Consequently, the developed models can be used to model the impacts of icy roadway conditions together with the distributions fitted in the previous section. In order to analyze the correlation between the parameters, scatter plots together with regression lines were generated. In the plots, the circles and triangles represent the parameters for dry and icy experiments, respectively. As can be seen in Figure 2.9, there is a positive correlation between the u_f and u_c parameters.

Figure 2.9 Scatter Plots and Regression Lines for Different Combinations of Variables (uf, uc, qc, and PRT)

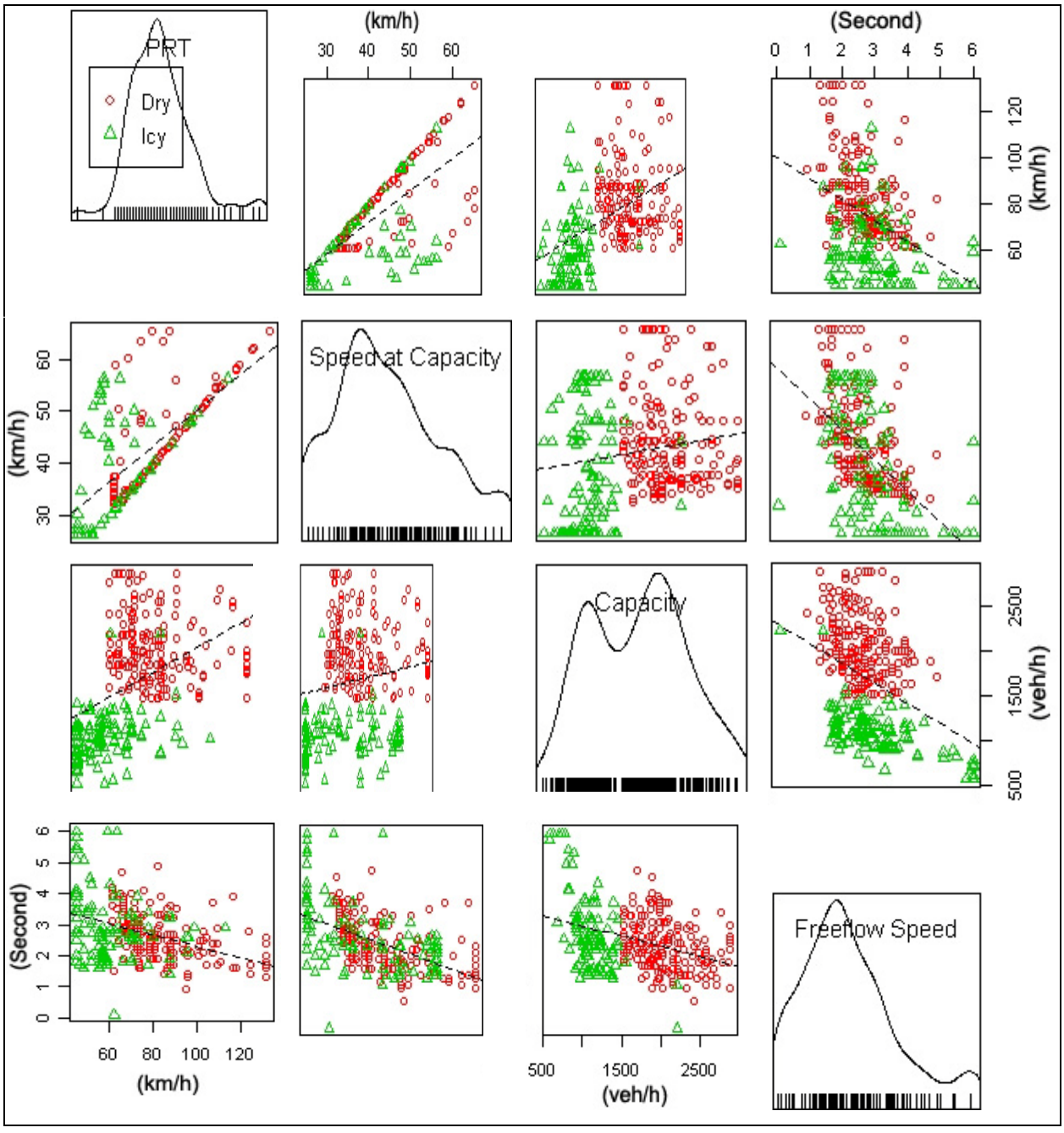

However, a relationship could not be established with the parameters. Thus, three linear regression models were developed using the following regression structure.

$$Y = \beta_0 + \beta_1 X_1 + \beta_2 X_2 + \varepsilon \quad (1)$$

Where *Y (*q_c, u_c, *or* PRT*)* is the dependent (response) variable, X_1 (u_f) and X_2 (roadway condition) are the independent variables, β_0, β_1, and β_2 are the model coefficients, and ε is the error term. Specifically, u_f and roadway condition (Dry = 0 and Icy = 1) were used as independent variables to develop the linear regression model of the u_c, q_c, and PRT parameters. From the regression model summary (Table 2.6), it appears that q_c is not related to u_f and thus can be modeled as an independent random variable with different coefficients to reflect icy and dry roadway conditions. For the PRT model, the adjusted R^2 of the regression model is very small and thus the parameter can be modeled as an independent random variable. Alternatively, since the u_c model has a relatively high adjusted R^2 (0.505) when compared to the other models while all the coefficients are significant, the regression model can be used to model the correlation between the speed-at-capacity and free-flow speed. Consequently, the modeling of differences in driver behavior is achieved by generating five uniformly distributed random numbers (X~U(0,1)). These uniformly distributed random variables generate realizations of u_f, q_c, k_j, and PRT that are GEV distributed. Alternatively, the mean u_c is computed using the regression parameters specified in Table 2.6. A normally distributed error term N~(0,σ_ε) is introduced to the speed-at-capacity to capture the driver variability about the average behavior.

Table 2.6 Summary of the Regression Models

	Model		Coefficients				
Classification	Adjusted R^2	P-Value	Coefficient	Estimate	Std. Error	T-value	P-Value
q_c	0.674	<2.2e-16	β_0	2,155.202	99.345	21.69	<2e-16
			β_1	-1.083	1.144	-0.95	0.344
			β_2	-983.615	48.125	-20.44	<2e-16
u_c	0.505	<2.2e-16	β_0	9.307	2.258	4.12	4.94e-05
			β_1	0.412	0.026	15.86	<2e-16
			β_2	4.231	1.094	3.87	0.000136
PRT	0.168	<2.073e-12	β_0	4.394	0.262	16.81	<2e-16
			β_1	-0.021	0.003	-6.97	2.29e-11
			β_2	-0.160	0.127	-1.26	0.207

2.4 Conclusions

The research presented in this chapter quantified the impacts of icy roadway conditions on driver car-following behavior. The data used in the study were gathered in Japan in a controlled environment under dry and icy roadway conditions. The collected data were used to calibrate the Van Aerde car-following model subject to vehicle acceleration and deceleration constraints. Using the calibrated car-following parameters, the effects of icy roadway conditions on the driver capacity (q_c), speed-at-capacity (u_c), free-flow speed (u_f), jam density (k_j), and the driver perception-reaction time (PRT) were compared using one-way ANOVA and Kruskal-Wallis tests.

The impact of icy roadway conditions on the roadway free-flow speed, speed-at-capacity, capacity, and PRT were found to be significant. Specifically, icy roadway conditions reduced the mean free-flow speed, speed-at-capacity, and capacity by 28 percent, 13 percent, and 46 percent, respectively, compared to dry roadway driving. The mean PRT for icy conditions was found to take 13 percent longer than driving under dry conditions. The longer PRTs could be attributed to the fact that the drivers drove at lower speeds and larger spacing compared to driving under dry conditions. The calibrated parameters were modeled using beta, gamma, lognormal, and generalized extreme value (GEV) distributions. The study demonstrated that the GEV distribution is most suited for modeling differences in driver behavior.

Additionally, the study demonstrated that the impacts of icy roadway conditions on the steady-state speed-flow-density relationship are significant. When comparing the flow rates and speeds at the same density levels, the maximum flow difference is 994 veh/h/lane, which happens at the density of 58 veh/km/lane. The maximum speed difference is 23 km/h, which happens at the density of 33 veh/km/lane.

The findings from this study have implications for weather responsive traffic management strategies because they can be used to calibrate microscopic simulation models in order to quantify the impact of icy conditions on transportation system performance.

3.0 Inclement Weather Impacts on Driver Left-Turn Gap Acceptance Behavior

3.1 Introduction

Several studies have quantified the effect of inclement weather on macroscopic traffic stream behavior, including its impact on the roadway capacity and speed. However, it is hard to find studies that characterize individual driver behavior under adverse weather conditions and that analyze the variability in driver behavior. One of the factors that affect the capacity and saturation flow rate at signalized and nonsignalized intersections is gap acceptance behavior. Gap acceptance is defined as the process that occurs when a traffic stream (known as the opposed flow) has to either cross or merge with another traffic stream (known as the opposing flow). This section focuses on crossing gap acceptance behavior for permissive left turns.

Within the context of crossing gap acceptance, a gap is defined as the elapsed-time interval between arrivals of successive vehicles in the opposing flow at a specified reference point in the intersection area. The minimum gap that a driver is willing to accept is generally called the critical gap. The Highway Capacity Manual (HCM) (2000) [13] defines the critical gap as the "minimum-time interval between the front bumpers of two successive vehicles in the major traffic stream that will allow the entry of one minor-street vehicle." When more than one opposed vehicle uses a gap, the time headway between the two opposed vehicles is called the follow-up time.

3.2 Literature Search

Attempts have been made in the literature to quantify the impact of various parameters on gap acceptance. However, none of the previous research efforts quantified the impact of adverse weather on gap acceptance behavior; except for a few studies that are described in the following section. Weather events are considered one of the factors that influence traffic regime by affecting roadway surface conditions, vehicle performance and driver behavior, which consequently reduce capacity.
The basic differences in the various studies of gap acceptance behavior were the underlying assumptions about driver behavior (consistent or inconsistent), the type of the developed gap acceptance model (deterministic versus probabilistic) and the independent variables used in the model.

The main objective of this study is to investigate the influence of weather precipitation (rain or snow) and roadway surface condition (icy, snowy, or wet) on left-turn gap-acceptance behavior. The weather condition in the study is divided into six categories for the different combinations of weather precipitation "rain and snow" and roadway surface condition "wet, icy, and snowy." Logit models are fit to the data to model driver gap acceptance behavior and compute driver-specific critical gap sizes.

The remainder of this report includes:

- The results of a literature search summarizing previous research efforts;
- A presentation of the study site and data acquisition procedures;
- A description of the data analysis process;
- A summary of preliminary results, including
    - A description of the different proposed models; and
    - Model calibration results, including the predicted critical gap and analysis of the impact of various factors on opposed saturation flow rates.
- Study conclusions; and
- Recommendations for further research.

Adverse weather conditions negatively affect surface transportation and accordingly impact roadway operating conditions, safety, and mobility. The adverse weather could be mainly precipitation (rain or snow), surface condition (wet, icy, or snowy), strong winds, fog or storms. Most of the literature on the effect of weather have focused on collision risk, traffic volume variations, signal control, travel pattern and traffic flow parameters, where some of them are presented in the Table 3.1. Studies 2 and 3 estimated the impact of adverse weather on traffic volumes while Studies 4 through 6 addressed how adverse weather impacts traffic flow variables, including speed, flow, density, headway, and capacity. Studies 7 through 15 all attempted to characterize driver on gap acceptance behavior and only studies 14 and 15 characterized the impact of inclement weather on driver gap acceptance behavior. These two studies, however, dealt only with rain.

Table 3.1 Summary of Literature Review

No.	Author/Source	Title	Comments
[13]	TRB, Transportation Research Board, 2000	''HCM:Highway Capacity Manual, 2000''	Used as source to define study variables.
[14]	S. Datla and S. Sharma, in Transportation Research Board TRB, 2010	''Association of Highway Traffic Volumes with Cold, Snow and Their Interactions''	Characterized highway traffic volume variations with severity of cold, amount of snowfall, and various combinations of cold and snowfall intensities.
[15]	M. Cools, E. Moons, and G. Wets, in Transportation Research Board TRB, 2008	''Assessing the Impact of Weather on Traffic Intensity''	Quantified the impact of weather conditions on traffic intensity and volume variations. The study considered: the daily precipitation, hail, snow and thunderstorm, cloudiness, temperature, wind speed, sunshine, and duration of diminished visibility due to fog.
[16]	W. Brilon and M. Ponzlet, Transp. Res. Rec., National Research Council, Washington, D.C., pages 91-98, 1996	''Variability of Speed-Flow Relationships on German Autobahns''	Investigated the impact of various weather conditions on capacity and on other traffic flow parameters on the Autobahn in Germany.
[17]	H. Rakha, M. Farzaneh, M. Arafah, and E. Sterzin, Transportation Research Board TRB, 2008	''Inclement Weather Impacts on Freeway Traffic Stream Behavior''	Earlier research conducted as part of this program. Quantified the impact of inclement weather (precipitation and visibility) on traffic stream behavior and key traffic stream parameters, including free-flow speed, speed-at-capacity, capacity, and jam density.
[18]	J. Daniel, J. Byun, and S. Chien, Transportation Research Board TRB, 2007	''Impact of Adverse Weather on Freeway Speeds and Flows''	Collected speed, flow, and density data under no adverse weather, as well as under rain, snow, darkness, and sun glare conditions.
[19]	N.G. Tsongos, Public Road, 35(7), pages 157-165, 1969	''Comparison of day and night gap-acceptance probabilities''	Quantified the impact of inclement weather on gap acceptance behavior, including day and nighttime effects.
[20]	K.C. Sinha, and Tomiak, W.W., Traffic Engrg. and control, 41(7), pages 28-33, 1971	''Gap acceptance phenomenon at stop controlled intersections''	Quantified the impact of inclement weather on gap acceptance behavior, including the speed of the opposing vehicle.
[21]	W. Brilon, Proc., Int. Workshop on Intersections without Traffic Signals, Bochum, Federal Republic of Germany, pages 111-153, 1988	''Recent developments in calculation methods for unsignalized intersections in West Germany, intersections without traffic signals''	Did not quantify the impact of inclement weather on gap acceptance behavior for unsignalized intersections.
[22]	A.W. Polus, Traffic Engrg. and control, 24(5), pages 255-258, 1983	''Gap acceptance characteristics at unsignalized urban intersections''	Did not quantify the impact of inclement weather on gap acceptance behavior for unsignalized intersections.

No.	Author/Source	Title	Comments
[23]	X. Yan, and Radwan, E., Journal of Transportation Engineering ASCE, Volume 134, February 2008	‘‘Influence of Restricted Sight Distances on Permitted Left-Turn Operation at Signalized Intersections’’	Did not quantify the impact of inclement weather on gap acceptance behavior. The variables that were considered included the driver sight distance.
[24]	M.M. Hamed and S. Easa, Journal of Transportation Engineering, Volume 123, February 1997	‘‘Disaggregate Gap-Acceptance Model for Unsignalized T-Intersections’’	Did not quantify the impact of inclement weather on gap acceptance behavior. Did consider the geometry of the intersection, the trip purpose, and the expected waiting time.
[25]	J.K. Caird and P.A. Hancock, R.E. Dewar and P. Olson, Eds.: Lawyers & Judges Publishing: Tucson, Arizona, 2002, pages 613-652	‘‘Left-Turn and Gap Acceptance Crashes,’’ in *Human factors in traffic safety*	Did not quantify the impact of inclement weather on gap acceptance behavior. Factors considered include gap acceptance crash patterns at intersections.
[26]	I. Zohdy, S. Sadek, and H. Rakha, Transportation Research Board TRB, 2010	‘‘Empirical Analysis of Wait Time and Rain Intensity Effects on Driver Left-Turn Gap Acceptance Behavior’’	Earlier research conducted as part of this project quantified the impact of rain intensity, waiting time, and travel time on driver left turn gap acceptance behavior using empirical and stochastic modeling approaches.
[27]	H. Rakha, S. Sadek, and I. Zohdy, in Transportation Research Board TRB, 2010	‘‘Modeling Stochastic Left-Turn Gap Acceptance Behavior’’	Earlier research conducted as part of this project quantified the impact of rain intensity, waiting time, and travel time on driver left turn gap acceptance behavior using empirical and stochastic modeling approaches.

3.3 Site and Equipment Description

The site analyzed in this study was the signalized intersection of Depot Street and North Franklin Street (Business Route 460) in Christiansburg, Virginia. A location map of the intersection is shown in Figure 3.1. A detailed schematic of the intersection is shown in Figure 3.2a. It consists of four approaches at approximately 90° angles. The posted speed limit for the eastbound and northbound approaches was 35 mph and for the westbound and southbound approaches was 25 mph at the time of the study.

Figure 3.1 Intersection of Depot Street and North Franklin Street (Business Route 460)

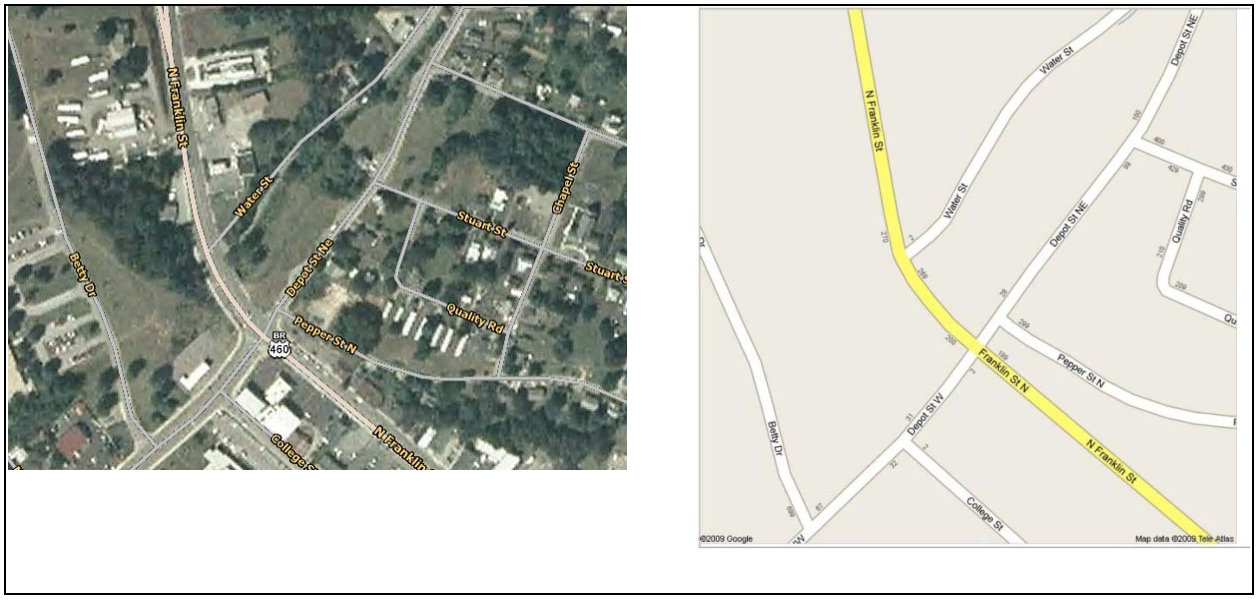

The signal phasing of the intersection included three phases, two phases for the Depot street North and South (one phase for each approach) and one phase for Route 460 (two approaches discharging during the same phase) with a permissive left turn movement. Figure 3.2a illustrates the movement of vehicles during the green phase of Route 460 and the dashed lines show the left turn vehicle trajectory where drivers are facing a gap acceptance/rejection situation. The dashed line is opposed by the through movements at three conflict points P1, P2, and P3, respectively. Each conflict point presents the location of possible collision with the through movement and reflect the locations of the offered gaps. The data acquisition hardware of the study site consisted of two components as follows:

1. Video cameras to collect the visual scene (Figure 3.2b). There were four cameras installed at the intersection (one camera for each approach) to provide video feed of the entire intersection environment at 10 frames per second.

2. Weather station (Figure 3.2c). The weather station provided weather information every minute. The collected weather data included precipitation, wind direction, wind speed, temperature, barometric pressure, and humidity level.

Figure 3.2 The Study Intersection and the Installed Data Acquisition Equipment

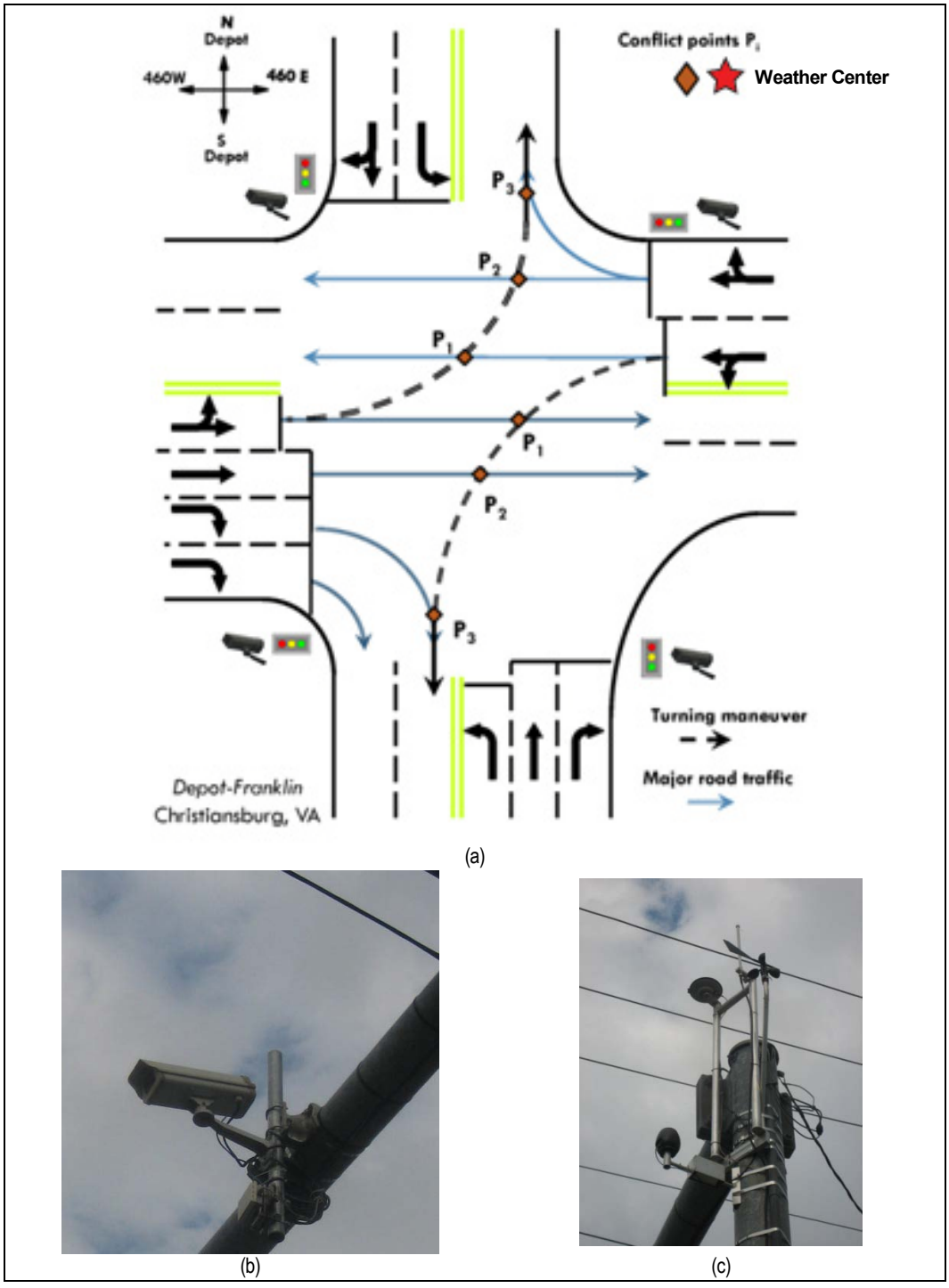

3.4 Data Analysis Procedures

Data were collected at the Franklin/Depot Street intersection over a six-month period from the beginning of December 2009 till the end of May 2010. The data output per each day consists of 15 hourly video files and the corresponding weather measurements. The video data were reduced manually by recording the time instant at which a subject vehicle initiated its search to make a left turn maneuver, the time step at which the vehicle made its first move to execute its left turn maneuver, and the time the left turning vehicle reached each of the conflict points. In addition, the time stamps were also recorded when each of the opposing vehicles passed the conflict points.

Gap Analysis Data

Each rejected or accepted gap for a left turn vehicle was recorded as an observation in the reduced dataset and the corresponding variables for each observation were also recorded. More than 5,000 observations of gaps were excluded because they were ended by a red signal indication. In other words, no gap was offered between a turning vehicle and an opposing vehicle due to the ending of the green phase. The final dataset that was analyzed consisted of a total of 11,114 gap observations, of which 1,176 were accepted and 9,938 were rejected. The reduced variables for each observation are as follows:

- Gap size(s);
- Weather condition;
- Weather station measurements (precipitation, wind speed, barometric pressure, temperature);
- Day or night;
- Lane number of the offered gap;
- Travel time to reach the conflict point; and
- Decision of the driver regarding the offered gap (accept or reject).

The gap size "g" was defined as a continuous variable measured in seconds and defined as the time headway difference between the passage of the front bumper of a lead vehicle and the following vehicle at a reference point (P1, P2, or P3) in the opposing direction, as was illustrated in Figure 3.2a. The analysis assumed that left turning vehicles heading for South Depot Street were similar in gap acceptance behavior to left turning vehicles heading for North Depot Street. Only considered the first vehicle in the queue was considered in studying the gap acceptance/rejection behavior.

Weather Condition Data

The dataset was classified into six categories for weather conditions depending on the precipitation type and roadway surface condition as illustrated in Table 3.2.

Table 3.2 Different Weather Condition Categories

Weather Category	Weather Condition	
	Precipitation	Roadway Surface
Category 1 (DD)	Dry	Dry
Category 2 (DW)	Dry	Wet
Category 3 (DI)	Dry	Icy
Category 4 (DS)	Dry	Snowy
Category 5 (RW)	Rain	Wet
Category 6 (SS)	Snow	Snowy

For the first four weather categories, Category 1 (DD), Category 2 (DW), Category 3 (DI), and Category 4 (DS), the precipitation condition is dry (i.e., no precipitation) but the roadway surface conditions are dry, wet, icy, and snowy, respectively. Figure 3.3 presents screen shots from the recorded videos at the studied intersection showing all six categories. For the last two weather categories, Category 5 (RW) presents the case of rain precipitation and wet surface condition, and the last category (SS) is for the snow precipitation and snowy surface condition.

Figure 3.3 **Screen Shots from the Recording Videos of the Intersection Showing the Four Types of Weather Surface Coverage**

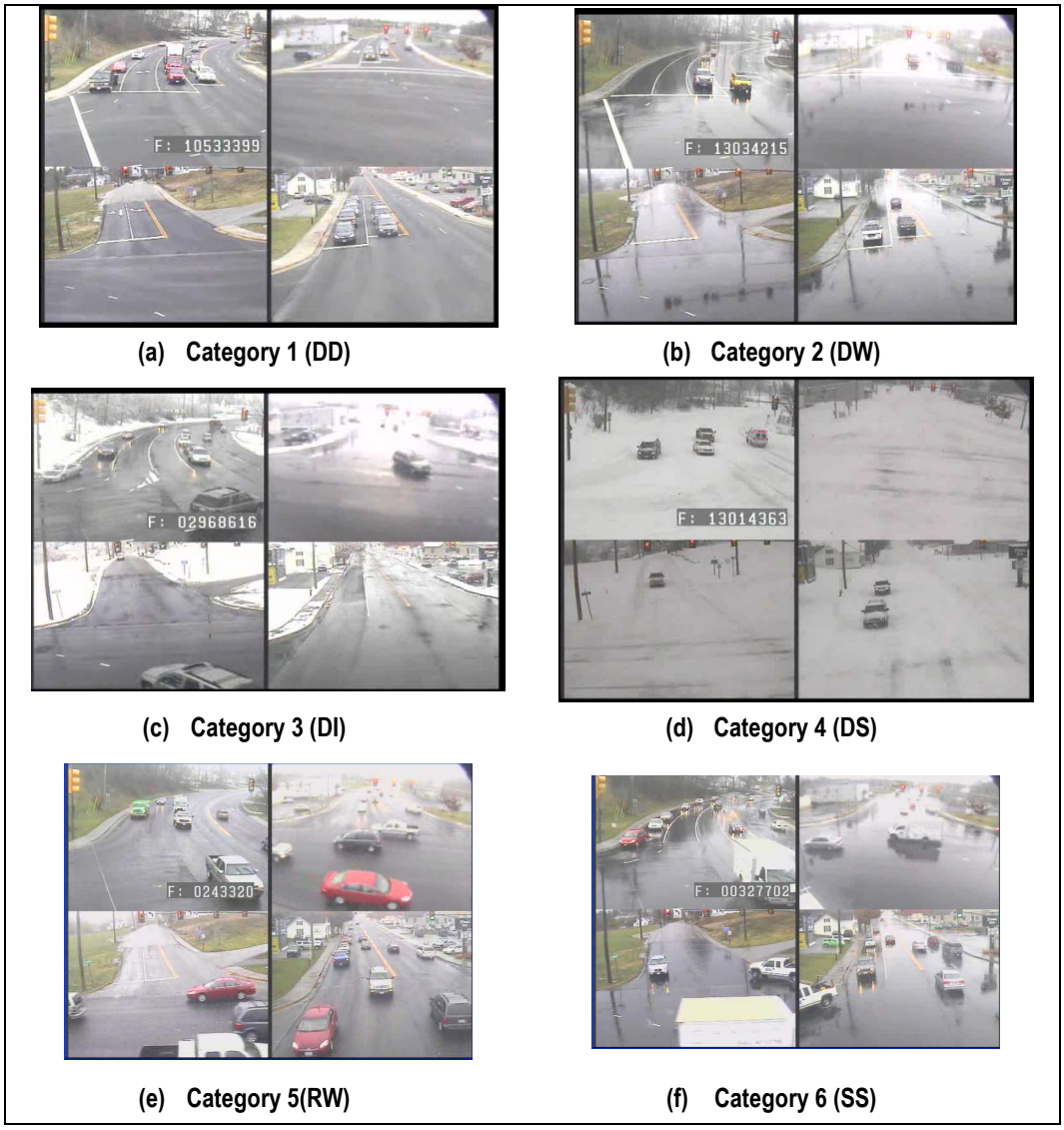

(a) Category 1 (DD)

(b) Category 2 (DW)

(c) Category 3 (DI)

(d) Category 4 (DS)

(e) Category 5(RW)

(f) Category 6 (SS)

Figure 3.4 Dataset Distributions for Different Weather Conditions

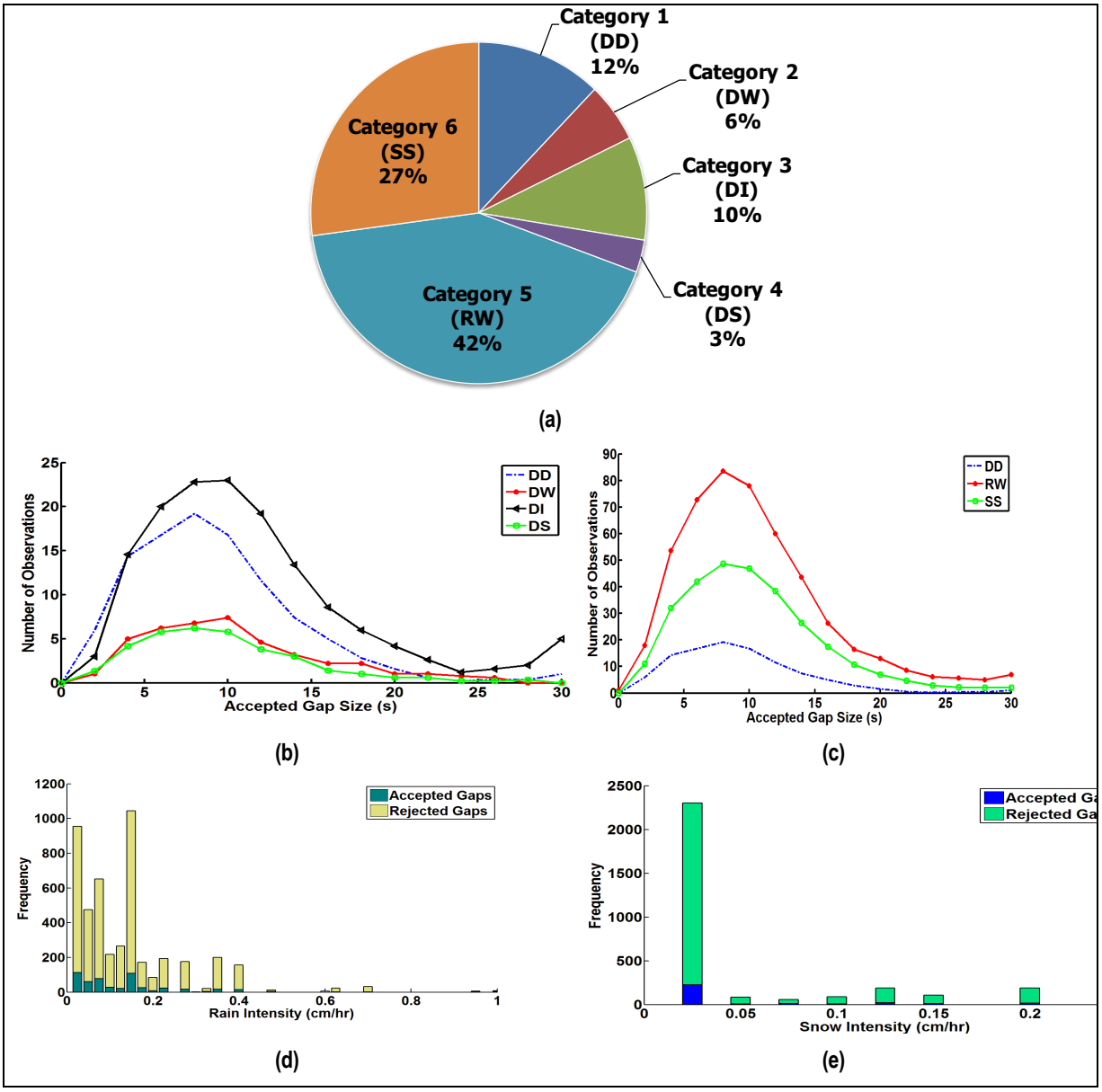

In summary, the weather condition for the collected dataset could be one of the following: DD, DW, DI, DS, RW, or SS as illustrated in Figure 3.3a. The distribution of accepted gap size dataset for the different weather conditions is shown in Figure 3.3b and Figure 3.3c. Figure 3.4b shows the relationship of gap acceptance to different surface conditions, all with no precipitation falling. The data indicate an increase in gap size under icy surface conditions, but minimal difference between dry, wet, and snowy conditions.

The weather station measurements were extracted every minute and related to the driver gap acceptance/rejection behavior. In the reduced dataset, the rain precipitation levels ranged from 0.025 cm/hr to 1 cm/hr and the snow precipitations ranged from 0.025 cm/hr to 0.25 cm/hr, as presented in Figure 3.4d and Figure 3.4c. The average recorded measurements for wind speed, barometric pressure,

and temperature were 3.45 km/hr, 106 millibar, and 3 Celsius, respectively. The day or nighttime conditions corresponding to each gap acceptance/rejection also were studied in this research. The day/night is considered as a binary variable (1 for day and 0 for night) and it was recorded for each observation. Figure 3.4c shows a comparison between gap acceptance for three conditions; DD, RW and SS. The data indicate a clear increase in gap size under rainy and wet conditions and increase, though smaller, under snowy conditions with snow on the road.

Figures 3.4e shows the proportion of gaps accepted and rejected at different precipitation rates under rainy, wet surface conditions while Figure 3.3f shows the same relationship for snowy conditions. In both cases, there is an increase in the proportion of rejected gaps as precipitation rates increase but the sample for heavier amounts of precipitation is relatively small.

Lane Usage Data

The lane number variable indicates the location of the offered gap for the left turn vehicle. The lane number variable is equal to 1, 2, or 3 corresponding to the three conflict points P1, P2, or P3 respectively. The travel time "τi" is a continuous variable measured in seconds and is defined as the time taken by left turning vehicle's front bumper to reach conflict point Pi. The mean and median (50^{th} percentile) values for travel time to reach each conflict point (P1, P2, and P3), respectively are presented in Table 3.3 for different weather categories.

Table 3.3 Travel Time Values for Different Weather Categories

Weather Category		Travel Time(s)		
		P 1	P 2	P 3
Category 1 (DD)	Mean	0.89	1.93	3.21
	Median	0.90	2.00	3.30
Category 2 (DW)	Mean	1.56	2.72	4.12
	Median	1.10	2.30	3.60
Category 3 (DI)	Mean	1.56	2.74	4.12
	Median	1.50	2.50	3.90
Category 4 (SS)	Mean	1.48	2.53	3.95
	Median	1.60	2.50	4.00
Category 5 (RW)	Mean	2.16	3.08	4.40
	Median	1.60	2.50	3.90
Category 6 (SS)	Mean	1.51	2.55	4.05
	Median	1.60	2.50	4.00

The Gap decision was recorded as a binary variable (0=rejection and 1=acceptance). The gap decision of the driver is the response for the different independent variables studied in this research. Logistic models were fit to the data to estimate the probability (*p*) of accepting a certain gap as will be described in the following section.

3.5 Analysis Results

Logistic Model Results

In this study, different models were considered to capture gap acceptance behavior in terms of the different observed variables. Given that the response variable is discrete (0 or 1) while the explanatory variables are continuous, a logistic model was fit to the data to estimate the probability (*p*) of accepting a gap as shown in Equation 1) and (2):

$$p = \frac{e^{U(x)}}{1+e^{U(x)}} \tag{1}$$

$$U(x) = \text{logit}(p) = \ln\left[\frac{p}{1-p}\right] = \beta_0 + \beta_1 x_1 + \beta_2 x_2 + ... + \beta_n x_n \tag{2}$$

Where; p is the probability of accepting a gap; x1, x2,…, xn are the explanatory variables; and β0, β1, β2, …, βn are the estimated regression coefficients.

By applying different statistical approaches for variables elimination, and treating the accepted and rejected decision as a binary choice (0 or 1), and assuming a logit link function for the generalized linear model (GLM), three different models were developed as follows:

Model 1, (M1)

$$\text{logit}(p) = \beta_o + g \times (\beta_1 + \beta_2 DW + \beta_3 DI + \beta_4 DS + \beta_5 RW + \beta_6 SS) + L \times (\beta_7 + \beta_8 RW + \beta_9 SS) \tag{3}$$

Model 2, (M2)

$$\text{logit}(p) = \beta_o + \beta_1 \tau + g \times (\beta_2 DD + \beta_3 DW + \beta_4 DI + \beta_5 DS + \beta_6 RW + \beta_7 SS) \tag{4}$$

Model 3, (M3)

$$\text{logit}(p) = \beta_o + \beta_1 g + (g - \tau) \times (\beta_2 DD + \beta_3 DW + \beta_4 DI + \beta_5 DS + \beta_6 RW + \beta_7 SS) \tag{5}$$

Where;

- logit(*p*)=ln(*p*/(1-*p*)); *p* is probability of accepting a gap;
- *g* is the gap size offered to the opposed vehicle (s);
- *L* is the lane indicator variable for the lane number of the offered gap (1=First lane, 2=Second lane and 3=Third lane);

- τ the corresponding travel time to reach the conflict point where the gap is offered for each individual left turn vehicle; and
- *DD*, *DW*, *DI*, *DS*, *RW*, *SS* are dummy variables indicating the six different weather categories that were mentioned previously.

Each weather independent variable is a dummy variable (0 or 1) and the existence of one weather category (=1) means that all other weather category variables are eliminated (=0). The contribution of the β for corresponding weather is changed by the switching on or off of the dummy variable (from 0 to 1 and Vice Versa) and thus the predicted value for logit (p) depends on the existing weather condition. The estimated parameters for the three proposed models are presented in Table 3.4.

For model 1 (M1), the independent variables presented are the gap size and lane number that are interacted with the different weather categories. The estimated coefficient of the gap size in M1 is the β1 value in case of category 1 (DD) and this value is increased in case of other weather categories by the value corresponding to βi of (DW, DI, DS, RW, or SS). For the lane number variable (L), the offered gap location is treated as a discrete variable (1, 2, or 3). It is noticeable that effect of "L" on the probability of acceptance (i.e., Logit(p)) is the same for the first four categories (i.e., no precipitation) and is only varied for the weather categories (RW and SS).

In the case of the second model (M2), the independent variables include the same interaction terms as the gap size variable presented in M1 in addition to the travel time as a continuous variable. The travel time in this model reflects the required time needed for each vehicle to reach the conflict point where the gap is offered. The different travel times (for P1, P2, and P3) are observed during the maneuver of each vehicle in case of gap acceptance, and for rejected gaps these values are applied depending on the location of each offered gap. This model is designed to estimate the impact on gap acceptance behavior of the offered gap size, the weather category and the travel time needed for each vehicle to reach the location of that gap (conflict point).

For the third model (M3), the independent variables include the gap size and the difference between the gap size and the travel time to the conflict point interacted with different weather categories. The difference between the gap size and the travel time is considered as the time remaining for a left turn driver to clear the conflict point (i.e., buffer of safety for the driver). Thus, this model presents the impact of the gap size and the buffer of safety needed for each driver on gap acceptance behavior based on the weather category.

Some variables were eliminated from the different models structure based on the Chi-Square significance test. The weather measurements precipitation, wind speed, barometric, and temperature were found not statistically significant on gap acceptance behavior. The insignificance of precipitation appears to be a function of the fact that most observations were concentrated in low precipitations values and the range of precipitation values is not large. Other weather measurements, were almost constant with very limited variation in the data. In addition, the daytime/nighttime variable was found not statistically significant, a finding that is consistent with other studies identified in the literature. [19]

Table 3.4 Estimated Parameters for the Three Proposed Models and the Statistics Tests

	Term	β_i	Estimated Mean Values	Std Error	L-R ChiSquare	Prob>ChiSq (p Values)	Lower CL	Upper CL
Model 1 (M1)	Intercept	β_0	-4.744	0.161	1293.569	<.0001	-5.060	-4.428
	g	β_1	1.021	0.052	784.843	<.0001	0.931	1.122
	g*DW	β_4	-0.188	0.051	13.351	0.0003	-0.288	-0.087
	g*DI	β_5	-0.126	0.040	9.649	0.0019	-0.206	-0.046
	g*DS	β_6	-0.137	0.055	6.062	0.0138	-0.245	-0.028
	g*RW	β_7	-0.237	0.057	17.275	<.0001	-0.349	-0.125
	g* SS	β_8	-0.270	0.060	20.421	<.0001	-0.387	-0.153
	L	β_7	-0.898	0.126	50.412	<.0001	-1.167	-0.650
	L*RW	β_8	0.357	0.142	6.313	0.0120	0.078	0.635
	L*SS	β_9	0.348	0.153	5.126	0.0236	0.047	0.649
	Model tests: LogLikelihood= -1531.998, ChiSquare= 4441.727, Prob>ChiSq (p-value) <0.0001							
Model 2 (M2)	Intercept	β_0	-4.956	0.127	2478.181	0.0000	-5.206	-4.706
	τ	β_1	-0.297	0.038	82.976	<.0001	-0.373	-0.220
	g*DD	β_2	0.844	0.034	866.951	<.0001	0.776	0.911
	g*DW	β_5	0.729	0.042	376.209	<.0001	0.646	0.811
	g*DI	β_6	0.780	0.029	1252.677	<.0001	0.723	0.836
	g*DS	β_7	0.765	0.046	327.776	<.0001	0.674	0.855
	g*RW	β_3	0.789	0.021	2969.196	0.0000	0.746	0.831
	g*SS	β_4	0.733	0.022	1964.470	0.0000	0.689	0.776
	Model tests: LogLikelihood= -1501.048, ChiSquare= 4448.177, Prob>ChiSq (p-value) <0.0001							
Model 3 (M3)	Intercept	β_0	-5.027	0.128	2541.336	0.0000	-5.277	-4.775
	g	β_1	0.500	0.038	169.706	<.0001	0.425	0.575
	(g- τ)*DD	β_2	0.449	0.054	67.738	<.0001	0.342	0.556
	(g- τ)*DW	β_5	0.186	0.065	8.018	0.0046	0.057	0.314
	(g- τ)*DI	β_6	0.311	0.049	39.307	<.0001	0.213	0.407
	(g- τ)*DS	β_7	0.264	0.071	13.732	0.0002	0.124	0.403
	(g- τ)*RW	β_3	0.295	0.042	47.552	<.0001	0.220	0.378
	(g- τ)*SS	β_4	0.236	0.041	31.849	<.0001	0.153	0.317
	Model tests: LogLikelihood= -1498.677, ChiSquare= 4456.928, Prob>ChiSq (p-value) <0.0001							

Comparison of Models

In comparing the different models (M1, M2, and M3), two criteria were considered: a) Success Rate factor (SR); and b) Corrected Akaike's Information Criterion (AICc). These criteria are briefly described.

Success Rate Factor

The SR is defined as the percentage of observations with acceptance/rejection outcomes from the each model (rounded to 0 or 1) that are identical to field responses. The model with the largest SR is the best model.
The negative log likelihood (or, equivalently, the deviance) can be used as a measure of how well a model fits a data set, with smaller values being indicative of a better fit. However, due to the difference in number of parameters from one model to the other, this criterion will be biased in favor of less parsimonious models. Therefore, the corrected Akaike's Information Criterion (AICc) is used for comparison as was suggested in the literature. [16]

Akaike's Information Criterion (AICc)

AICc is a measure of the goodness of fit of an estimated statistical model and is a tool for model selection that could be employed regardless of sample size. Given a data set, several competing models may be ranked according to their AICc, with the one having the lowest AICc being the best as:

$$AICc = -2 \times LL + 2 \times N + \frac{2N(N+1)}{N-p-1} \quad (6)$$

Where; LL is the posterior expected log likelihood, p is the number of parameters used by the model, and N is the number of datum points (number of observations).

Model Performance

By applying the two criteria on the three proposed models (M1, M2, and M3), the SR values were found to be 95.11 percent, 95.12 percent and 95.07 percent, respectively. The AIC measure was 3,084, 3,074, and 3,065 for the M1, M2, and M3 models, respectively.

In the case of the SR criteria, the M1 and M2 offer the highest success rates; therefore. Alternatively, in the case of the AIC criterion, the M2 and M3 models are superior to the M1 model.

In summary, given the small differences for the three models with respect to the two evaluation criteria, identification of the optimum model is not simple. Each of the three models provides similar inferences concerning the relation between gap acceptance and lane number (or travel time) for different weather categories. Specifically, the models demonstrate that the probability a driver accepts a gap decreases as the travel time needed to reach the gap increases (i.e., the further the gap is). The main difference between the proposed models is the definition of the offered gap location. The M1 model can be applied in a simulation environment where the lane width information may not available. Alternatively the M2 model is more general given that the time to reach the conflict point is a continuous variable. The drawback of the M3 is that the estimated buffer of safety (the difference between the gap size offered and the required time to reach the offered gap) could be a very large number in the case of large gap sizes but the driver in reality could accept smaller buffers of safety.

In conclusion, the M2 model is considered more general. The proposed model explicitly captures the vehicle constraints on driving behavior (presented in the travel time value) and the driver's deliberation in accepting or rejecting a gap in different weather conditions. The model can be generalized to capture different vehicles, roadway, movement, intersection characteristics, and weather effects on driver gap acceptance behavior. Consequently, the remainder of the report considers the analysis of the second model "M2." Figure 3.5 presents the probability distribution of gap acceptance per lane separately for different weather and roadway surface conditions.

Figure 3.5 The Proposed Model (M2) Probability Distribution of Gap Acceptance per Each Lane for Each Weather Category

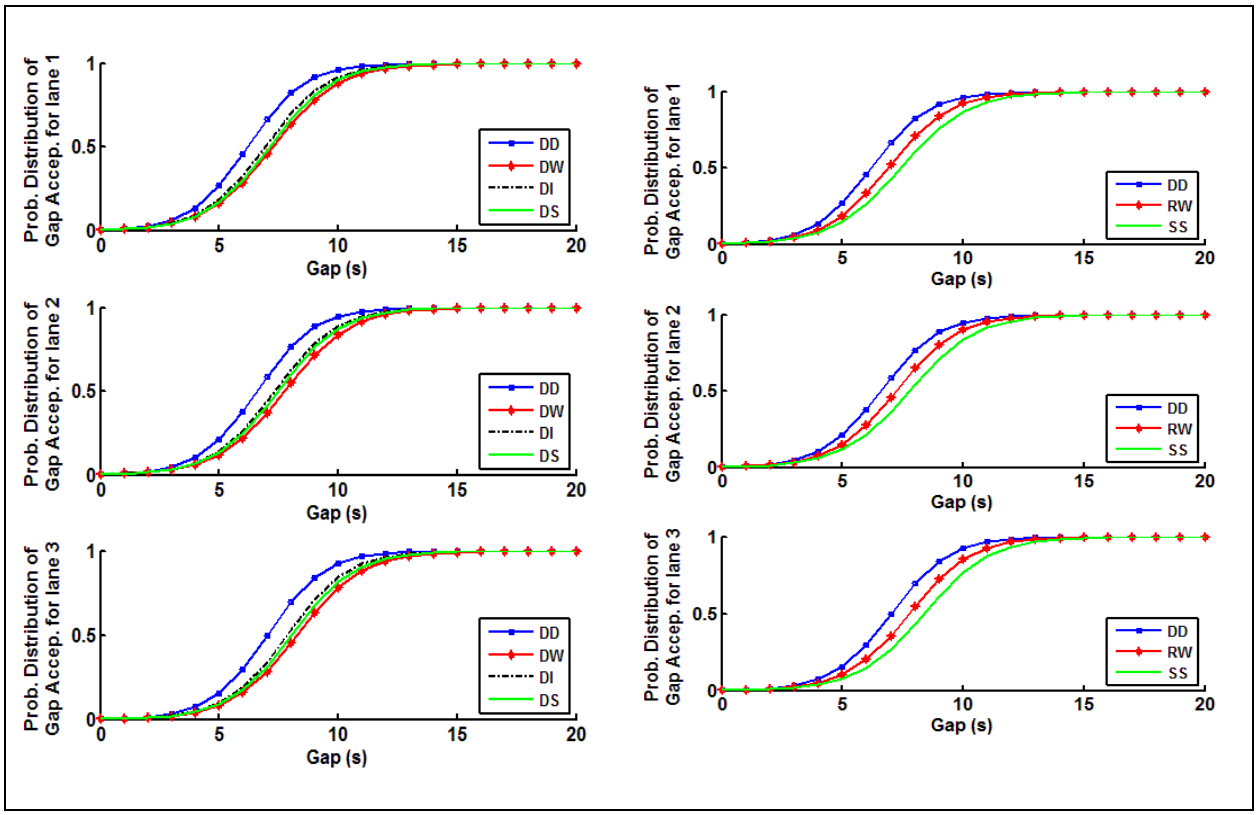

The model demonstrates that by wetting the roadway surface, the gap acceptance curve shifts to the right (DW right of DD curve). Furthermore, a larger gap is required for a wet surface (DW) compared to a snowy (DS) and icy surface (DI) followed by a dry surface (DD). For the precipitation weather categories (Category 5 and 6), rain precipitation results in an increase in the required gap (curve shifted to the right) followed by snow precipitation (SS). In summary, drivers are less aggressive for the snow precipitation compared to the rain precipitation and dry conditions.

Critical Gap Estimation Based on Logistic Regression

As mentioned before, the critical gap is considered the minimum gap size that a driver is willing to accept in order to make a gap acceptance maneuver. The critical gap value is considered as the gap size used to determine the saturation flow rate and is typically computed as the 50th percentile gap size (probability of acceptance equal to zero). The fundamental assumption is that drivers accept all gaps that are larger

than their critical gap and reject all smaller gaps. The critical gap is defined as the gap size that is equally likely to be accepted and rejected; and thus corresponds to the median of the probability of accepted gaps.

For permissive left-turn traffic, The HCM (2000) [13] estimates the opposed saturation flow rate based on the critical gap and follow-up time. The HCM considers the critical gap accepted by left-turn drivers as a deterministic value equal to 4.5 s at signalized intersections with a permitted left-turn phase and this value is independent of the number of opposing-through lanes to be crossed and the weather condition.

The American Association of State Highway and Transportation Officials (AASHTO, 2001) [17], classifies the left turning movements from the major road across opposing traffic as Case *F*. The AASHTO (2001) recommends that for case *F* opposed movements that the critical gap for left-turning passenger cars be set equal to 5.5 s (for passenger cars) and for left-turning vehicles that cross more than one opposing lane to add an additional 0.5 s for each additional lane of travel.

The critical gap can be computed for the proposed model (M2) by setting the probability of accepting a gap equal to 0.5 which entails setting the Logit function to zero. Consequently, the critical gap (t_c) for the proposed model (M2) can be computed using Equations (7).

$$t_c = \frac{-\beta_o - \beta_1 \tau}{\beta_2 DD + \beta_3 DW + \beta_4 DI + \beta_5 DS + \beta_6 RW + \beta_7 SS} \quad (7)$$

The different critical gap values for the proposed model is summarized in Table 3.5 using the median travel time values corresponding to each weather category (referring to Table 3.3).

Table 3.5 The Different Critical Gap Values per Each Lane (Conflict Point) for Different Weather Categories

Weather Category	(tc) Critical Gap(s)		
	P 1	P 2	P 3
Category 1 (DD)	6.19	6.58	7.03
Category 2 (DW)	7.25	7.74	8.27
Category 3 (DI)	6.93	7.31	7.84
Category 4 (DS)	7.09	7.45	8.03
Category 5 (RW)	6.88	7.22	7.75
Category 6 (SS)	7.41	7.77	8.38

First, it should be stated that the three proposed models were consistent in the hierarchy of the different gap size values. For the six categories of weather condition, the critical gap values increase with an increase in the lane number. In other words, the minimum acceptable gap increases with the increase in distance traveled to proceed through the offered gap. Comparing the 6 categories for the same conflict point, the lowest critical gap is for DD followed by RW, DI, DS, DW, and SS. It is noticeable that the RW condition has the lowest critical gap size (after DD) comparing to all other weather conditions and that has many interpretations. One of these interpretations is that drivers are familiar with these weather conditions and consequently are more aggressive in accepting a gap. Second, the driver could overestimate the offered gap size value compared to other weather conditions due to low visibility condition during rain falling. However, the inclement weather impact on gap acceptance behavior requires further data collection at other locations in other cities to validate these findings.

The critical gap values that are presented in Table 3.5 are significantly larger than the HCM [13] recommended value of 4.5 s and slightly larger than the AASHTO recommended value of 5.5s. One possible explanation for the higher critical gaps is the geometry of the intersection. Specifically, the intersection approaches were slightly curved and thus drivers might have had a difficult time establishing which lane the opposing vehicles were in and which movement they were executing (left, through, or right). An earlier study [11] showed that the opposing vehicles turning left may block a driver's view of oncoming traffic, which results in larger accepted gap sizes. Specifically, the study indicates that in case of no opposing left turn vehicles (no sight blockage) the critical gap is 5.6 s and increases by 2.1 s in the case of sight blockage.

The difference between the critical gap values for different opposing lanes is approximately 0.5 s for all weather and roadway conditions and thus is consistent with the recommended value in the AASHTO 2001 design procedures [17].

In general, for different weather categories, the critical gap values increase with an increase in the lane number or in other words, the drivers require larger gaps when the conflict point is farther way.

Impact on Opposed Saturation Flow Rates

Once the critical gap is determined, the opposed saturation flow rate(s) can be computed using Equation (8). Here v0 is the opposing flow (veh/h), tc is the critical gap size(s) which can be computed using one of the three models that were presented earlier (M1, M2, and M3), and tf is the follow-up time(s). The follow-up time is the discharge time headway for the unopposed saturation flow rate (i.e., when the opposing flow is zero) between consecutive vehicles accepting the same gap. HCM (2000) [13] recommends a 2.5 s value for the follow-up time.

$$s = v_0 \frac{e^{\frac{-v_0 t_c}{3600}}}{1 - e^{\frac{-v_0 t_f}{3600}}} \tag{8}$$

The opposed saturation flow rates were computed for various weather categories and opposing flow levels using the M2 model for a different number of opposing lanes. Opposed saturation flow rate adjustment factors (SF_{ij}) (saturation flow rate relative to the saturation flow rate of dry conditions "Category 1") were then computed, as illustrated in Figure 3.6 and Equation (9)

$$s_j = s \times SF_{ij} \tag{9}$$

Where sj is the inclement weather opposed saturation flow rate; j is the weather/roadway condition category (DW, DI, DS, RW, or SS); s is the opposed saturation flow for dry conditions (DD); SFij is the saturation flow reduction factor corresponding to each weather/roadway condition category and the number of opposing lanes i (1, 2, or 3).
Figure 3.6 clearly demonstrates a decrease in the opposed saturation flow rate as the opposing flow increases for various weather categories. The figure also shows that for a specific opposing flow rate (v0), the minimum saturation flow rate (s) (or the minimum value for an adjustment factor) is for SS followed by DW, DS, RW, DI, then DD, respectively. Noteworthy is the fact that the increase in the number of opposing lanes needed to be crossed by the driver leads to a decrease in the saturation flow rate for the same weather category. These findings are similar to those documented in discussion of Table 3.5.

Figure 3.6 Saturation Flow Reduction Factor and Opposing Volume Relationship for Different Weather Categories Depending on the Number of Opposing Lanes

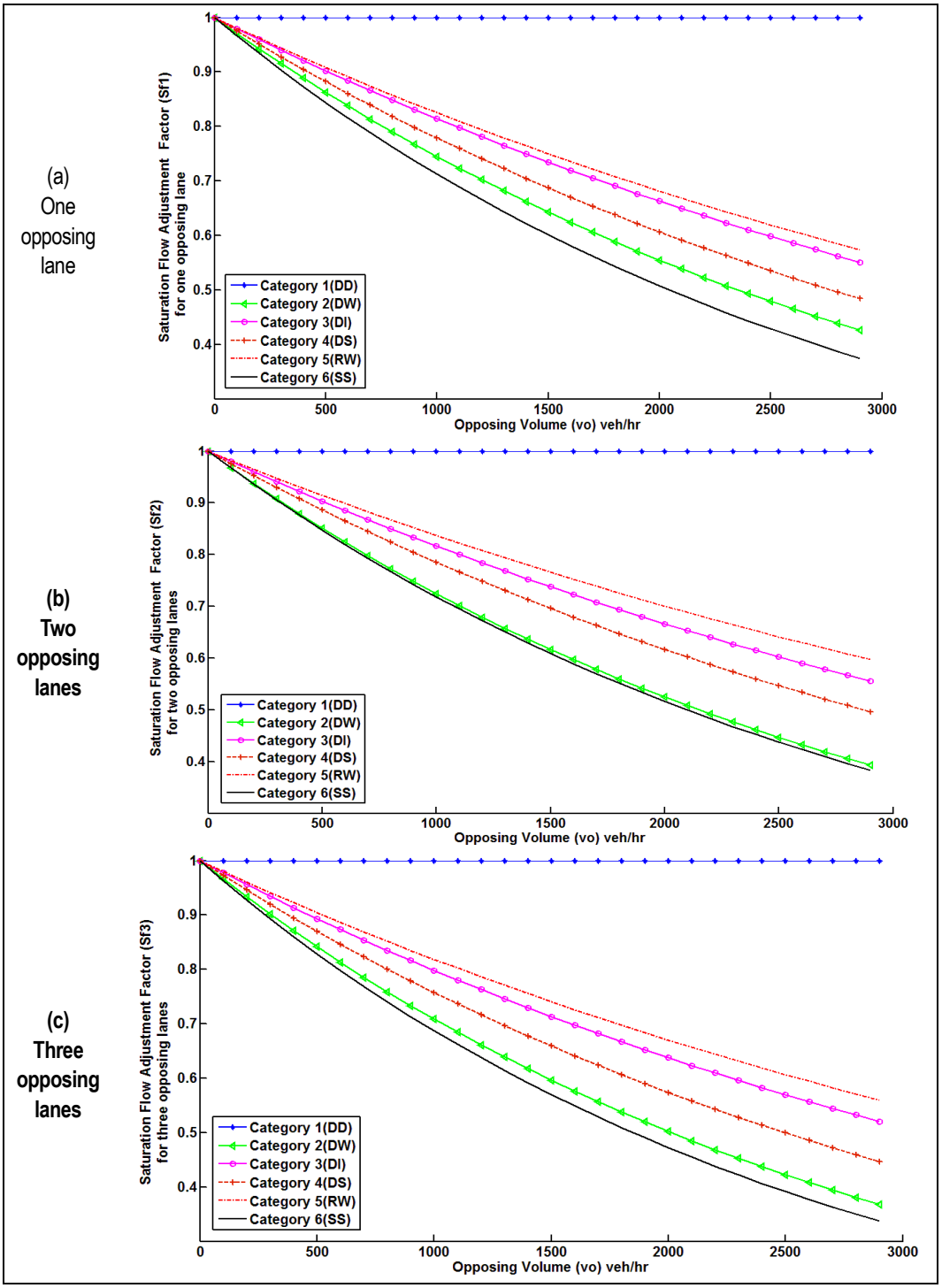

3.6 Conclusions and Recommendations for Further Research

The study gathered field data at a signalized intersection (a total of 11,114 observations of which 1,176 were accepted and 9,938 were rejected gaps) over a six-month period in an attempt to characterize driver left-turn gap acceptance behavior under various weather and roadway surface conditions. Logistic regression models were calibrated to the data and compared in order to identify the best model for capturing driver gap acceptance behavior. The models reveal that drivers are more conservative during snow precipitation compared to rain precipitation. In the case of the roadway surface condition, drivers require larger gaps for wet surface conditions compared to snowy and icy surface conditions, and, as would be expected, require smallest gaps for dry roadway conditions. In addition, the models show that the drivers require larger gaps as the distance required to clear the conflict point increases. The study also illustrates how inclement weather and number of opposing lanes affects permissive left-turn saturation flow rates. Using the study findings inclement weather signal timings can be implemented within traffic signal controllers. The traffic signal controller could include an inclement weather signal timing plan that accounts for the reduction in the opposed saturation flow rates. It is anticipated that this research will contribute to enhance intelligent transportation system (ITS) and IntelliDrive™ applications.

4.0 Modeling Inclement Weather Impacts on Traffic Behavior Using VISSIM and INTEGRATION Software

4.1 Overview

Analysis and implementation of weather-responsive traffic management strategies are goals of FHWA's Road Weather Management Program. These strategies need to be analyzed using microsimulation models that can evaluate the traffic flow impacts of those strategies, and help determine whether they meet desired objectives. This requires that analysts be able to modify microsimulation parameters to reflect the impact of weather on driver behavior. Earlier research under this project has concentrated on the first challenge; obtaining empirical data to determine what those impacts are and developing factors that can be used in simulations. The second challenge, adjusting the models to reflect adverse weather conditions, is the subject of this report.

The objective of the work documented in this section is to identify the methodologies for modeling traffic stream behavior under inclement weather conditions using state-of-the-art microscopic simulation software. Specifically, this study investigates general approaches to construct simulation models accounting for the impact of rain and snow precipitation by means of calibrating car-following, lane-changing, and gap-acceptance models. Thereafter, the general approach is applied to the calibration of the VISSIM and INTEGRATION software. The original project plan called for use of the CORSIM model rather than INTEGRATION. However, an evaluation of both models showed that the CORSIM model has a limited ability to incorporate weather-related adjustment factors. INTEGRATION, on the other hand, offers much greater capability to incorporate weather-related factors.

CORSIM does not track a vehicle through the entire trip but instead assigns probabilities to vehicles as they approach decision points. INTEGRATION on the other hand does track vehicles throughout the entire trip. INTEGRATION, unlike other microscopic tools, explicitly models the vehicle dynamics and thus can explicitly capture the impact of roadway surface condition on vehicle acceleration behavior. In addition, CORSIM uses a Pipes car following model that does not allow the independent calibration of free-flow speed and speed at capacity. It would be difficult to model weather-related adjustment factors without this capability.

Subsequent sections of this report include:

- Process for Modeling the Traffic Stream Under Inclement Weather;
- Inclement Weather Impact on the Simulation Parameters of VISSIM, INTEGRATION and CORSIM Software;

- Demonstration of Modeling Weather-Related Adjustment Factors in VISSIM and INTEGRATION; and
- Summary and Conclusions.

4.2 Process for Modeling the Traffic Stream Under Inclement Weather

Previous studies have quantified the impact of inclement weather on traffic stream behavior by quantifying the changes in key traffic stream model parameters as a function of weather and roadway conditions [1, 2]. Specifically, field-measured weather data were synchronized with traffic stream data and then the relationship between inclement weather and traffic stream parameters was derived. The traffic stream model parameters include four parameters that define the steady-state, car-following relationship. These parameters include the free-flow speed (uf), speed-at-capacity (uc), capacity (qc), and jam density (kj). Using these four parameters the space-mean speed (u), density (k), and flow rate (q) can be estimated. Subsequently, the vehicle headway can be estimated as the inverse of the flow rate. Similarly, the inverse of the traffic stream density is the approximation of the average vehicle spacing. Consequently, the car-following model needs to be calibrated using the quantified changes in the traffic stream parameters. In other words, all the parameters characterizing the car-following behavior need to be calibrated.

Vehicle Deceleration Model Adjustment

Another set of driving behavior models to be calibrated are the vehicle deceleration models. This calibration is required because inclement weather conditions can affect both the condition of roadway surfaces and the driver behavior, which would limit the performance of deceleration. The maximum braking force can be computed as shown below in Equation 1[32]:

$$d_{max} = \eta_b \mu g (1 - d_a) \quad (1)$$

Where:

- ηb = braking efficiency;
- μ = coefficient of roadway adhesion, also known as the coefficient of friction;
- g = gravitational acceleration (9.8066 m/s2); and
- da = the driver adjustment factor.

As can be seen in the equation, the coefficient of friction needs to be adjusted to reflect the roadway surface conditions. If the driver adjustment factor to inclement weather is available then it can be incorporated into the equation, otherwise it can be set to zero. Rakha, et al. quantified the inclement weather impacts on driver deceleration behavior [33]. The maximum values of coefficients of road adhesion are summarized in Table 4.1.

Table 4.1 Maximum Values of Coefficients of Road Adhesion

Pavement	Coefficient of Road Adhesion	
	Maximum	Slide
Good, Dry	1.00	0.80
Good, Wet	0.90	0.60
Poor, Dry	0.80	0.55
Poor, Wet	0.60	0.30
Packed Snow or Ice	0.25	0.10

Vehicle Acceleration Model Adjustment

The next step is to calibrate vehicle acceleration behavior. The rolling resistance force, which can be affected by roadway surface conditions, is used in the calculation of the maximum acceleration level using vehicle dynamics models as can been seen in Equations 2 and 3. The acceleration model parameters corresponding to weather conditions need to be fed into the microscopic simulation tools.

$$a = f_p \frac{F - (R_a + R_r + R_g)}{m} . \quad (2)$$

$$R_r = C_r \left(c_2 u + c_3\right) \frac{mg}{1000} . \quad (3)$$

Where:

- a = the vehicle acceleration (m/s^2);
- F = the vehicle tractive force (N);
- R_a = the aerodynamic resistance force;
- R_r = the rolling resistance force (N);
- R_g = the grade resistance force;
- (N), m is the vehicle mass (kg);
- f_p = the proportion of the maximum acceleration that the driver is willing to employ (field studies have shown that it is typically 0.62);
- C_r, c_2, c_3 =the rolling coefficients; and
- u = speed.

If the simulation tool uses the vehicle dynamics models then the rolling coefficients corresponding to different weather conditions can be directly used as input parameters. Otherwise the user needs to modify the acceleration performance functions based on the vehicle dynamics models. Typical values for the rolling coefficients (C_r, c_2, and c_3), as a function of the road surface type, condition, and vehicle tires, are provided in the literature [34]. Typical values of C_r as a function of the roadway surface are summarized in Table 4.2.

Table 4.2 Rolling and Friction Coefficient Values Based on Roadway Surface Condition

Pavement Type	Pavement Condition	C_r	Coefficient of Friction
Concrete	Excellent	1.00	0.80
	Good	1.50	0.70
	Poor	2.00	0.60
Asphalt	Good	1.25	0.60
	Fair	1.75	0.50
	Poor	2.25	0.40
Macadam	Good	1.50	0.55
	Fair	2.25	0.45
	Poor	3.75	0.35
Cobbles	Ordinary	5.50	0.50
	Poor	8.50	0.40
Snow	2''	2.50	0.20
	4''	3.75	0.15
Dirt	Smooth	2.50	0.30
	Sandy	3.75	0.20
Mud		3.75-15.0	0.15
Sand	Level Soft	6.0-15.0	0.15
	Dune	16.0-30.0	0.10

Gap Acceptance Model Adjustment

Gap acceptance is defined as the process that occurs when a traffic stream (known as the opposed flow) has to either cross or merge with another traffic stream (known as the opposing flow). Attempts have been made in the literature to quantify the impact of various parameters on gap acceptance. However research on the impact of adverse weather on gap acceptance has been limited. Weather events are considered one of the factors that affect roadway surface conditions, vehicle performance, driver behavior, and consequently reduce capacity. Within the context of crossing gap acceptance, a gap is defined as the elapsed-time interval between arrivals of successive vehicles in the opposing flow at a specified reference point in the intersection area. The minimum gap that a driver is willing to accept is generally called the critical gap. The Highway Capacity Manual (HCM) (2000) defines the critical gap as the "minimum time interval between the front bumpers of two successive vehicles in the major traffic stream that will allow the entry of one minor street vehicle [35]."

The critical gap value is considered as the gap size used to determine the saturation flow rate and is typically computed as the 50th percentile gap size (probability of acceptance equal to zero). The fundamental assumption is that drivers accept all gaps that are larger than their critical gap and reject all smaller gaps. The critical gap is defined as the gap size that is equally likely to be accepted and rejected; and thus corresponds to the median of the probability of accepted gaps. Weather is one of the many factors affecting the critical gap value, including: weather precipitation (rain or snow), roadway surface

condition (wet or snowy), number of opposing lanes, and time needed to cross the conflict point. In summary, corresponding critical gap values for different weather conditions can be implemented as one of the microsimulation parameters used to determine the saturation flow rates.

The general approach to calibrate microscopic traffic simulation models to capture the impact of inclement weather requires the calibration of the steady-state car-following, deceleration, acceleration, and gap-acceptance models.

4.3 Inclement Weather Impact on Simulation Parameters

This section describes the process for incorporating weather-related adjustment factors into two different microsimulation software packages: VISSIM and INTEGRATION. In addition, instructions are provided for incorporating factors into CORSIM, a software package which is commonly used but has more limited capability to model adverse weather impacts. Use of weather-related factors were actually simulated in VISSIM and INTEGRATION in order to demonstrate the process. The results of this demonstration are documented in Section 4.4 of this report.

VISSIM Software

In VISSIM software, there is an option called: "Driver Behavior Parameter Sets" where several driving behavior parameters can be adjusted reflecting different weather conditions as described in the following sections [36].

Car Following Model

The car following model allows selection of the basic model for the vehicle following behavior. Depending on the selected model, the model parameters change. The two model options area: 1) Wiedemann 74 which is mainly suitable for urban traffic; and 2) Wiedemann 99 which is mainly suitable for interurban (motorway) traffic. There also is an option of "No Interaction," in which vehicles do not recognize any other vehicles. VISSIM entry screens for car following parameters are shown in Figure 4.1 a) and b). For the Wiedemann 74 car following model, the corresponding parameters are:

- Average standstill distance – spacing from front bumper of a stopped vehicle to the rear bumper of the vehicle ahead of it;
- Additive part of safety distance – a factor added to the average standstill distance to account for randomness; and
- Multiplicative part of safety distance – a factor multiplied by the average standstill distance to account for randomness.

Those parameters can be adjusted for different weather conditions so that the simulation results can be consistent with field-measured traffic stream parameters. For Wiedemann 99, two model constants, CC0 and CC1 (also known as the Driver Sensitivity Factor) could be adjusted for the impact of inclement weather and they are computed as:

$$CC0 = \frac{1000}{k_j} - \bar{L} \tag{4}$$

$$CC1 = 3600\left(\frac{1}{q_c} - \frac{1}{k_j u_f}\right) \tag{5}$$

CC0 is the spacing between the front bumper of the subject vehicle and the rear bumper of the lead vehicle. This equals the jam density spacing minus the average vehicle length. The Driver Sensitivity Factor (CC1) can be calibrated using three macroscopic traffic stream parameters, namely: the expected roadway capacity, jam density, and free-flow speed.
The detailed descriptions of the calibration procedures are available in the literature [8, 9]. Rakha and Guo proposed methodologies to calibrate the Wiedemann models using macroscopic traffic stream model parameters [38].

Figure 4.1 Car Following Parameters in the VISSIM Software

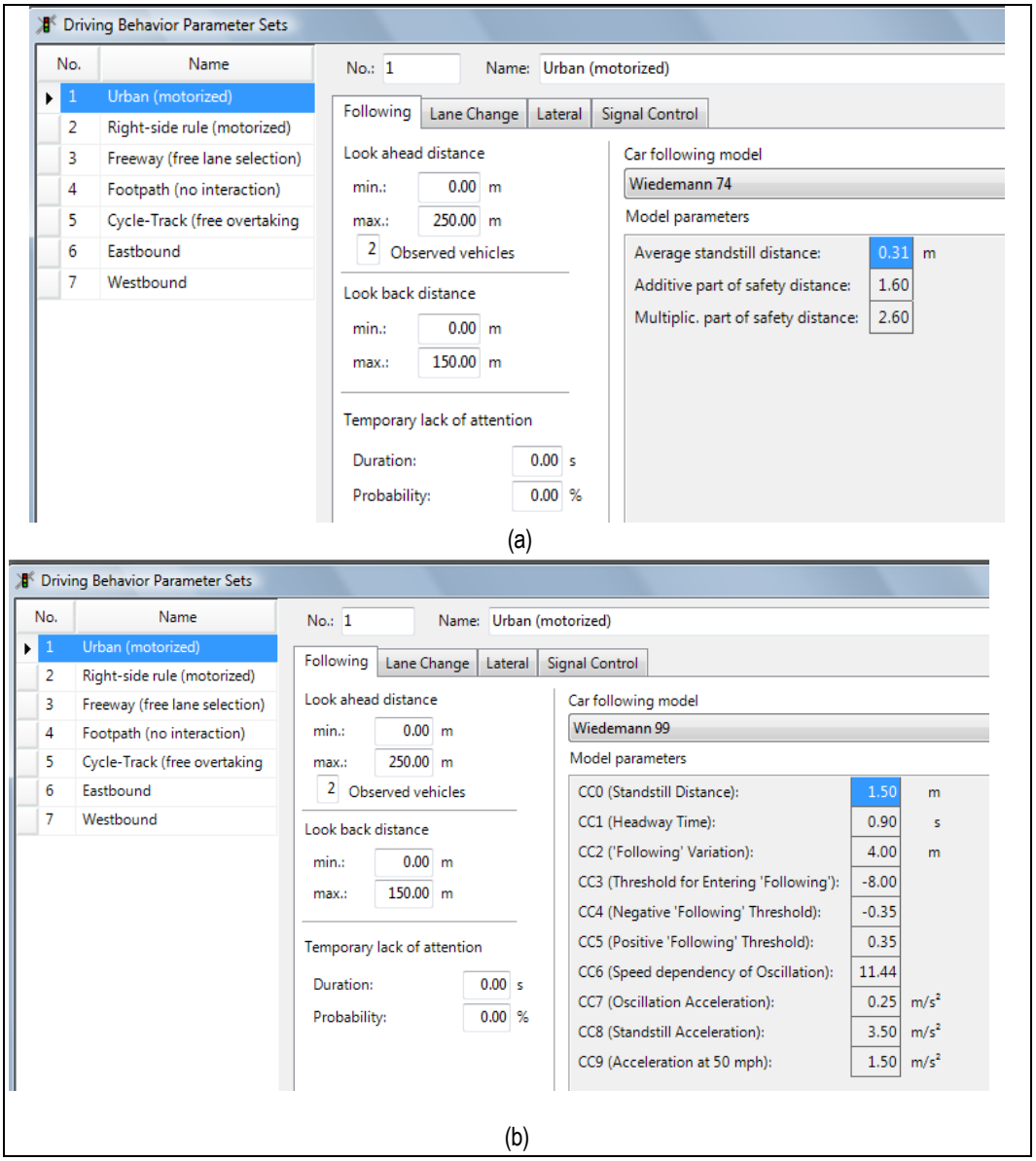

Lane-Changing Model

There are two kinds of lane changes, namely: necessary lane changes and free lane changes. As the names imply, the necessary lane change is made to maintain route decisions while the free lane change is made to maintain some desired speed. In both cases, when a driver tries to change lanes, the first step is to find a suitable gap (time headway) in the destination flow. The gap size is dependent on the speeds of the lane changer and the vehicle that "comes from behind" (on the lane where the lane changer switches to). In case of a necessary lane change it also is dependent on the level of deceleration.

In case of a necessary lane change, the driving behavior parameters contain the maximum acceptable deceleration for the vehicle and the trailing vehicle on the new lane, depending on the distance to the emergency-stop position of the next connector of the route.

For the free lane change, VISSIM checks for the desired safety distance of the trailing vehicle on the new lane. This safety distance depends on the trailing vehicle speed and the speed of the lane changer. There currently is no way for the analyst to change the "aggressiveness" for these lane changes. However, changing the parameters for the desired safety distance (which are used for the vehicle following behavior) will affect the free lane changes as well. Consequently, the lane-changing model is closely related to the car-following model [36].

In the VISSIM software, the aggressiveness of lane change of a specific driving behavior can be defined with a set of parameters:

- Maximum Deceleration;
- -1 ft/s^2 per Distance; and
- Accepted Deceleration for the vehicle and the trailing vehicle on the new lane.

These parameters are shown on the entry screen Figure 4.2. In the Lane Change tab, there are five additional parameters:

- Waiting Time Before Diffusion – Defines the maximum amount of time a vehicle can wait at the emergency-stop position waiting for a gap to change lanes in order to stay on its route. When this time is reached the vehicle is taken out of the network (diffusion) and a message will be written to the error file denoting the time and location of the removal. The default value in VISSIM is 60 seconds.
- Minimum Headway (front/rear) – Minimum distance to the front vehicle for a lane change in standstill condition.
- To Slower Lane if Collision Time – Describes the minimum time headway towards the next vehicle on the slow lane so that a vehicle on the fast lane changes to the slower lane. The value for *To Slower Lane if Collision Time* is used only if *Lane Change Behavior* is set to *Right Side Rule* resp. *Left Side Rule*.
- Safety Distance Reduction Factor – The ratio multiplied to the original safety distance to calculate the reduced safety distance during lane changes.
- Maximum Deceleration for Cooperative Braking – The maximum deceleration that a vehicle uses to cooperate with a vehicle trying to change into the target lane [36].

Figure 4.2 Lane Change Parameters in the VISSIM Software

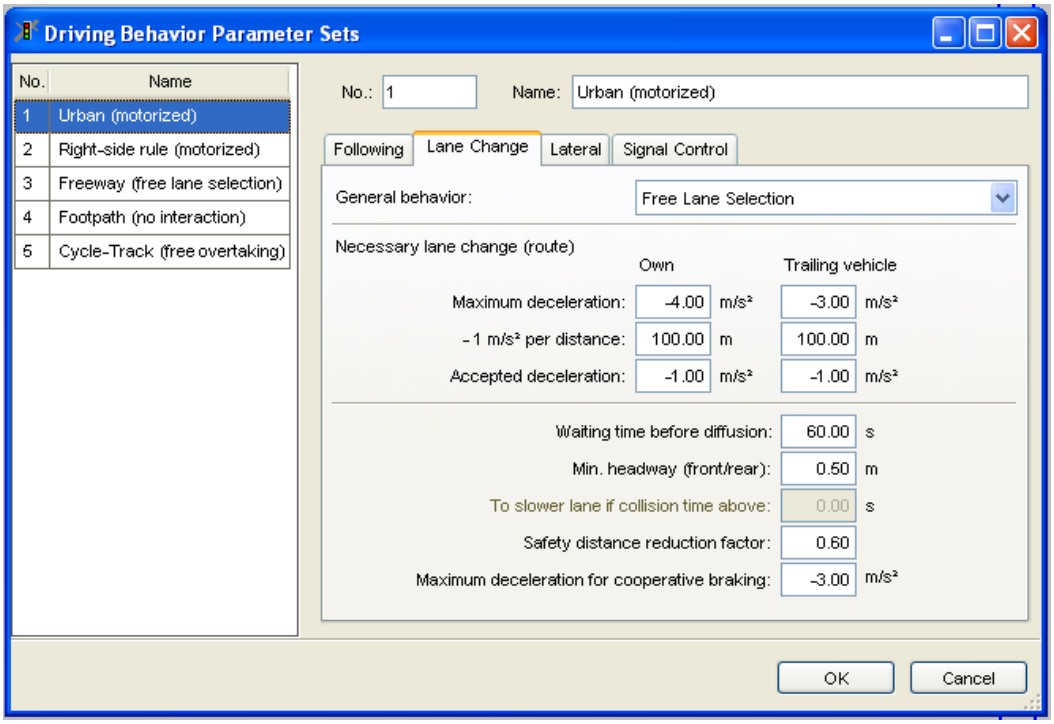

Vehicle Acceleration and Deceleration Models

VISSIM uses functions, which are defined as a set of points that are linearly connected with each other, to calculate vehicle acceleration and deceleration values. For each vehicle type, there are two acceleration and two deceleration functions that are predefined as default. These functions include: 'maximum acceleration,' 'desired acceleration,' 'maximum deceleration,' and 'desired deceleration.' Maximum acceleration is a function that defines the technically achievable maximum acceleration as the name implies. Similarly, maximum deceleration is a function that defines the maximum deceleration. Desired acceleration and deceleration functions are used for other situations in which the maximum acceleration and deceleration are not needed. These functions can be adjusted or newly created as needed through the "Base-Data-Functions" menu, as seen in Figure 4.3.

Figure 4.3 Maximum Acceleration

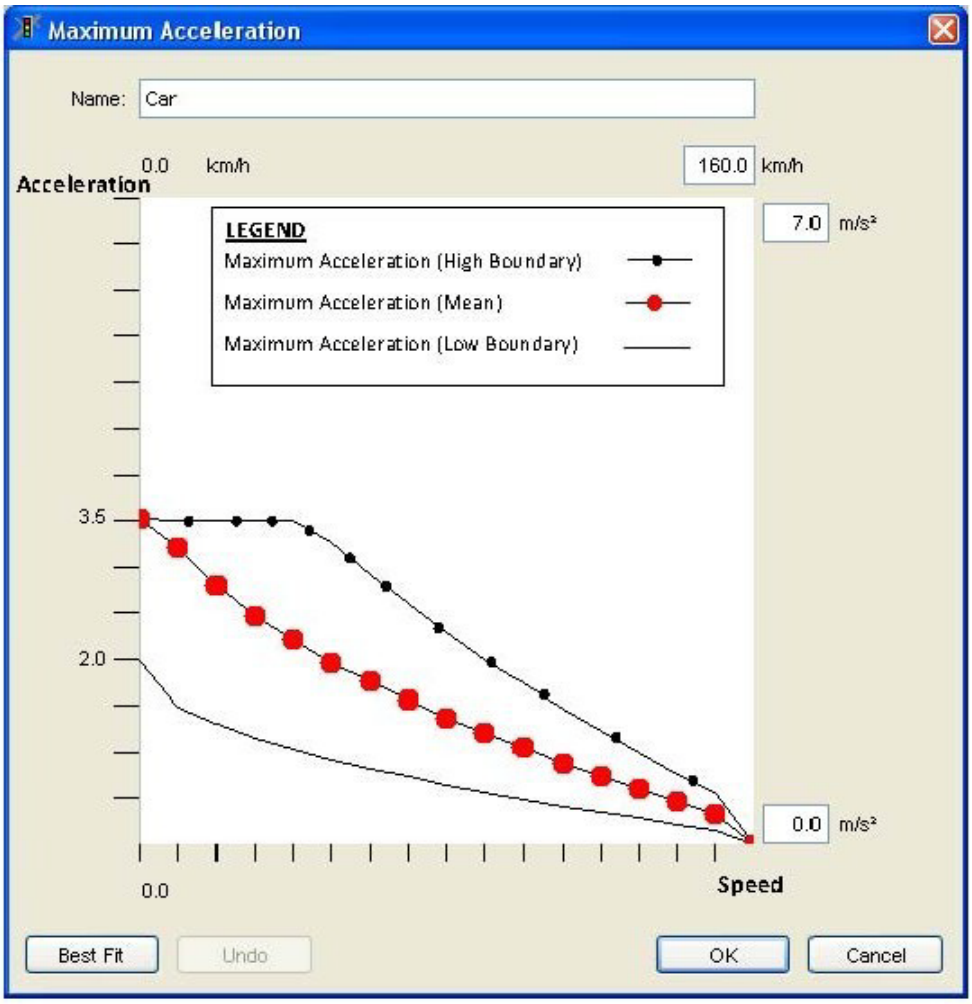

Gap Acceptance Model

The gap acceptance model in the VISSIM software is mainly divided into two categories: Priority Rule and Conflict Areas, as will be described in the following sections.

Priority Rule Control

The VISSIM software provides the user two ways to define gap acceptance behavior locally. The user can define a rule to assign the right-of-way for conflicting movements and to specify a minimum gap size at any location on the network.

The first method is to define a Priority Rule that consists of a stop line and a conflict marker or more. The stop line is defined as the location where lower priority vehicles wait until a suitable gap time or distance headway is available as shown in Figure 4.4 (a). The conflict marker is defined as the location where the user checks the gap time and headway. The right-of-way for non-signal protected conflicting movements

is modeled with priority rules. This applies to all situations where vehicles on different links/connectors should recognize each other. Vehicles within the same link will implicitly see each other, even if the link has multiple lanes. In the VISSIM software, the priority rule option provides two parameters for weather impact implementation: minimum gap time and minimum headway. The minimum gap time and the minimum headway should be defined at each of the conflict markers regardless of the number of opposing lanes as illustrated in Figure 4.4 (b). The maximum speed parameter controls the driver dependence on either the minimum gap time or headway; thus, the minimum gap time is the relevant condition for free flow traffic on the higher priority road and the minimum headway is the relevant condition for slow moving or queuing traffic [36].

It should be stated that for each signal control intersection in VISSIM, all conflicting movements that can run at the same time need to be secured using priority rules. In other words, in the case of signalized intersections with permissive left turns, the minimum gap time accepted by each driver could be adjusted using the Priority Rule option. Consequently, the impact of inclement weather on the gap acceptance behavior is possible.

Figure 4.4 Priority Rules Intersection

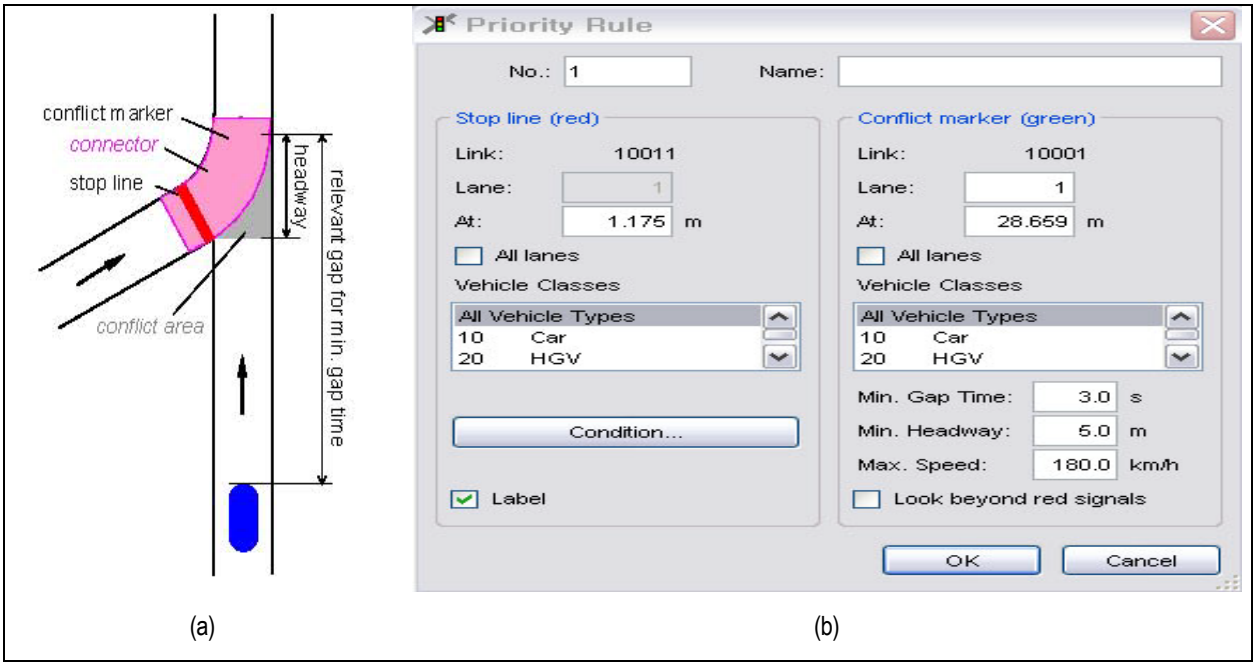

Conflict Area

The second method is to define a conflict area. A conflict area can be defined as a place where two links/connectors in the VISSIM network overlap as shown in Figure 4.5 (a). For each conflict area, the user can select which of the conflicting links has right-of-way (if any). For the definition of the conflict area, the priority conditions of the conflict, Visibility of the Links, Front Gap, Rear Gap, and Safety Distance Factor are used.

The priority of the conflict can be defined from the screen, as illustrated in Figure 4.5 (b). In the figure, while the green indicates the main road (right-of-way), the red represents the minor road. The Visibility is the maximum distance that a vehicle approaching can see on the other link. The Front Gap is the minimum gap time between the rear end of a higher priority vehicle and the front end of a lower priority

vehicle. The Rear Gap is the minimum gap time between the rear end of a lower priority vehicle and the front end of a higher priority vehicle. Finally, the Safety Distance Factor is a scale factor that is multiplied by the normal desired safety distance of a higher priority vehicle. The scaled distance is used to determine the minimum headway for a lower priority vehicle trying to merge in the main road [36]. Therefore, by adjusting the Front Gap and/or the Rear Gap value, the impact of the studied weather condition will be captured. Similarly, the same concept could be applied for stop sign control, weaving, and merging sections and roundabout intersections.

Figure 4.5 Conflict Areas

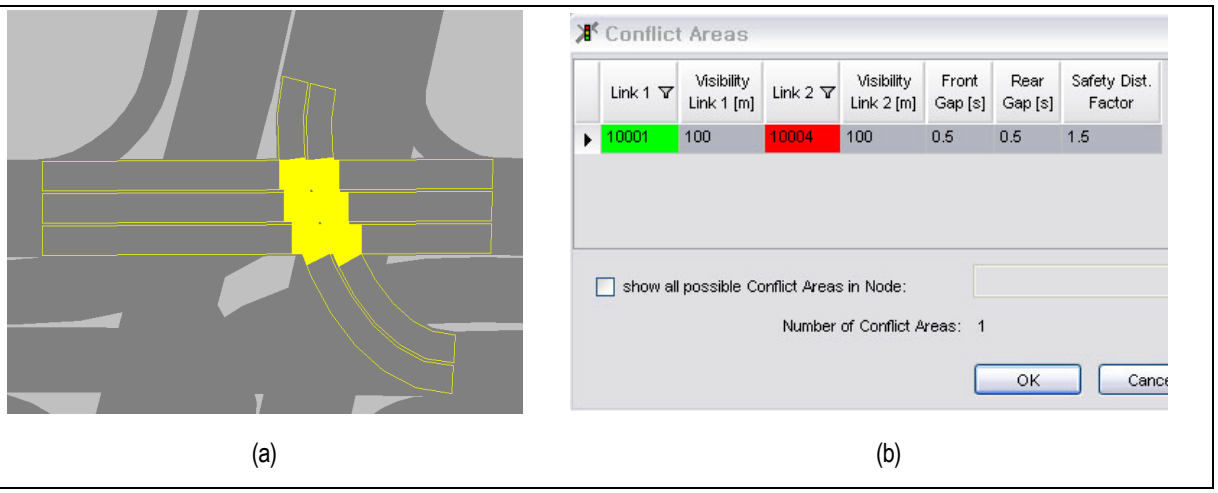

Integration Software

INTEGRATION software is a fully microscopic simulation model, as it tracks both the lateral and longitudinal movements of individual vehicles at a resolution of up to one deci-second. This microscopic approach permits the analysis of many dynamic traffic phenomena, such as shock waves, gap acceptance, and weaving [39].

The input data that are required to run the model are divided into fundamental data and advanced data. The fundamental data are essential to run the model (global simulation parameters, node characteristics, link structure, signal timing plan, Origin-Destination (O-D) traffic demands, and incidents description), while the advanced data allow optional model features to be activated (link-specific output options, the placement of lane additions, the degree of variability in vehicle speeds, and the critical gap sizes for opposed movements).

The following sections describe the models that can be modified to adjust for weather-related impacts.

Car Following Model

Once the vehicle has selected which lane to enter, the vehicle computes its desired speed on the basis of the distance headway between it and the vehicle immediately downstream of it, but within the same lane. This computation is based on a link-specific microscopic car following relationship that is calibrated

macroscopically to yield the appropriate target aggregate speed flow attributes for that particular link. The simulation process in INTEGRATION software uses the Van Aerde steady-state car-following model. The INTEGRATION car-following model, like the Gipps model, computes the vehicle speed as the minimum of the maximum vehicle speed based on vehicle dynamics and the desired speed based on the Van Aerde model formulation as:

$$u_n(t+\Delta t) = \min\left\{\begin{array}{l} u_n(t) + 3.6 \cdot \dfrac{F_n(t) - R_n(t)}{m}\Delta t, \\ \dfrac{-c_1' + c_3 u_f + \tilde{s}_n(t) - \sqrt{\left[c_1' - c_3 u_f - \tilde{s}_n(t)\right]^2 - 4c_3\left[\tilde{s}_n(t)u_f - c_1' u_f - c_2\right]}}{2c_3} \end{array}\right\} \quad (6)$$

Where:

- un(t) speed of vehicle n at time t (km/hr).
- c1, c2, c3 and c1' are variable headway constants.
- uf is the free flow speed (km/h).
- uc is the speed at capacity (km/h).
- sn(t) is the spacing at time (t).
- Fn(t) and Rn(t) are the resultant forces acting on vehicle n at time t.

The parameters c1, c2, c3, and c1' are calculated using the traffic stream model parameters as shown in Equations 7) and (8).

$$c_1 = \frac{u_f}{k_j u_c^2}\left(2u_c - u_f\right); \quad c_2 = \frac{u_f}{k_j u_c^2}\left(u_f - u_c\right)^2; \quad c_3 = \left(\frac{1}{q_c} - \frac{u_f}{k_j u_c^2}\right) \quad (7)$$

$$c_1' = \frac{u_f}{k_j u_c^2}\left(2u_c - u_f\right) + \max\left(\frac{u_n^2(t) - u_{n-1}^2(t)}{2b}, 0\right) \quad (8)$$

Where:

- u_c is the speed at capacity,
- u_f is the free-flow speed,
- k_j is the jam density, and
- q_c is the capacity.

As can be seen in the Equations (6), (7), and (8), the car-following model is characterized by the traffic stream model parameters. Consequently, the user needs to adjust these parameters to calibrate the car-following model corresponding to weather conditions through the use of File 2, which defines the link characteristics.

Lane-Changing Model

When a vehicle travels down a particular link, it may make discretionary lane changes, mandatory lane changes, or both. Discretionary lane changes are a function of the prevailing traffic conditions, while mandatory lane changes are usually a function of the prevailing network geometry and routing conditions. In the INTEGRATION software, in order to determine if a discretionary lane change should be made, each vehicle computes three speed alternatives each deci-second. The first alternative represents the potential speed at which the vehicle could continue to travel in its current lane, while the second and third choices represent the potential speeds that this vehicle could travel in the lanes immediately to the left and to the right of its current lane. These speed comparisons are made on the basis of the available headway in each lane, and pre-specified biases for the vehicle to remain in the lane in which it already is traveling or to move to the shoulder lane. In addition the vehicle computes the speeds that it could travel on across all the lanes every 0.5s so that it could potentially try to move to an HOV lane that is a couple of lanes away depending on the level of congestion on the lane.

For the vehicle headway in INTEGRATION, the user may specify the degree of randomness in the vehicle departure headways. When completely random headways are requested, they will follow a negative exponential distribution. Less randomness is obtained by utilizing a shifted negative exponential distribution. The above randomness is only imparted into the traffic stream by modifying the intervehicle trip departure headways. However, once the vehicles enter the network, subsequent en-route headways become modified as a function of vehicle speeds, lane-changing activities, merges and diverges, and traffic controls.

The file 'lanebias.dat' is an optional file in INTEGRATION that biases vehicles to change lanes within a specified distance of a downstream link. The parameters included in the file will override the lane bias internal to the model. The bias is only effective on the upstream link (field 2). Once the vehicle leaves the link the bias factor is no longer effective. Consequently, if the user wants to maintain a bias over a number of links, a separate line is required for each of the links. The bias is achieved by reducing the perceived speed in the lanes other than the biased lane. The user determines the reduction factor of perceived speed. We recommend a factor of 2.0, which results in a perceived speed that is half the actual speed. A factor of 2.0 entices vehicles to use the desired lane at low volumes; however, it has a minor effect at high volumes. If the user would like a more aggressive lane allocation a higher factor should be utilized. The distance at which the lane bias occurs is measured from the downstream end of the downstream link towards the upstream link. The location is varied randomly across the different vehicles in order to ensure that not all lane changing occurs at the same location. In addition, there is an optional file in INTEGRATION software called "lanechange.dat" that can be utilized to alter the default lane change parameters incorporated within the software [39].

INTEGRATION does allow for the bias factors to be adjusted for differences in behavior due to adverse weather by changing the bias towards different lanes. At this point we do not have adequate empirical data to calibrate the bias for inclement weather conditions. A technical report prepared for the FHWA study on Data Mining and Gap Analysis for Weather Responsive Traffic Management Studies used ESS and traffic detector data from Salt Lake City to show how shifts in lane usage could be evaluated under adverse weather conditions. However, calibration of bias factors would require an extensive study that accounts for a variety of factors such as precipitation intensity, lane configuration, spacing of exit and merge ramps and roadway geometry.

Vehicle Acceleration and Deceleration Models

INTEGRATION uses Equation 1) to calculate the maximum deceleration levels. Thus, in order to calibrate the maximum deceleration level the user just needs to adjust the friction coefficient values. INTEGRATION provides an additional input file called 'Max_acc.dat', which allows the user to specify vehicle characteristics. The characteristics include vehicle weight, vehicle length, proportion of mass on tractive axle, coefficient of friction, vehicle power, transmission efficiency, drag coefficient, frontal area, and rolling coefficients [39].

Vehicle dynamics models are used in the INTEGRATION software to calculate the maximum acceleration levels as described earlier with Equations 2 and 3. So the user can calibrate the acceleration model by adjusting the rolling coefficients through the 'Max_acc.dat' file.

Gap Acceptance Model

One of the most complex modeling tasks in estimating the capacity of both isolated and coordinated traffic signals is the treatment of permissive left turns and/or right turns on red. Within INTEGRATION, a microscopic gap acceptance model is utilized to reflect the impact of opposing flows on opposed left turners and right turners on red. This opposition is automatically customized by the model at each intersection by means of built-in logic. This logic specifies which opposing movements are in conflict with the movement of interest. The internal logic also determines which of the turning movements are opposed within a shared lane or shared link. The incorporation of this logic within INTEGRATION permits the model to evaluate the impact of protected versus permissive left turns. In addition, the gap acceptance logic can work concurrently with the queue spill-back model to determine when, or if, vehicles in a left-turn bay spill back into the through lanes, or conversely, when the through lanes spill back to cut-off entry into the left turn bays. The combination of lane striping, to change certain lanes from being exclusive to being shared, and the selective opposition of vehicles (depending upon the direction in which they are turning), permits the implicit computation of shared lane-saturation flow rates within the model. Exactly the same mechanism of the simulation of permissive left turns at traffic signals can be utilized to model the impact of stop or yield signs. In this case, different critical gap sizes may need to be identified, and several links may concurrently oppose a given turning movement. The simulation logic within INTEGRATION also automatically models the hierarchy in gap acceptance priority of one movement over a lower priority movement.

Vehicles are often required to find acceptable gaps in an opposing flow, typically when attempting unprotected movements at either signalized or partially controlled intersections. The user has the option to specify the number of links that may oppose the current link, in which case the default gap size is assumed. Alternatively, all of the neighboring links may be set to represent an opposition to the current link and an acceptable base gap size may be specified. This feature is invoked by specifying the negative equivalent of the desired gap size (seconds) in the field of the first opposing link. The base gap size default to the model, if an opposing link is specified explicitly, is set to 4.5 seconds. In addition, if the number of opposing lanes for the vehicle to cross is limited to one, then 0.5 seconds will be subtracted to the acceptable gap for a right turn movement and 0.5 seconds will be added to the acceptable gap for a left turn movement. An additional 1.5 seconds is added for a stop sign. No additional time will be added to the basic gap size if a straight through movement is being attempted, but another 0.5 seconds will be added to the acceptable gap size for each additional lane the vehicle must cross in order to complete the maneuver. For example, if a vehicle must turn left across two lanes of opposing flow, the acceptable gap size will be 5.5 seconds, assuming a base gap size of 4.5 seconds.

It has been observed that drivers will typically accept a smaller gap size as they wait longer. The INTEGRATION model incorporates this behavior by utilizing a linear decay function, which reduces the acceptable gap size from the computed maximum value to zero over a period of 120 seconds. The decay process is initiated each time the speed of a waiting vehicle makes the transition from above the speed-at-capacity to below this threshold value. The user has more flexibility to override the gap acceptance logic using the 'ops_gaps.dat' file, as will be described later. The 'ops_gaps.dat' is an optional file that permits the user to set link-specific gap acceptance critical gaps. This file could be used to input the critical gap size corresponding to each opposing lane separately which is considered more relevant compared to other simulation software [39].

The critical gap in the INTEGRATION software can be estimated as

$$t_c = \frac{-\beta_o - L \times (\beta_7 + \beta_8 RW + \beta_9 SS)}{\beta_2 DD + \beta_3 DW + \beta_4 DI + \beta_5 DS + \beta_6 RW + \beta_7 SS} \quad (9)$$

Where β1, β2, …, βn are the estimated regression coefficients as defined in Table 4.3; L is the lane indicator variable of the offered gap (1=First lane, 2=Second lane and 3=Third lane); DD, DW, DI, DS, RW, SS are dummy variables indicating the six different weather categories as defined in Table 4.4. Each weather independent variable is a dummy variable (0 or 1) and the existence of one weather category (=1) means that all other weather category variables are eliminated (=0).

Table 4.3 Coefficients for Gap Analysis Equation

β_i	Estimated Mean Values	Std Error	L-R ChiSquare	Prob>ChiSq (p Values)	Lower CL	Upper CL
β_o	-4.744	0.161	1,293.569	<.0001	-5.060	-4.428
β_1	1.021	0.052	784.843	<.0001	0.931	1.122
β_4	-0.188	0.051	13.351	0.0003	-0.288	-0.087
β_5	-0.126	0.040	9.649	0.0019	-0.206	-0.046
β_6	-0.137	0.055	6.062	0.0138	-0.245	-0.028
β_2	-0.237	0.0571	17.275	<.0001	-0.349	-0.125
β_3	-0.270	0.060	20.421	<.0001	-0.387	-0.153
β_7	-0.898	0.126	50.412	<.0001	-1.167	-0.650
β_8	0.357	0.142	6.313	0.0120	0.078	0.635
β_9	0.348	0.153	5.126	0.0236	0.047	0.649

Table 4.4 Different Weather Condition Categories

Weather Category	Weather Condition	
	Precipitation	Roadway Surface
Category 1 (DD)	Dry	Dry
Category 2 (DW)	Dry	Wet
Category 3 (DI)	Dry	Icy
Category 4 (DS)	Dry	Snowy
Category 5 (RW)	Rain	Wet
Category 6 (SS)	Snow	Snowy

Actual critical values by lane that could be implemented directly into the INTEGRATION software for the different weather categories are summarized in Table 4.5.

Table 4.5 Critical Gap Values by Lane for Different Weather Categories

Weather Category	(tc) Critical Gap(s)		
	Lane 1	Lane 2	Lane 3
Category 1 (DD)	6.19	6.58	7.03
Category 2 (DW)	7.25	7.74	8.27
Category 3 (DI)	6.93	7.31	7.84
Category 4 (DS)	7.09	7.45	8.03
Category 5 (RW)	6.88	7.22	7.75
Category 6 (SS)	7.41	7.77	8.38

Summary of Parameters used in VISSIM and INTEGRATION Software

As explained earlier, the car-following, deceleration, acceleration, and gap-acceptance models are the most critical components in the microscopic simulation software tools and need to be adjusted to capture the impacts of inclement weather. The functions and parameters related to those models vary depending on the structure of simulation software. The parameters and functions or additional files are used in the VISSIM and INTEGRATION software in order to adjust the models corresponding to inclement weather conditions. The descriptions of detailed parameters, functions, and files are summarized in Table 4.6.

Table 4.6 VISSIM and INTEGRATION Parameters

Models	VISSIM	INTEGRATION
Car-Following Model	‘‘Driving Behavior Parameter Sets’’ • Wiedemann 74 parameters • Wiedemann 99 parameters	‘‘File2’’: Link characteristics file • Free-flow speed, speed-at-capacity, and saturation flow rate
Deceleration Model	‘‘Base Data – Functions’’ • ‘‘Maximum deceleration’’	‘‘Max_acc.dat’’ file • Coefficient of friction
Acceleration Model	‘‘Base Data – Functions’’ • ‘‘Maximum acceleration’’	‘‘Max_acc.dat’’ file • Rolling coefficients and coefficient of friction
Gap-Acceptance Model	‘‘Priority Rules’’ and ‘‘Conflict Areas’’	‘‘File2’’: Link characteristics file • Critical gap or ‘‘Ops_gaps.dat’’ • Critical gap

Inclement Weather Impact on the Simulation Parameters of CORSIM Simulation Software

Introduction of CORSIM Software

The CORSIM (CORridor SIMulation) simulation software consists of an integrated set of two microscopic simulation models that represent the entire traffic environment ‘‘NETSIM and FRESIM.’’ NETSIM represents traffic on urban streets (and arterial streets) and intersections, and FRESIM represents traffic on freeways [30]. Microscopic simulation models represent movements of individual vehicles, which include the influences of driver behavior. The time-varying portion of the simulation analysis of CORSIM simulation Software consists of a sequence of ‘‘time periods’’ specified by the user. For each time period, the specified input data remains the same unless changed in a subsequent time period. In CORSIM, the user can specify up to 19 time periods and must specify the conditions that have changed during each period. The first time period is distinctive as it contains the input data that remains the same for all simulation time. Thus, the first time period is used for global network data that is applied to all subnetwork data (the bus operation routes as an example), including a NETSIM subnetwork and/or a FRESIM subnetwork [30].

Consequently, the input stream consists of a sequence of ‘‘blocks’’ of data records, with each block defining the conditions that apply to one time period. Each block of data records for a time period is subdivided into ‘‘sections’’ of data records. Accordingly, the user can allocate the traffic stream parameters related to the specific weather condition in the corresponding time period. The input data file (*.trf) is divided into a series of 80-column records and many Text Editor program can be used for creating/editing this file. Each file consisting of Record Types 00 through 210 where each record type (row number) indicate a specific list of input data [30].

Calibration of Traffic Stream Parameters

Traffic parameters provide CORSIM with a description of how traffic behaves, and they can be specified by a variety of record types. Examples of traffic parameters include the response to gaps in traffic for turning vehicles, the distribution of the desired free-flow speed, and vehicle types. There are several CORSIM inputs that are known as calibration parameters. These calibration parameters include driver behavior and vehicle performance parameters for the NETSIM and the FRESIM simulation models [30].

The driver behavior parameters of NETSIM model consist of: queue discharge headway and start-up lost time, distribution of free flow speed by driver type, mean duration of parking maneuvers, lane change parameters, maximum left and right turning speeds, probability of joining spillback, probability of left turn jumpers and laggers, gap acceptance at stop signs, gap acceptance for left and right turns, pedestrian delays and driver familiarity with their path [30]. For FRESIM model, the driver behavior parameters include: mean start-up delay at ramp meters, distribution of free flow speed by driver type, incident rubbernecking factor, car-following sensitivity factor, lane change gap acceptance parameters, maximum deceleration values and parameters that affect the number of discretionary lane changes [30]. Vehicle performance calibration parameters for both NETSIM and FRESIM include speed and acceleration characteristics, fleet distribution, and passenger occupancy.

Subsequently, the traffic stream parameters that should be calibrated for the inclement weather impact could be divided into parameters on freeway facilities using Freeway Simulation (FRESIM) and parameters on arterial streets using Network Simulation (NETSIM), as described in the following paragraphs.

NETSIM

As mentioned before, the NETSIM simulation models deals with urban streets and intersections in the simulation network. Consequently, the calibration of gap acceptance models at intersections for different weather conditions is considered a part of NETSIM simulation models.

Firstly, the type of intersection control (Stop sign, yield sign, or signal control) is specified on Record type (number) 35 and 36 of the input data file [30].

Thereafter, for changing the minimum acceptable gap (critical gap) value for the drivers corresponding to different weather conditions, the following input data records could be changed [1, 2]:

- Record Types 142 and 143: the acceptable gaps values for turning vehicles pulling out onto a main street at stop signs, or
- Record Type 145: the acceptable gaps values in the opposing traffic for vehicles turning onto a side street across traffic (for permissive left turn maneuver at signalized intersections).

FRESIM

The calibrated FRESIM network parameters could be focused on the car following (the Pitt model), lane changing, and free-flow speed, in addition to vehicle acceleration and deceleration behavior variables, because the other driver behavior parameters apply to intersections on surface streets.

The CORSIM simulation software uses the Pitt car-following model as

$$s_n(t) = s_j + c_3 \frac{u_n(t+\Delta t)}{3.6} + bc_3 \frac{\Delta u_n(t+\Delta t)^2}{3.6^2} \quad (10)$$

where $s_n(t)$ is the vehicle spacing between the front bumper of the lead vehicle and front bumper of following vehicle at time t(m), s_j is the vehicle spacing when vehicles are completely stopped in a queue (m), c_3 is the driver sensitivity factor (s), b is a calibration constant that equals 0.1 if the speed of the following vehicle exceeds the speed of the lead vehicle, otherwise it is set to zero (h/km), Δu is the difference in speed between lead and following vehicle (km/h) at instant $t + \Delta t$, and u_n is the speed of the following vehicle at instant t (km/h).

Rakha and Gao [32] developed procedures for relating steady-state car-following model parameters to the four key macroscopic traffic stream parameters: free flow speed, speed at capacity, capacity, jam density (uf, uc, qc, and kj, respectively) as

$$c_3 = 3600\left(\frac{1}{q_c} - \frac{1}{k_j u_f}\right) \quad (11)$$

Using these calibration procedures the impact of inclement weather can be captured by adjusting the four traffic stream parameters using the WAFs that were presented earlier in [32], and then modifying the car-following parameters using Equation (11).

For the calibration of vehicle acceleration behavior under inclement weather in CORSIM, the modeler can provide a speed-acceleration relationship. The relationship can be derived using the vehicle dynamics procedures.

For the case of deceleration model calibration, the CORSIM software does not allow for the calibration of vehicle deceleration levels (not possible given that the calibration constant "b" is fixed at 0.1).
As a result, for simulating the impact of inclement weather in CORSIM, the following records (parameters) of the input file for modeling car following behavior could be changed [1, 2]:

- Record Type 68: the embedded car-following sensitivity factors;
- Record Type 69: the lag to accelerate and decelerate when drivers are making required maneuvers;
- Record Type 70: the minimum separation for vehicle generation and lane-changing parameters, such as the time to complete a lane change, the percentage of cooperative drivers, and non-emergency deceleration; and
- Record Type 147: Variation of free flow speed around the user-specified free-flow speed (variance of mean free flow speed).

CORSIM Summary

The CORSIM simulation software algorithm is divided into two types of simulation models (NETSIM and FRESIM). Each simulation model needs specific parameters for the data file input.

The weather-related traffic parameters in the CORSIM traffic microsimulation software are then specified for each simulation model. Simply, the values of the calibrated traffic stream parameters could be

allocated in the specific Record Type (row identification number) depending on the desired weather condition for each time period.

In order to determine the calibrated values for all traffic stream parameters of the CORSIM, more field data needs to be collected beside the past research results. Given that this is often not possible and/or practical for some parameters; the correct parameter values could only be estimated through the findings of past research and/or based on engineering judgment [31].

4.4 Demonstration of Inclement Weather Modeling

In order to demonstrate how inclement weather can be modeled in traffic simulation software, a single signalized intersection is constructed and modeled using the INTEGRATION and the VISSIM software. The geometry of the intersection used in this demonstration is illustrated in Figure 4.6. (There is no significance in the color of the vehicles. The red and green bars represent the stop lines.) Note that the left turns from the west and east approaches are modeled as permissive left turns.

Figure 4.6 Geometry of Intersection

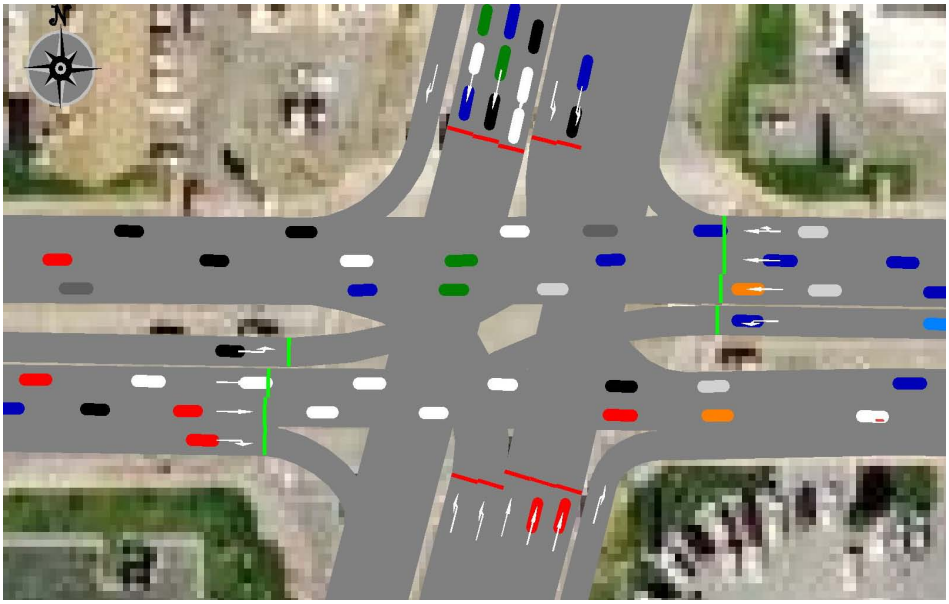

There are several ways to incorporate weather in traffic simulation models depending on the objectives of the study. However, this demonstration mainly focuses on the calibration of the car-following and gap-acceptance models to capture the weather impacts. The simulation demonstration can be summarized in two steps. The first step involves calculating the adjusted traffic stream parameters based on the weather conditions of interest in order to calibrate the car-following models. In this study, we demonstrate three weather conditions, dry, rain and snow conditions. Specifically, the weather adjustment factors that were developed in our previous study were utilized to update the traffic stream parameters. The second step involves calibrating the gap acceptance behavior.

Car-Following Parameters Corresponding to Rain and Snow Conditions

For the simulation of dry condition (base case), the traffic stream parameters, which are described in Table 4.7 were used for the car-following model calibration. Those parameters were multiplied by the weather adjustment factors (WAF), described in Table 4.8, to model the impact of inclement weather on the traffic stream parameters. For examples, the rain WAF for qc, which is 0.89, was multiplied by the base case capacity (1,900 vph) to compute the capacity, qc (1,695 vph) corresponding to the rain condition. The updated traffic stream parameters were used as input parameters to the INTEGRATION software. Specifically, File 2, which is the Link Characteristic file, includes the traffic stream parameters that were input to the software.

Table 4.7 Traffic Stream Parameters for Dry Conditions

Classification	North and South Arterial (N-S)	East and West Arterial (E-W)
Free-flow speed (u_f) (km/hr)	88	72
Speed-at-capacity (u_c) (km/hr)	70	40
Capacity (q_c)	1,900	1,900
Jam density (k_j)	170	170

Table 4.8 Weather Adjustment Factors and Updated Traffic Stream Parameters

	Rain			Snow		
		(a) Adj. Value			(b) Adj. Value	
Classification	WAF	N-S	E-W	WAF	N-S	E-W
Free-flow speed (u_f) (km/hr)	0.91	80.4	65.8	0.96	84.0	68.8
Speed-at-capacity (u_c) (km/hr)	0.84	58.5	33.4	0.96	66.9	38.2
Capacity (qc)	0.89	1,695	1,695	0.88	1,666	1,666

While the INTEGRATION software uses traffic stream parameters to calibrate the car-following model, the VISSIM software uses different procedures and parameters. First, the desired speeds should be changed based on the changes in the free-flow speeds. In this demonstration, the updated free-flow speeds in Table 4.8 were used as the mean desired speeds for the North-South and East-West arterials. Second, the traffic stream parameters in Table 4.7 need to be converted to the corresponding VISSIM car-following parameters. Among the VISSIM parameters, the standstill distance can be derived from the jam density since the jam density is the inverse of the standstill vehicle spacing. For the calculation, a vehicle length of 4.45 meter was used because it is the mean length of passenger vehicles modeled in the VISSIM software. There are two other parameters, which are BXadd and BXmult. The two parameters are used to calculate the safety distance (BX). In this demonstration, the methodologies that Rakha and Gao proposed were used to compute these parameters using the traffic stream parameters [30]. A brief description of the procedures follows.

First, the expected value of the desired safety distance E(BX) is calculated using Equation (12). In this demonstration, the value of α was set to 2.

$$E(BX) = 1000\sqrt{3.6}\sqrt{u_f}\left(\frac{1}{\alpha q_c} - \frac{1}{k_j u_f}\right) \tag{12}$$

Where,

- α = ratio of the maximum following distance (SDX) to the minimum following distance (ABX), which ranges from 1.5 to 2.5.;
- q_c = capacity;
- u_f = free-flow speed; and
- k_j = jam density.

$$BX = BX_{add} + BX_{mult} \times RND \tag{13}$$

Where,

- *RND* = a normally distributed random variable with a default mean value of 0.5 and a standard deviation of 0.15.

Given that the value of *BX* already is known, the values of BX_{add} and BX_{mult} can be calculated if the value of *RND* and the relationship between BX_{add}, and BX_{mult} are known. For the calculation, the value of 0.5 was used as *RND* because this is the mean value. Also, the relationship described in Equation 3 was derived from the default parameters used in the VISSIM software.

$$BX_{mult} = BX_{add} + 1 \tag{14}$$

The standstill, E(BX), BXadd and BXmult corresponding to the weather conditions were calculated using the described procedures and are summarized in Table 4.9.

Table 4.9 Car-Following Parameters for VISSIM

Classification	(a) Dry		(b) Rain		(c) Snow	
	N-S	E-W	N-S	E-W	N-S	E-W
Standstill Distance	1.43					
E(BX)	3.49	2.92	3.77	3.16	4.00	3.38
BXadd	2.00	1.61	2.18	1.78	2.33	1.92
BXmult	3.00	2.61	3.18	2.78	3.33	2.92

Gap-Acceptance Parameters Corresponding to Rain and Snow Conditions

As described earlier, the critical gaps used as input to the simulation software were calculated using the previous study results. Specifically, the ratios of critical gaps under the rain and snow conditions to that of

the dry condition, which were obtained from the previous studies, can be seen in Table 4.10, Column (a),. For the simulation of dry condition (base case) using the INTEGRATION software, the default critical-gap parameters were used and those values were updated based on the corresponding weather conditions by multiplying the corresponding ratios by the default values shown on Table 4.10.
For the VISSIM models, the critical gaps used in the INTEGRATION models were also used. Specifically, Priority Rules were used and they require minimum gap times, which are the times required for approaching vehicles to reach the conflict marker (the beginning of conflicting area), as their critical input. The values of critical gap in Table 4.10 were used as the minimum gap times.

Table 4.10 Calculation of Critical-Gaps

Weather Condition	(a)[a] Ratio of Critical Gap to Dry Condition	(b) Critical Gap (sec)
Dry	1.000	5.00
Rain	1.104	5.52
Snow	1.190	5.95

Figures in Column (a)[a] are the field-measured values from the previous study.

Using the INTEGRATION and VISSIM Software

Using the weather-specific calibrated car-following and gap-acceptance parameters, the weather impact on the network performance was modeled using the INTEGRATION and VISSIM software. In summary, Table 4.11 describes the list of parameters, the values, and which file or module the users should use to incorporate the parameters.

Table 4.11 Summary of Model Parameters

Classification			INTEGRATION	VISSIM
Free-flow speed (Speed limit)			Free-flow speed in File2	Desired Speed Distribution
Car-following model	Associated file or module name		File2 – Link characteristics file	Driving behavior
	List of Parameters		Free-flow speed Speed-at-capacity Jam density Capacity	Average standstill distance Additive part of safety distance Multiplicative part of safety distance
	Values of Parameters	Dry	Table 4.1	Table 4.3 (a)
		Rain	Table 4.2 (a)	Table 4.3 (b)
		Snow	Table 4.2 (b)	Table 4.3 (c)
Gap-acceptance model	Associated file or module name		Ops_gaps.dat	Priority Rule
	List of Parameters		Critical gap	minimum gap time
	Values of Parameters		Table 4.4 (b)	Table 4.4 (d)

Simulation Results

Given the INTEGRATION and VISSIM models, one hour of simulation was repeated 20 times with different random number seeds for each simulation model. The impact of the rain and snow were evaluated by comparing the network-wide measures of effectiveness (MOE). The INTEGRATION simulation results demonstrate that the impacts of the rain and snow are significant, as summarized in Table 4.12. The results demonstrate a reduction in the average speed and an increase in the total delay, stopped delay, number of vehicle stops, and vehicle fuel consumption levels with the introduction of rain and snow, as illustrated in Figure 4.7. The impact of snow conditions was found to produce more significant negative impacts.

While the mean INTEGRATION MOEs were significantly different from each other at a 5 percent significance level, the differences in MOEs for the VISSIM model were less evident as demonstrated in Figure 4.8. For example, the differences in the average speed between the dry, rain and snow conditions were less than 1 km/h in the INTEGRATION analysis although they were statistically different. The differences observed in VISSIM were not significant, however.

Table 4.12 Mean Values of MOEs

		Average Statistics					Total Statistics			
Classification	Weather	Speed (km/h)	Total Delay (sec/veh)	Stopped Delay (sec/veh)	Stops (stops/veh)	Fuel (l/veh)	Total Trip	Total Delay (h)	Stopped Delay (h)	Total Stop
INTEGRATION	Dry	45.7	61.0	28.9	1.25	0.1459	7,882	133.6	63.2	9,851
	Rain	38.2	79.7	34.5	1.35	0.1486	7,803	172.8	74.7	10,537
	Snow	34.7	98.7	41.0	1.41	0.1578	7,701	211.1	87.6	10,882
VISSIM	Dry	36.5	69.2	53.1	1.29	[a]-	6,813	136.8	105.0	9,211
	Rain	35.6	70.6	53.8	1.29	[a] -	6,788	139.2	106.1	9,145
	Snow	35.6	72.3	55.0	1.29	[a] -	6,783	142.5	108.4	9,139

[a] Fuel consumption is not directly calculated in VISSIM.

Figure 4.7 Plots of Means and 95 Percent Confidence Intervals for the INTEGRATION Results

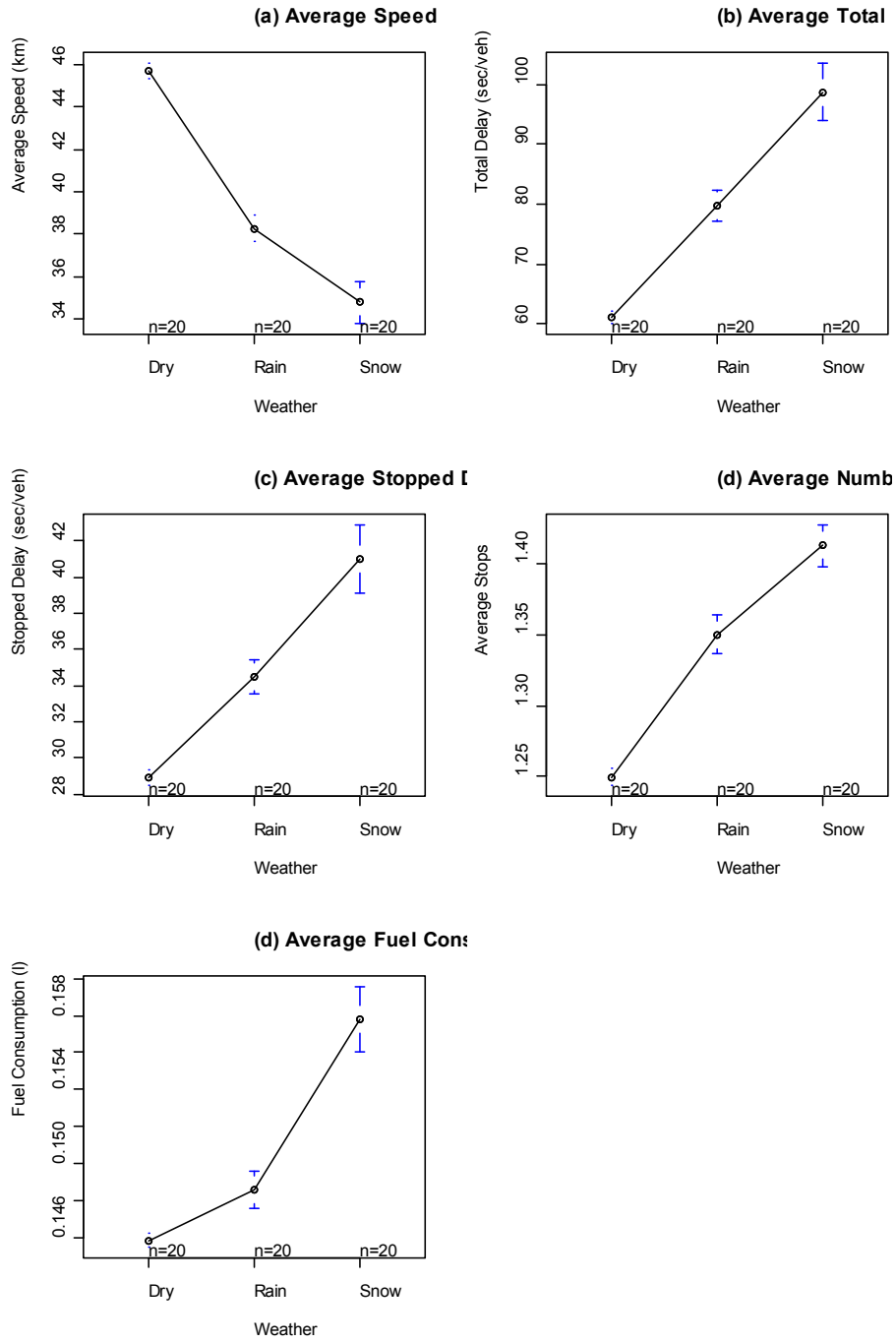

Figure 4.8 Plots of Means and 95 Percent Confidence Intervals for the VISSIM Results

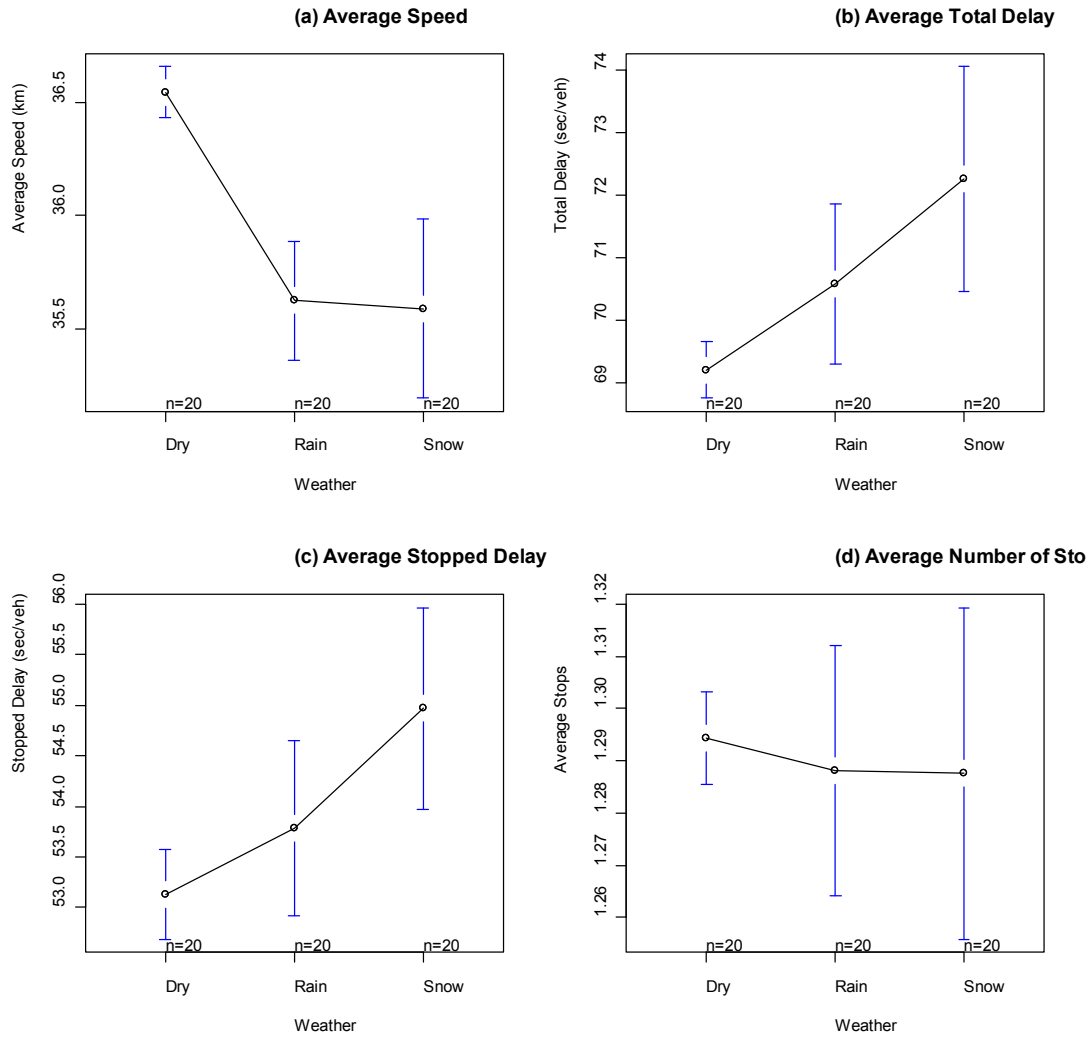

Model Demonstration Findings

The study demonstrated the procedures for calibrating the car-following and gap-acceptance parameters within the INTEGRATION and VISSIM models in order to quantify the impact of inclement weather on traffic behavior. Specifically, the demonstration identified the associated files and/or modules for the calibration of inclement weather parameters.

While the rain and snow conditions significantly affected the traffic flow conditions in the case of the INTEGRATION simulation runs, the weather impacts were not significant for the VISSIM results. It is difficult to identify the reason the simulation results were different from each other. Although the INTEGRATION simulation results appear to be more logical, we need to validate these results against field observations. Because of these differences, which cannot be explained based on the existing analysis, we recommend modeling the intersection in Christiansburg and comparing the simulation results to the field observations for various weather conditions. This exercise will serve as an effort to

validate the simulation findings. The results of this demonstration appear to warrant using the INTEGRATION model for intersection car-following and gap acceptance analyses since more intuitive results were produced. Additional experience is needed, however, to reach a definitive conclusion.

4.5 Findings and Conclusions

The research identified a general approach to calibrate microscopic simulation models to reflect inclement weather and roadway conditions. Specifically, the research identified the car-following, deceleration, acceleration, and gap-acceptance parameters that require calibration and demonstrated why they need to be calibrated. The research then identified the simulation parameters that require calibration in the VISSIM and INTEGRATION software.

First, in the case of the VISSIM software the car-following sensitivity factors and deceleration and acceleration functions were presented. Subsequently, modeling the impact of inclement weather on gap acceptance behavior was demonstrated. The gap acceptance situation in the software can be divided into two categories: Priority Rule and Conflict areas. For the Priority Rule, a stop line and a conflict marker or more are defined. The stop line is defined the location where lower priority vehicles wait until a suitable gap time or a sufficient distance headway is available. The signalized intersection with permissive left turn is considered a special case for priority rule option in VISSIM by only adjusting the minimum acceptable gap regardless the number of opposing lanes and waiting time. The second category is the Conflict Area option which can be defined wherever two links/connectors in the VISSIM network overlap. For each conflict area, the user can select which of the conflicting links has right-of-way (if any), Visibility of the links, Front Gap, Rear Gap, and Safety Distance Factor are used.

Finally, the parameter adjustments for the INTEGRATION software were explained. The INTEGRATION software follows the Van Aerde steady-state car-following model which can be calibrated to different weather and roadway conditions by changing three traffic stream parameters (free-flow speed, speed-at-capacity, and saturation flow rate). Thereafter, the parameters, which include friction coefficient and rolling coefficients, used to adjust the acceleration and deceleration models were presented. The gap acceptance modeling also was presented. The simulation logic within INTEGRATION automatically models the hierarchy in gap acceptance priority of one movement over a lower priority movement. Vehicles are often required to find acceptable gaps in an opposing flow, typically when attempting unprotected movements at either signalized or partially controlled intersections. The user has the option to specify the number of links that may oppose the current link, and the corresponding minimum acceptable gap per lane. The gap acceptance modeling process in INTEGRATION gives the user, flexibility for studying different weather conditions for any type of intersection control and geometric design.

These findings could be used for further research related to the impact of inclement weather on driving behavior using different simulation software packages. Additionally, in the future, the procedures presented could be applied to a sample network to demonstrate the potential network-wide impacts of inclement weather.

Finally, the calibration of microscopic simulation models for the quantification of the weather impacts on the traffic flow conditions was demonstrated using the INTEGRATION and VISSIM tools so that the users can better understand the modeling procedures from a practical standpoint. Specifically, the demonstration described which parameters need to be calibrated and how to adjust these parameters to

reflect inclement weather conditions. This demonstration constructed the simulation models for dry, rainy, and snowy conditions. In each of the models, the car-following and gap-acceptance model parameters were calibrated to model the corresponding weather conditions. Based on the simulation results from the INTEGRATION model, the impact of the rain and snow on the average speed, average total delay, average stopped delay, average number of stops, and average fuel consumption were found to be statistically significant. However, the differences in the MOEs for the VISSIM results were less evident. Consequently, further validation is required using field measurements.

5.0 Summary and Recommendations

This report documents the results of three distinct but related research projects. Each of these projects confirmed the hypotheses that weather-related adjustment factors can be developed from both test-track and field data, and utilized in microsimulation models. It is clear however that additional research is needed, particularly for ice and snow conditions, so that weather-responsive traffic management strategies can be more thoroughly modeled before they are tested in the field. The results of the three research efforts are summarized below.

5.1 Impact of Icy Conditions on Driver Car Following Behavior

The objective of this task was to quantify the impact of icy roadway conditions on driver car-following behavior. The data used in the study were gathered in Japan in a controlled environment under dry and icy roadway conditions. The collected data were used to calibrate the Van Aerde car-following model subject to vehicle acceleration and deceleration constraints. Using the calibrated car-following parameters, the effects of icy roadway conditions on the driver capacity (qc), speed-at-capacity (uc), free-flow speed (uf), jam density (kj), and the driver perception-reaction time (PRT) were compared using one-way ANOVA and Kruskal-Wallis tests.
The impact of icy roadway conditions on the roadway free-flow speed, speed-at-capacity, capacity, and PRT were found to be significant. Specifically, icy roadway conditions reduced the mean free-flow speed, speed-at-capacity, and capacity by 28 percent, 13 percent, and 46 percent, respectively, compared to dry roadway driving. The mean PRT for icy conditions was found to take 13 percent longer than driving under dry conditions. The longer PRTs could be attributed to the fact that the drivers drove at lower speeds and larger spacing compared to driving under dry conditions. The calibrated parameters were modeled using beta, gamma, lognormal, and generalized extreme value (GEV) distributions. The study demonstrated that the GEV distribution is most suited for modeling differences in driver behavior.

Additionally, the study demonstrated that the impacts of icy roadway conditions on the steady-state speed-flow-density relationship are significant. When comparing the flow rates and speeds at the same density levels, the maximum flow difference is 994 veh/h/lane, which happens at the density of 58 veh/km/lane. The maximum speed difference is 23 km/h, which happens at the density of 33 veh/km/lane. The study demonstrated that the GEV distribution is suitable for modeling differences in driver behavior.

The findings from this study have implications for weather responsive traffic management strategies because they can be used to calibrate microscopic simulation software in order to quantify the impact of icy conditions on transportation system efficiency. However, additional tests of driver response in icy conditions are needed, preferably field test under operating conditions. This will probably require targeted demonstrations, since ice is a rare condition and many ESS do not measure icy conditions accurately enough for research purposes. Naturalistic driving studies and On-Board Unit data gained through the IntelliDrive program provide a good potential opportunity to increase the effectiveness of research on icy conditions.

5.2 Inclement Weather Impact on Driver Left-Turn Gap Acceptance Behavior

The study gathered field data at a signalized intersection near Blacksburg, Virginia (a total of 11,114 observations of which 1,176 were accepted and 9,938 were rejected gaps) over a six-month period in an attempt to characterize driver left-turn gap acceptance behavior under various weather and roadway surface conditions. Logistic regression models were calibrated to the data and compared in order to identify the best model for capturing driver gap acceptance behavior. The models revealed that drivers are more conservative during snow precipitation compared to rain precipitation. In the case of the roadway surface condition, drivers surprisingly require larger gaps for wet surface conditions compared to snowy and icy surface conditions, but as would be expected, require the smallest gaps for dry roadway conditions. There are several possible explanations to these results. One of these interpretations is that drivers are more cautious on rainy and wet surface conditions compared to snowy and icy conditions and therefore are less aggressive in accepting a gap. Drivers may also not immediately see or perceive ice or thin snow on the road compared to a wet surface, which underscores the importance of road weather advisory strategies during these conditions. Moreover, these findings may reflect visibility more than surface condition and a driver could overestimate the offered gap size value compared to other weather conditions due to low visibility condition during rain. However, the inclement weather impact on gap acceptance behavior requires further data collection at other locations in other cities to validate these findings.

In addition, the models show that the drivers require larger gaps as the distance required to clear the conflict point increases. The study also illustrates how inclement weather and number of opposing lanes affects permissive left-turn saturation flow rates. Using the study findings inclement weather signal timings can be implemented within traffic signal controllers. The traffic signal controller could include an inclement weather signal timing plan that accounts for the reduction in the opposed saturation flow rates. It is anticipated that this research will contribute to enhance intelligent transportation system (ITS) and IntelliDrive™ applications.

5.3 Modeling Inclement Weather Impacts on Traffic Stream Behavior

The research identified a general approach to calibrate microscopic simulation models to reflect inclement weather and roadway conditions. Specifically, the research identified the car-following, deceleration, acceleration, and gap-acceptance parameters that require calibration and demonstrated why they need to be calibrated. The research then identified the simulation parameters that require calibration in the VISSIM and INTEGRATION software and demonstrated use of the methodology. Use of weather-related factors also was documented for CORSIM, although these were not demonstrated.

First, in the case of the VISSIM software the car-following sensitivity factors and deceleration and acceleration functions were presented. Subsequently, modeling the impact of inclement weather on gap acceptance behavior was demonstrated. The gap acceptance situation in the software can be divided into two categories: Priority Rule and Conflict areas. For the Priority Rule, a stop line and a conflict marker or more are defined. The stop line is defined the location where lower priority vehicles wait until a suitable gap time or a sufficient distance headway is available. The signalized intersection with permissive left turn is considered a special case for priority rule option in VISSIM by only adjusting the

minimum acceptable gap regardless the number of opposing lanes and waiting time. The second category is the Conflict Area option which can be defined wherever two links/connectors in the VISSIM network overlap. For each conflict area, the user can select which of the conflicting links has right-of-way (if any), Visibility of the links, Front Gap, Rear Gap, and Safety Distance Factor are used.

Finally, the parameter adjustments for the INTEGRATION software were explained. The INTEGRATION software follows the Van Aerde steady-state car-following model which can be calibrated to different weather and roadway conditions by changing three traffic stream parameters (free-flow speed, speed-at-capacity, and saturation flow rate). Thereafter, the parameters, which include friction coefficient and rolling coefficients, used to adjust the acceleration and deceleration models were presented. The gap acceptance modeling also was presented. The simulation logic within INTEGRATION automatically models the hierarchy in gap acceptance priority of one movement over a lower priority movement. Vehicles are often required to find acceptable gaps in an opposing flow, typically when attempting unprotected movements at either signalized or partially controlled intersections. The user has the option to specify the number of links that may oppose the current link, and the corresponding minimum acceptable gap per lane. The gap acceptance modeling process in INTEGRATION gives the user, flexibility for studying different weather conditions for any type of intersection control and geometric design.

6.0 References

1. Pisano, P.A., L.C. Goodwin, and M.A. Rossetti, *U.S. Highway Crashes in Adverse Road Weather Conditions*, in 24th Conference on IIPS, 2008.
2. Hranac, R., et al., *Empirical Studies on Traffic Flow in Inclement Weather*. Publication No. FHWA-HOP-07-073, U.S. DOT FHWA, 2006.
3. Rakha, H., et al., *Inclement Weather Impacts on Freeway Traffic Stream Behavior*. Transportation Research Record: Journal of the Transportation Research Board, No. 2071, TRB, National Research Council, Washington, D.C., pages 8-18, 2008.
4. Zhang, L., P. Holm, and J. Colyar, *Identifying and Assessing Key Weather-Related Parameters and Their Impacts on Traffic Operations Using Simulation*. Publication No. FHWA-HRT-04-131, U.S. DOT FHWA, 2004.
5. Sterzin, E.D., *Modeling Influencing Factors in a Microscopic Traffic Simulator*, in Department of Civil and Environmental Engineering, 2004, Massachusetts Institute of Technology: Cambridge, Massachusetts.
6. Gurusinghe, G.S., et al., *Multiple Car-Following Data with Real-Time Kinematic Global Positioning System*. Transportation Research Record: Journal of the Transportation Research Board, No. 1802, TRB, National Research Council, Washington, D.C., pages 166-180, 2002.
7. Ranjitkar, P., et al., *Human Driving Behavior Under Icy Road Conditions: Trajectory-Based Study*, in Transportation Research Board 88th Annual Meeting, 2009: Washington, D.C.
8. M. Van Aerde and H. Rakha. *Multivariate Calibration of Single Regime Speed-Flow-Density Relationships*, in Proceedings of the 6th 1995 Vehicle Navigation and Information Systems Conference, 1995, Seattle, Washington, U.S.A., pages 334-341.
9. M. Van Aerde, *Single Regime Speed-Flow-Density Relationship for Congested and Uncongested Highways*, in 74th TRB Annual Conference, Washington, D.C., 1995.
10. Rakha, H., *Validation of Van Aerde's Simplified Steady-State Car-Following and Traffic Stream Model*.
11. H. Rakha, P. Pasumarthy, and S. Adjerid, *A Simplified Behavioral Vehicle Longitudinal Motion Model*. Transportation Letters: The International Journal of Transportation Research, Volume 1, pages 95-110, 2009.
12. Rakha, H. and Lucic I., *Variable Power Vehicle Dynamics Model for Estimating Maximum Truck Acceleration Levels*. ASCE Journal of Transportation Engineering, Volume 128(5), September/October, pages 412-419, 2002.
13. TRB, "HCM: Highway Capacity Manual 2000," in *Transportation Research Board*, 2000.
14. S. Datla and S. Sharma, "Association of Highway Traffic Volumes with Cold, Snow and Their Interactions," in *Transportation Research Board TRB, 2010*.
15. M. Cools, E. Moons, and G. Wets, "Assessing the Impact of Weather on Traffic Intensity," in *Transportation Research Board TRB, 2008*.

16. W. Brilon and M. Ponzlet, "Variability of Speed-Flow Relationships on German Autobahns," *Transp. Res. Rec., National Research Council, Washington, D.C.,* pages 91-98, 1996.

17. H. Rakha, M. Farzaneh, M. Arafah, and E. Sterzin, "Inclement Weather Impacts on Freeway Traffic Stream Behavior," in *Transportation Research Board TRB*, 2008.

18. J. Daniel, J. Byun, and S. Chien, "Impact of Adverse Weather on Freeway Speeds and Flows," in *Transportation Research Board TRB, 2007*.

19. N.G. Tsongos, "Comparison of day and night gap-acceptance probabilities," *Public Road, 35(7),* pages 157-165, 1969.

20. K.C. Sinha, and Tomiak, W.W., "Gap acceptance phenomenon at stop controlled intersections," *Traffic Engrg. and control, 41(7),* pages 28-33, 1971.

21. W. Brilon, "Recent developments in calculation methods for unsignalized intersections in West Germany, intersections without traffic signals," *Proc., Int. Workshop on Intersections without Traffic Signals, Bochum, Federal Republic of Germany,* pages 111-153, 1988.

22. A.W. Polus, "Gap acceptance characteristics at unsignalized urban intersections," *Traffic Engrg. and control, 24(5),* pages 255-258, 1983.

23. X. Yan, and Radwan, E., "Influence of Restricted Sight Distances on Permitted Left-Turn Operation at Signalized Intersections," *Journal of Transportation Engineering ASCE,* Volume 134, February 2008.

24. M.M. Hamed and S. Easa, "Disaggregate Gap-Acceptance Model for Unsignalized T-Intersections," *Journal of Transportation Engineering,* Volume 123, February 1997.

25. J.K. Caird and P.A. Hancock, "Left-Turn and Gap Acceptance Crashes," in *Human factors in traffic safety*, R.E. Dewar and P. Olson, Eds.: Lawyers & Judges Publishing: Tucson, Arizona, 2002, pages 613-652.

26. I. Zohdy, S. Sadek, and H. Rakha, "Empirical Analysis of Wait Time and Rain Intensity Effects on Driver Left-Turn Gap Acceptance Behavior," in *Transportation Research Board TRB, 2010*.

27. H. Rakha, S. Sadek, and I. Zohdy, "Modeling Stochastic Left-Turn Gap Acceptance Behavior" in *Transportation Research Board TRB, 2010*.

28. K. Burnham and D. Anderson, "Multimodel inference:Understanding AIC and BIC in model selection," *Amsterdam Workshop on Model Selection,* 2004.

29. AASHTO, "A policy on geometric design of highways and streets," Washington, D.C., 2001.

30. Hranac, R., et al., *Empirical Studies on Traffic Flow in Inclement Weather*. Publication No. FHWA-HOP-07-073, U.S. DOT FHWA, 2006.

31. Rakha, H., et al., *Inclement Weather Impacts on Freeway Traffic Stream Behavior*. Transportation Research Record: Journal of the Transportation Research Board, No. 2071, TRB, National Research Council, Washington, D.C., pages 8-18, 2008.

32. Mannering, F.L. and W.P. Kilareski, *Principles of Highway Engineering and Traffic Analysis*. Second edition 1998: John Wiley and Sons.

33. Rakha, H., M. Arafeh, and S. Park, *Modeling Inclement Weather Impacts on Traffic Stream Behavior*, in Transportation Research Board 88th Annual Meeting. 2009: Washington, D.C.

34. Rakha, H., et al., *Vehicle Dynamics Model for Predicting Maximum Truck Acceleration Levels.* Journal of transportation engineering, 2001. **127**(5): pages 418-425.

35. TRB, *HCM:Highway Capacity Manual 2000*, in *Transportation Research Board*. 2000.

36. Cassidy, M.J., et al., *Unsignalized Intersection Capacity and Level of Service: Revisiting Critical Gap.* Transportation Research Record, 1995(1484): pages 16-23.

37. Rakha, H., F. Dion, and H.G. Sin, *Using Global Positioning System Data for Field Evaluation of Energy and Emission Impact of Traffic Flow Improvement Projects: Issues and Proposed Solutions.* Transportation Research Record, 2001. **n 1768**: pages 210-223.

38. Rakha, H. and Y. Gao. *Calibration of Steady-State Car-Following Models Using Macroscopic Loop Detector Data*. Symposium on The Fundamental Diagram: 75 Years. 2008. Woods Hole, Massachussetts.

39. *INTEGRATION Software Guide, Release 2.3.* February 2007

Appendix A. Car-Following Model Equations

A.1 Van Aerde Car-Following Model

Van Aerde proposed a traffic stream model that integrates the Greenshields and Pipes car-following models.[2], [3] The model has four degrees of freedom and is formulated as

$$h_{n+1}(t-T) = c_1 + c_3 u_{n+1}(t) + \frac{c_2}{u_f - u_{n+1}(t)} \quad [1]$$

Where $h_{n+1}(t-T)$ is the distance headway (km) of vehicle *n+1* at instance *t-T*, $u_{n+1}(t)$ is the speed of vehicle *n+1* at instance t (km/h), u_f is the facility free-flow speed (km/h), c_1 is a fixed distance headway constant (km), c_2 is a variable headway constant (km^2/h), c_3 is a variable distance headway constant (h^{-1}), and *T* is PRT.

c_1, c_2, and c_3 can be formulated as a combination of four traffic parameters[4] q_c, k_j, u_c, and u_f as

$$c_1 = \frac{u_f}{k_j u_c^2}\left(2u_c - u_f\right); \quad c_2 = \frac{u_f}{k_j u_c^2}\left(u_f - u_c\right)^2; \quad c_3 = \frac{1}{q_c} - \frac{u_f}{k_j u_c^2} \quad [2]$$

According to Equation 1, the vehicle speed at instance *t* depends on the headway between the lead vehicle at instance *t-T*. Thus, for the easy calculation of the speed of following vehicle, the equation can be rearranged as[5]

$$u_{n+1}(t) = \frac{-c_1 + c_3 u_f + h_{n+1}(t-T) - \sqrt{\left[c_1 - c_3 u_f - h_{n+1}(t-T)\right]^2 - 4c_3\left[h_{n+1}(t-T)u_f - c_1 u_f - c_2\right]}}{2c_3} \quad [3]$$

A.2 Vehicle Dynamics Model

The state-of-practice car-following models can estimate unrealistic vehicle accelerations. Consequently, a variable vehicle dynamics model that was developed by Rakha and Lucic was introduced to ensure that the estimated accelerations were feasible. Specifically, the vehicle speed was constrained by the maximum acceleration. The maximum vehicle speed was calculated as

$$\widehat{u}_{n+1}(t) = u_{n+1}(t - \Delta t) + \widehat{a}_{n+1}(t)\Delta t \quad [4]$$

Where $a_{n+1}(t)$ is computed as the maximum acceleration of the following vehicle (vehicle *n+1*) at instance *t* as

$$\widehat{a}_{n+1}(t) = \frac{F_{n+1}(t) - R_{n+1}(t)}{M} \quad [5]$$

Where $F_{n+1}(t)$ is the effective propulsive force of vehicle *n+1* at instance *t*; $R_{n+1}(t)$ is the total resistance force, including the aerodynamics, rolling, and grade resistance forces on vehicle *n+1* at instance *t*; and *M* is the vehicle mass. The details of the calculation of tractive and resistance forces are available in the literature.[6]

A.3 Collision Avoidance Model

In addition to the vehicle dynamics model, the vehicle speed estimated by the car-following model was checked with the maximum speed at which the vehicle can traverse without resulting in a collision with the leading vehicle. The maximum collision avoidance speed is calculated as

$$\breve{u}_{n+1}(t) = \sqrt{u_n^2(t) + 2\mu g\left(h_{n+1}(t) - h_j\right)} \quad [6]$$

Where μ is the coefficient of friction between the vehicle tires and the pavement surface and *g* is the gravitational acceleration. The normal value for the coefficient of friction, 0.6, was used for dry roadway conditions. For the icy roadway experiments, the coefficient of friction was reduced to 0.13 based on field measurements conducted at the time of the experiments.

Appendix B. Metric/English Conversion Factors

ENGLISH TO METRIC	METRIC TO ENGLISH
LENGTH (APPROXIMATE)	**LENGTH (APPROXIMATE)**
1 inch (in) = 2.5 centimeters (cm)	1 millimeter (mm) = 0.04 inch (in)
1 foot (ft) = 30 centimeters (cm)	1 centimeter (cm) = 0.4 inch (in)
1 yard (yd) = 0.9 meter (m)	1 meter (m) = 3.3 feet (ft)
1 mile (mi) = 1.6 kilometers (km)	1 meter (m) = 1.1 yards (yd)
	1 kilometer (km) = 0.6 mile (mi)
AREA (APPROXIMATE)	**AREA (APPROXIMATE)**
1 square inch (sq in, in^2) = 6.5 square centimeters (cm^2)	1 square centimeter (cm^2) = 0.16 square inch (sq in, in^2)
1 square foot (sq ft, ft^2) = 0.09 square meter (m^2)	1 square meter (m^2) = 1.2 square yards (sq yd, yd^2)
1 square yard (sq yd, yd^2) = 0.8 square meter (m^2)	1 square kilometer (km^2) = 0.4 square mile (sq mi, mi^2)
1 square mile (sq mi, mi^2) = 2.6 square kilometers (km^2)	10,000 square meters (m^2) = 1 hectare (ha) = 2.5 acres
1 acre = 0.4 hectare (he) = 4,000 square meters (m^2)	
MASS – WEIGHT (APPROXIMATE)	**MASS – WEIGHT (APPROXIMATE)**
1 ounce (oz) = 28 grams (gm)	1 gram (gm) = 0.036 ounce (oz)
1 pound (lb) = 0.45 kilogram (kg)	1 kilogram (kg) = 2.2 pounds (lb)
1 short ton = 2,000 pounds (lb) = 0.9 tonne (t)	1 tonne (t) = 1,000 kilograms (kg)
	= 1.1 short tons
VOLUME (APPROXIMATE)	**VOLUME (APPROXIMATE)**
1 teaspoon (tsp) = 5 milliliters (ml)	1 milliliter (ml) = 0.03 fluid ounce (fl oz)
1 tablespoon (tbsp) = 15 milliliters (ml)	1 liter (l) = 2.1 pints (pt)
1 fluid ounce (fl oz) = 30 milliliters (ml)	1 liter (l) = 1.06 quarts (qt)
1 cup (c) = 0.24 liter (l)	1 liter (l) = 0.26 gallon (gal)
1 pint (pt) = 0.47 liter (l)	
1 quart (qt) = 0.96 liter (l)	
1 gallon (gal) = 3.8 liters (l)	
1 cubic foot (cu ft, ft^3) = 0.03 cubic meter (m^3)	1 cubic meter (m^3) = 36 cubic feet (cu ft, ft^3)
1 cubic yard (cu yd, yd^3) = 0.76 cubic meter (m^3)	1 cubic meter (m^3) = 1.3 cubic yards (cu yd, yd^3)
TEMPERATURE (EXACT)	**TEMPERATURE (EXACT)**
[(x-32)(5/9)] °F = y °C	[(9/5) y + 32] °C = x °F

QUICK INCH - CENTIMETER LENGTH CONVERSION

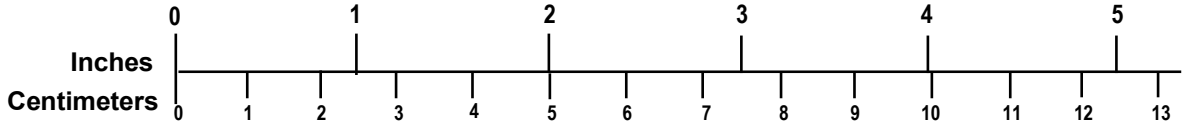

QUICK FAHRENHEIT - CELSIUS TEMPERATURE CONVERSIO

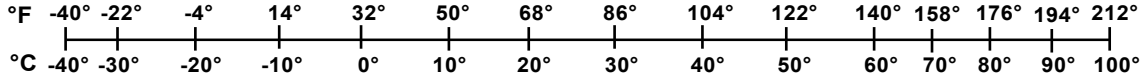

For more exact and or other conversion factors, see NIST Miscellaneous Publication 286, Units of Weights and Measures. Price $2.50 SD Catalog No. C13 10286

U.S. Department of Transportation
Research and Innovative Technology Administration (RITA)
1200 New Jersey Avenue, SE
Washington, DC 20590

www.its.dot.gov

FHWA- JPO-11-020